Final Technical Report

National Institute of Justice Award Number: 2008-DN-BX-K165

Biomarkers of Human Decomposition Ecology and the Relationship to Postmortem Interval

Franklin E. Damann, PhD
National Museum of Health and Medicine
Silver Spring, MD 20910

30 September 2012

Abstract

Microbial putrefaction of a corpse leaves signatures in the landscape and bone. Within this relationship exists the potential for refining models of postmortem interval (PMI) estimation based on increased understanding of the physicochemical characteristics and bacterial metagenomic profiles of the human decomposition environment. Therefore, microbial biomarkers and characterization of gravesoil ecology have a great potential to benefit the work of forensic anthropologists in interpreting postmortem history. Unfortunately, this potential is only recently becoming realized and suffers from a lack of basic research. Using bone and soil samples acquired from The University of Tennessee Anthropology Research Facility (ARF), this study provides baseline physicochemical and bacterial community data for developing methods to estimate better estimate PMI.

This project evaluated the physicochemical and microbial characteristics of ARF soils, non-ARF soils, and skeletal tissue exposed to various levels of human decomposition and advancing PMIs. Soil was evaluated for eight different physicochemical parameters and a biological similarity matrix of identified bacterial taxa from sequencing the 16S rRNA gene was generated from soil and bone.

Results of the physicochemical analyses from ARF landscape soils demonstrated no differences among the decomposition sample groups inside the facility, while all sample groups inside were significantly different ($p \leq 0.05$) from the non-ARF samples. Bacterial community data augmented the physicochemical data, by identifying significant differences inside the ARF between decomposition sites with constant decomposition and those with little to no decomposition, suggesting microbial sensitivity to slight ecological change. Sites with a lot of decomposition contained elevated levels of chemoorganotrophic and sulfate-reducing bacteria, and a reduction in Acidobacteria, indicating a change in the community of underlying bacteria in response to carcass enrichment and ammonification of the soil.

Temporally-related trends in bacterial metagenomic profiles were observed among the PMI samples of gravesoil and bone. Regardless of origin (gravesoil or bone), the same bacterial phyla (Proteobacteria, Actinobacteria, Acidobacteria, Firmicutes, Bacteroidetes, Gemmatimonadetes) were observed; only the relative abundance changed over time. Proteobacteria were most abundant in all samples and the most fluctuation among samples

occurred with Firmicutes, Bacteroidetes, and Actinobacteria. Firmicutes appeared more frequently in the earlier samples than did Bacteroidetes and Actinobacteria. Bacteroidetes dominated the middle phase to the 20 month PMI sample, at which time Actinobacteria dominated the three phyla at the 48 month terminus of this project.

Thirty years of decomposition research at the ARF has forced a shift in the underlying bacterial community in response to the enrichment of the soil with increased nitrogen and carbon-containing compounds. The results of this basic research provide baseline data for further exploration regarding the biogeochemical relationships among microbial organisms, soil characteristics, cadaver decomposition, and advancing PMI.

Table of Contents

List of Figures

List of Tables

Executive Summary

The ecology of human decomposition is a complex series of occurrences that are driven by physicochemical and biological processes. Among the postmortem biological processes, the microbial communities are significant modulators. Enteric microbes initiate putrefaction, which are then replaced by edaphic microorganisms during late stage decomposition (Evans 1963), eliciting micro- and macroscopic destruction of soft and hard tissues.

Microbially-mediated human decomposition is a significant biologic function that facilitates the transformation of a once living organism to a resource of energy and nutrients that become available to various decomposer guilds. Therefore, the cadaver-soil interface has a highly complex ecology, and should be an important area of forensic investigation for identifying potential changes in soil parameters and microbial diversity that relate to time since death.

Little is known about postmortem microbiology and biodiversity at human cadaver decomposition sites, and even less is known about the relationship between microbial structure and the human decomposition ecosystem. New laboratory methods and techniques, such as next generation sequencing, allow characterization of microbial communities at a breadth and depth previously unattainable. For example, the individuating nature of the human gut microbiome is now well established (Costello et al. 2009). This microbial fingerprint may explain some of the significant variation observed with cadaver decomposition (c.f. Shirley et al. 2011). Understanding and appreciating the variability in modulators of decomposition and their effect on the rate of human decomposition is important in order to increase our understanding of the observable patterns of how humans decompose and how those patterns and changes may be used to better estimate time since death.

Given the limited information that currently exists on postmortem microbiology and gravesoil ecology, this basic research project investigates the physicochemical and microbiological characteristics of human decomposition. Our primary interest was to create a baseline dataset of physicochemical parameters and bacteria associated with human decomposition to which future studies may expand upon to further our understanding of human decomposition ecology.

Goals. The goal of this research was based on the premise that if the characteristics of a site that has experienced a lot human decomposition is systematically different from those with little

or no decomposition, then the same characteristics would be expected to differ with advancing PMI. Therefore, this basic research program devised two core questions: (1) what is the physicochemical and microbial composition of human decomposition in the terrestrial landscape, and (2) do the physicochemical and microbiological data associated with human decomposition conform to a pattern that has the potential to improve postmortem interval (PMI) estimation?

In order to answer these questions, soil samples were taken from the University of Tennessee Anthropology Research Facility (ARF) to evaluate general landscape patterns in physicochemical properties and microbial community structure. Once evaluated, a series of laboratory tests were devised to investigate potential effects of PMI on the physicochemical and microbial structure of gravesoil and bone.

Methods. The ARF was selected as the site of study, since it is well known for its unique history as a site of human decomposition research in a natural environment. The ARF has been integral to our understanding of the processes of human decomposition.

Given the slope and structures inside the ARF, bodies are often placed in areas that are easily accessible and on relatively flat terrain. In order to demonstrate the nonrandom spatial distribution and density of decomposing corpses at the ARF, the facility was mapped and overlaid with a 5-x-5-meter grid. The GPS locations of bodies were recorded plotted. The number of human corpses decomposing per unit was then tabulated. All units across the facility were structured on an ordinal scale. Units with six or more decomposing bodies were recorded as ‘‘High’’, while ‘‘Middle’’ decomposition units included 2 to 5 bodies. Units with one body were listed as ‘‘Low’’, and units inside the facility with no recorded history of human decomposition over the five-year data subset were listed as ‘‘None’’. The density distribution facilitated the partitioning of the facility into areas of increasing cadaver decomposition that permitted a test of the hypothesis that human decomposition changed the underlying soil characteristics.

In order to address possible temporal trends in physicochemical parameters and bacterial communities, gravesoil directly below the abdomen and a lower rib (11 or 12) from different corpses decomposing on the surface of the ARF were collected. The corpses varied in time since death and decomposition.

Results of ARF Landscape Evaluation. The characteristics of the ARF physicochemical soil landscape (Chapter 3) were significantly different from samples that were taken outside the ARF

(one-way ANOVA; $p < 0.05$). Soil moisture content, soil organic content, soil pH, total nitrogen, carbon to nitrogen ratio, and lipid-bound phosphorus all contributed to the significant ANOVA model. Post hoc Tukey's tests indicated significant differences ($p < 0.05$) between the samples collected outside the facility (non-ARF) and all samples included in the analysis from within the facility (None, Low, Middle, and High) for the variables of soil pH, moisture content, and organic content. Additional pairwise differences included non-ARF and High for the CN ratios ($p < 0.05$), and non-ARF to None for lipid-bound phosphorus ($p < 0.05$).

The six significant gravesoil parameters for all ARF landscape samples were then subject to principal components analysis (PCA). Seventy-nine percent of the total variation was explained in the first two components, with each component being significant ($p < 0.05$). The two-dimensional ordination plot indicated clear separation of non-ARF soil samples from the general landscape samples taken inside the facility.

The metagenomic data obtained from the same ARF landscape samples (Chapter 4) remained concordant with the physicochemical data, and demonstrated significant differences within the facility between the areas of High decomposition to those with no history of decomposition (i.e., None). The High decomposition samples were marked by increased levels of chemoorganotrophic and sulfate-reducing bacteria, and a reduction in members of the bacterial phyla Acidobacteria, suggesting that 30 years of decomposition research at the ARF likely forced a shift in the underlying bacterial community in response to the enrichment of the soil with increased nitrogen, moisture, and organic matter in the areas where bodies are constantly decomposing (i.e., the High sample group).

Results of PMI Investigations. The analyses of data collected from actively decomposing corpses were obtained from gravesoils and lower human ribs.

Physicochemical parameters from gravesoil samples taken below actively decomposing corpses varied in PMI from 1-48 months (Chapter 5). A PCA of the pooled and unstructured physicochemical parameters of gravesoil and non-ARF samples extracted two components that were significant ($p < 0.05$). The first two component scores accounted for 83% of the observed variation among the variables recorded. An evaluation of the sample distribution suggested a pattern by which there was a temporal shift along the PC2 axis. The non-ARF samples and the samples with the shortest PMI (< 1 month) shared similar PC2 values, and the greatest deviation along this axis occurred between samples of one to 18 months. The late-stage decomposition

samples (47 and 48) became more similar to non-ARF soil samples. This shift was likely driven by decreasing values of total carbon, total nitrogen, lipid-bound phosphorus, and soil organic matter, as they all correlated well with the extracted component score.

The bacterial community profiles from gravesoils collected below decomposing bodies covered a PMI of 1-47 months (Chapter 6). Classified sequences revealed Proteobacteria, Actinobacteria, Acidobacteria, Bacteroidetes, Firmicutes, and Gemmatimonadetes as the six major bacterial phyla present in each sample. As the postmortem interval increased the relative distribution of the individual phyla changed and appeared to follow time since death, as the sample distribution became more similar to that observed in the non-ARF "normal" soil samples. Phyla that were observed to change more drastically than others were the Firmicutes, Bacteroidetes, and Acidobacteria. Firmicutes and Bacteroidetes were most abundant in the early samples (< 7 months), which were followed by Bacteroidetes alone between 7 and 20 months postmortem. Acidobacteria were abundant early, decreased through the middle of the sample distribution, and increased in relative abundance by the 20 month PMI sample.

In addition to soils, bone was investigated as a potential source of microbiological data for estimating PMI. Bone samples were first investigated to determine the total concentration of microbial biomass (bacteria and fungi) contained in each bone sample (Chapter 7). Over time, the concentration of microbial DNA decreased, and showed temporally related ecological patterns in the dominance of bacterial DNA over fungal DNA in samples from the first 12 months after death. After 12 months, bacterial concentration decreased and maintained levels similar to fungi.

Bacterial community analysis of the bone samples (Chapter 8) identified a pattern in bacterial relative abundance similar to that of the gravesoil samples (Chapter 6). The same six bacterial phyla observed in the gravesoil samples were observed for each bone sample. Again, the relative abundance of each phylum changed over time becoming more similar to normal soil conditions at 47 and 48 months postmortem. The bacterial phyla in bone that fluctuated most drastically and therefore may have the most importance for PMI estimation were the Firmicutes, Bacteroidetes, and Actinobacteria. The Firmicutes were present early (≤ 9 months) and nearly nonexistent in the later stages. Their dominance in the early postmortem period in both gravesoil and bone suggested human gut origin. Bacteroidetes, a diverse bacterial phylum whose members are widely distributed in soils, sea water and the human gut, was most abundant between 11 and

20 months postmortem. Actinobacteria are widely distributed in soil and were the dominate phylotype of the 24 and 48 month samples.

This work demonstrated-a relationship between higher soil pH values, nitrogen content and a lower carbon to nitrogen ratio of soil in areas devoted to human decomposition. These observations may have elicited the significant changes observed in the underlying bacterial communities. Therefore, it is suggested that research facilities incorporate an evaluation of the saturation hypothesis into their long-term strategic plans by performing ecological surveys, early and repeatedly, throughout the lifecycle of a decomposition facility. In doing so, a better understanding of the relationship between ecological change and the forensic goals of providing better models for estimating postmortem intervals may be forthcoming.

In order to realize the full potential of decomposition ecology to forensic sciences, additional taphonomic research is certainly required. Both experimental and evidenced-based data collection should continue to be employed to identify patterns of change in the physicochemical (e.g., soil pH, total carbon, nitrogen, and moisture content, ninhydrin reactive nitrogen, volatile fatty acids) and biological (e.g., bacteria, fungi, and nematodes) constituents of gravesoils. These measures should be considered in addition to the descriptive gross observations and plotting of daily mean temperatures. The methods of collection, recording, and analysis of such information should be standardized to facilitate comparison between and among the various recovery sites and decomposition facilities across the United States. Standardized data collection may permit establishment of a nationwide registry of experimental and evidence-based data that would create the opportunity for the necessary increase in sample size and the development of regional models of human decomposition.

Chapter 1 Introduction

1.1 Statement of the Problem

Microbially-mediated human decomposition is a significant biologic function that facilitates the transformation of once living organisms to a pool of energy and nutrients that become available to living organisms in the surrounding landscape. Therefore the cadaver-soil interface has a highly complex ecology and should be an important area of forensic investigation for identifying potential changes in soil parameters and microbial diversity of soil and bone during the postmortem interval.

To that end, the microbial structure and biodiversity at human cadaver decomposition sites has only recently been investigated (Parkinson 2009; Damann 2010) and remains poorly understood. Little is known about the structure of the microbial community its relationship to the changing human decomposition ecosystem, and how the shifting community structure can be used as a temporal biomarker of forensic investigation.

1.2 Statement of Research Rationale

This research project evaluated the composition of various soil parameters and microbial communities associated with human decomposition in the terrestrial setting at the University of Tennessee Anthropology Research Facility (ARF). The rationale behind the research was based on the premise that if the characteristics of a site that has experienced a lot human decomposition is systematically different from those with little or no decomposition, then the same characteristics would be expected to differ with increasing PMI. Therefore, in conducting this basic research project, two core questions were asked:

1. What are the physicochemical parameters and microbial communities of human decomposition in the terrestrial landscape?

2. Do the physicochemical and microbiological data associated with human decomposition conform to a pattern that has the potential to improve PMI estimation?

A series of independent laboratory tests were devised in order to answer these two basic research questions (Figure 1-1). By achieving our primary goal of providing a baseline survey of physicochemical and microbial structure of soil at the ARF, the first question was addressed (see Chapters 3 and 4). The second question was addressed through four additional laboratory tests investigating the relationship of PMI to physicochemical parameters of gravesoil (Chapter 5), the

bacterial community structure of gravesoils (Chapter 6), the concentration of bacteria and fungi in bone (Chapter 7), and the bacterial communities of bone (Chapter 8).

By evaluating human decomposition in a broad ecological context this research developed an understanding of gravesoil microbial ecology and identified potential trends in temporal variation of edaphic characteristics and microbial diversity of a decomposing human corpse. With this at hand, the forensic scientist has acquired baseline data for furthering our understanding of human decomposition ecology and for developing new methods for refining postmortem interval estimations.

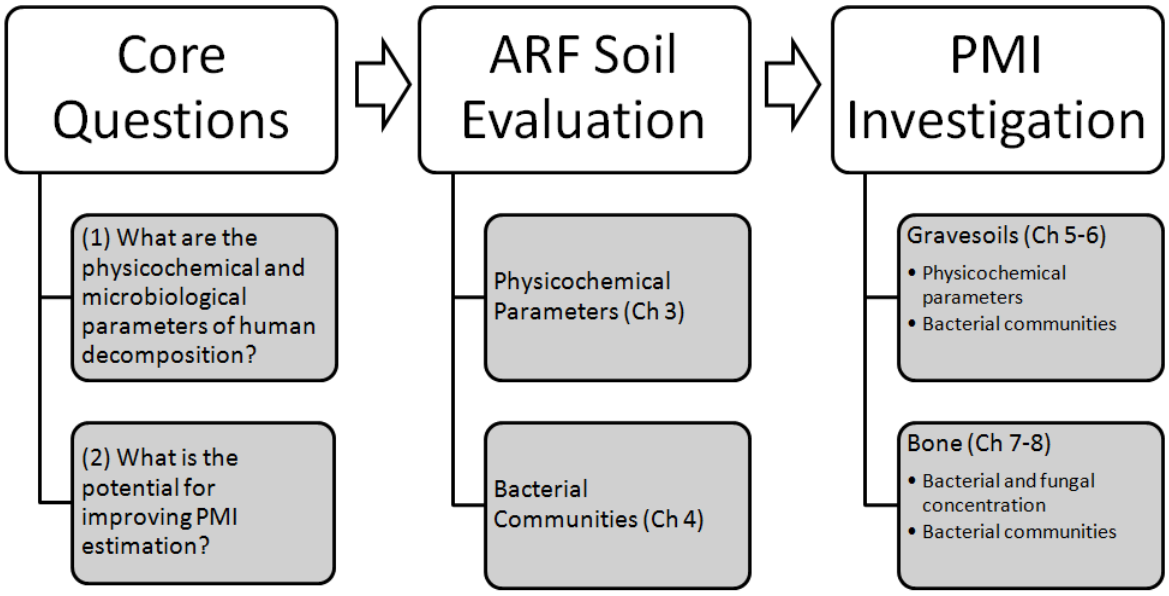

Figure 1-1. Diagram outlining the approach taken during this basic research on the evaluation and investigation of human decomposition ecology.

1.3 Literature Review

The breakdown of a corpse involves a complex hub of activity, where the mobilization of nutrients occurs through a localized pulse of water (Carter et al. 2010), carbon, nitrogen, phosphorus and energy into the surrounding ecosystem in both time and space (Carter et al. 2007). Benninger and colleagues (2008) identified significant changes in the soil solution soon after death, only to have the affected soil mimic control soils 60 to 80 days postmortem; thus reflecting the ephemeral pulse of nutrients and energy suggested first by Vass et al. (1992). This observation suggested that it may be possible to identify microbial markers of human

decomposition in the landscape, as the structure of the microbial population is sensitive to the changing nutrient availability.

During decomposition, the bacterial flora transition from the aerobic groups, exemplified by the coliform-staphylococcal-proteus varieties, to the anaerobic, in which the Clostridia predominate (Evans 1963). Similar observations have suggested that the destruction of soft tissue was caused by enteric obligate and facultative anaerobic microorganisms from the genera *Clostridium, Bacteroides, Staphylococcus,* and the Enterobacteriaceae family (Melvin et al. 1984; Carter et al. 2007).

With regard to bone tissue, the fungus *Mucor sp*. (Marchiafava et al. 1974) and the bacterium *Fusarium sp.* (Hackett 1981) have been isolated from bone. Child (1995) isolated fungi and bacteria from archaeological bone and associated soil and identified various microbial agents (Figure 1-2). Recently, Lorielle (personal communication, 2010) applied high-throughput sequencing to a 50 year-old bone, and identified 1,038 different sequences with bacteria and fungi representing 45% and 12%, respectively. Members of the bacterial genus *Streptomyces* represented the major microbial component. Carter and Tibbett (2003) presented a guild of taphonomic fungi associated with mammalian decomposition and listed fungi according to either early or late stage succession, differentiating them based on nitrogen utilization. Early stage fungi included Ascomycetes, Deuteromycetes, and saprotrophic Basidiomycetes, while late stage fungi included ectomycorrhizal basidiomycetes that typically fruit from one to four years after fertilization (Carter and Tibbett 2003). Subsequently, species of *Aspergillus*, *Penicillium* and *Candida* were indentified in the bloat and putrefactive stages, while *Aspergillus sp.*, *Penicillium sp*., and *Mucor sp*. were the primary residents during the late stage of skeletonization (Sidrim et al. 2010).

By way of molecular cloning and sequencing of the 16S rRNA gene, 23 different bacterial orders were identified from over 500 cloned sequences (Figure 1-3) (Parkinson 2009). This work demonstrated the complexities of the bacterial community structure of gravesoils associated with human cadaver decomposition.

These studies have provided important ecological information related to components of the microbial community (Parkinson 2009; Parkinson et al. 2009; Damann 2010) and changes in soil solution in response to cadaver decomposition (Vass et al. 1992, 2002, 2008; Carter et al. 2007; Benninger et al. 2008). In so doing, the data were derived from observations of decomposition

events with little attention placed on the diversity of microbial communities of gravesoils and skeletal remains. Furthermore, the indigenous landscape typically used in human decomposition studies has not been evaluated for physicochemical parameters or microbial diversity with an eye toward how the level of basal soil properties and diversity is affected given the constant input of a rich nutrient source. With the development of next generation sequencing greater resolution of once unculturable microbial-rich environments is now possible.

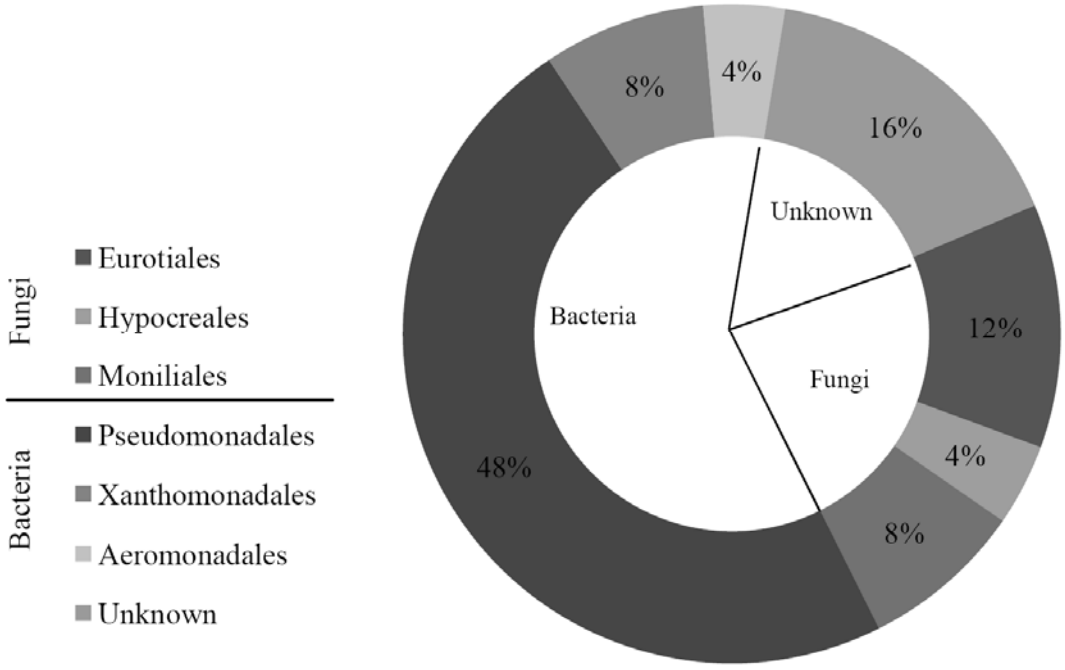

Figure 1-2. Fungal and bacterial orders recovered from archaeological bone (after Child 1995).

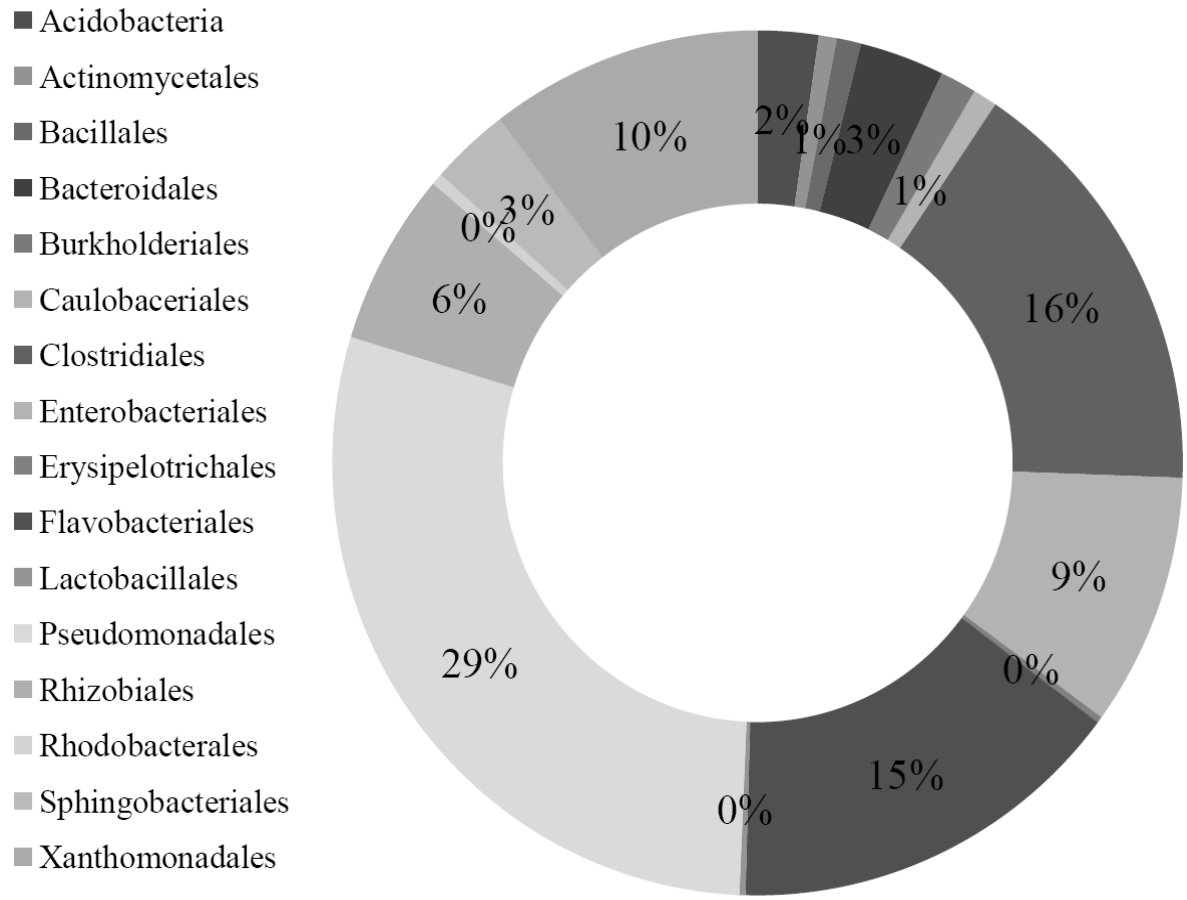

Figure 1-3. Bacterial orders from soil and sand below human and pig corpses (Parkinson 2009).

Chapter 2 General Field and Laboratory Methods

2.1 Sample Collection

The Soil Landscape. The University of Tennessee Anthropology Research Facility (ARF) soils are listed as Coghill-Corryton complex, and are divided into two units at the ARF: one having slope between 12% and 25%, and the second having slope greater than 25% and rocky (Hargrove 2006). Coghill-Corryton are described as very deep, well drained, clayey soils that formed in residuum derived from interbedded, leached, calcareous sandstone and shale (Hartgrove 2006). Surface sediments are further defined by Hartgrove (2006) as partially decomposed hardwood leaf litter and dark reddish brown loam (Munsell 5 YR 3/3) as the major component, with the residuum consisting of yellowish brown loam (Munsell 10 YR 5/4).

The specific location of each decomposing corpse at ARF has been recorded using a Trimble Pak Global Positioning System (GPS) since 2000. The coordinate data was mapped using previously established geographic-referenced data points and ArcGIS 9.1 (ESRI: Redlands, CA). Prior to 2000, body decomposition sites were sketched on multiple maps by multiple individuals using various reference points across the ARF. The GPS data provided more accurate locational information than the sketch maps, and was therefore used in lieu of the sketch maps.

The GPS location of each corpse was layered on the map to show the nonrandom spatial distribution of human decomposition at the ARF. A grid consisting of contiguous 5-x-5-meter units was superimposed. The frequency of human decomposition per unit was tabulated. Bodies that overlaid two units were included in the unit based on the south and/or west baseline of each unit. Five strata were established that included units with 0; 1; 2 to 5; 6 to 10; ≥ 11 decomposing corpses per unit (Figure 2-1). The units were then partitioned based on the tabulation of decomposition events per unit, and listed as None, Low, Middle, and High.

While the frequency tabulation was an absolute figure for the five year period, the purpose of the plot demonstrated the nonrandom placement of bodies on the surface at the ARF. The five year distribution was consistent with placement in previous years, as anyone that has worked at or visited the ARF quickly recognized that the areas that are flat, near the road and trails typically had more bodies decomposing; and therefore, would be expected to have a greater influence on the underlying soil data structure.

Soil Collection. Soil samples used in this study were taken from the A-horizon, which was encountered within the first five centimeters. All samples were placed on ice and transported to

the laboratory where samples were sifted using ASTM-standard soil sieve No. 10 (2 mm mesh). Large detritus and debris that did not pass through the sieve were discarded. The sieved samples were stored at -20°C until analyses.

Negative Soil Samples. Soil samples were taken outside the ARF, approximately one kilometer south. The samples came from the A-horizon and were located in a similar temperate forest biome. The Soil Survey of Knox County, Tennessee (Hartgrove 2006) identified the sample area as Coghill-Corryton Complex with 12 to 25 percent slopes, which is the same as the area west of the access road inside the ARF. These samples served as a control for "normal" basal soil properties to which ARF soils and bones were compared.

Postmortem Interval Assessment. Samples collected from cadavers and associated gravesoils were used to evaluate the relationships of the physicochemical and microbial environments to PMI. In doing so, a cross-sectional sampling of soil and cadavers from different locations across the ARF was performed. Samples consisted of soil and bone. The top five centimeters of soil was taken from below the abdomen, while either the 11th or 12th rib was selected. The soil was handled in the same manner as the other soil samples described above. The excised ribs were placed in a plastic bag on dry ice and transported to the laboratory where they were stored at -20°C until analysis. As a result of troubleshooting various laboratory techniques and the amount of destructive testing on the collected bone and soil, sample sizes varied slightly among the different laboratory tests performed. A table of samples used in each assay was included in each chapter that investigates the effect of PMI on gravesoil and bone characteristics.

2.2 Physicochemical Parameters

Soil Moisture Content. An average of 20.0 g of soil was used for determining soil moisture content. Moisture content was expressed as a percentage of the difference between wet and dry masses. Samples were dried in a Fisher Scientific Isotemp hybridization incubator (Fisher Scientific, Pittsburgh, PA) at 85°C until there was no more loss of mass per sample tested. Measurements of soil were repeated until the difference between subsequent measures was negligible. A negligible difference was defined as a plus or minus 0.1 g difference between measures. Mass was recorded using a PL1502-S Mettler Toledo balance (Columbus, OH).

Soil pH. Three to five gram aliquots of homogenized soil were suspended in 1:5 (w/v) distilled water (pH = 7.55) slurry in a 30 mL glass beaker. Soil acidity and alkalinity was tested using an Accumet® Research AR20 pH meter with a glass body, single junction silver (Ag) /

silver chloride (AgCl) electrode (Fisher Scientific, Trenton) and calibrated using auto buffer recognition of USA standardized buffer groups 4, 7, and 10.

Soil Organic Matter. Soil organic matter (SOM) is the contribution of plant and animal residues to the soil. SOM was determined by loss on ignition from 3.0 g aliquots of homogenized, oven-dried sediment following Heiri et al. (2001). The percent mass loss between pre- and post-bake values (Storer 1984) defined SOM content, since organic material turns to ash when baked at high temperatures. Samples were fired in ceramic crucibles and a Barnstead Thermoline Type 4800 muffle furnace (Dubuque, IA) at 550°C for four hours.

Total Carbon and Nitrogen. The total percent carbon and nitrogen content of the soil was determined by combustion in a pure oxygen environment using a LECO CNS-1000 elemental analyzer (LECO Corporation: St. Joseph, MI). The resulting gases were homogenized and extracted under controlled conditions of pressure, temperature, and volume using a chromatographic column. The homogenized gases were separated in a stepwise steady-state manner and quantified as a function of their thermal conductivities.

Carbon to Nitrogen Ratio. The carbon to nitrogen ratios were derived from individual sample measurements of total carbon and nitrogen. The CN ratio is typically applied in soil science and agriculture and has been used as an indication of overall soil quality. In this study, CN was applied in a fashion similar to Swift (1979) to indicate the quality of a substrate or resource being decomposed. Therefore, a low CN radio implies a high quality resource.

Lipid-bound Phosphorous. Estimation of microbial biomass by lipid-bound phosphorus was conducted following previously reported extraction and quantification methods described in Drijber et al. (2000) and Benninger et al. (2008). Lipid extraction from soil was performed following a modified Bligh and Dryer lipid extraction, and isolated phospholipid-phosphorus was quantified by colorimetric assay described by Kates (1986). Studies in microbial ecology often use Lipid-P as a measure of microbial biomass. In cadaver decomposition studies this measurement was interpreted differently since Lipid-P cannot be differentiated from the cell walls of microbes or from the cadaver itself (Benninger et al. 2008). Therefore, Lipid-P was used as a measure of total lipid-bound phosphorus influx to the soil landscape.

Analysis of the Physicochemical Data. Standard parametric statistical testing was applied to the physicochemical data, unless specified elsewhere in this report. The raw values were tested for normality and equality of variances. Outliers were removed from the dataset and the

remaining values were normalized by log transformation. One-way ANOVA and Tukey's post hoc test for pairwise differences in sample groups were applied to the log-transformed data. Principal Components Analysis (PCA) on Euclidian distances was performed on the ANOVA-determined significant variables in order to evaluate the distribution of samples in two-dimensional space. Significance of the first and second components was assessed by ANOVA. All statistical analyses of the physicochemical data were performed using SPSS 16.0 (Chicago, IL, USA), unless stated otherwise.

2.3 Molecular Methods

DNA Extraction from Soil. Extraction of total DNA from soil was completed using the Fast DNA Spin Kit for Soil (MP Biomedicals: Solon, OH) given its success in previous extractions from difficult samples (Layton et al. 2006). Following manufacturers' reference, 400 mg aliquots of homogenized sediment were subject to extraction. Post extraction clean-up of isolated DNA was performed using the MinElute PCR purification column (Qiagen: Germantown, MD). The purification procedure removed impurities that co-eluted during the DNA extraction. All extracted and concentrated samples were stored at 4°C for downstream applications.

DNA extraction from Bone. Two-hundred milligrams of pulverized bone were extracted following the demineralization protocol of Loreille et al. (2007), which is a modification of Edson et al. (2004) for degraded samples. The extracted DNA was purified using the Qiagen MinElute PCR Purification Kit following the manufacture's procedures. The DNA was eluted from the filter in a final volume of 100 µL of sterile water.

Bacterial Amplification. A highly-conserved region of the bacterial 16S rRNA gene of the small ribosomal subunit was targeted in order to evaluate bacterial diversity. Amplification was completed using previously reported universal primers targeting regions of the bacterial 16S rRNA gene (Table 2-1). Unless specified elsewhere in this report, PCR reactions were carried out in a 50 µL reaction volume. Each reaction tube contained 2.0 µL of each primer (10uM), 5 µL of 10X PCR buffer, 5 µL of 25 mM $MgCl_2$, 4 µL of 10 mM dNTPs, 5 µL of non-actylated BSA (2.5 mg mL^{-1}), 1.5µL of Taq Gold polymerase, and 2 µL of DNA template. The final volume was adjusted to 50 µL by addition of uv-treated water. Thermocycling conditions varied depending on annealing temperature of the primer sequence and amplicon length.

Table 2-1. Primer sequences, target regions, and annealing temperatures.

	Position	Sequence (5' → 3')	T_A [a]	Reference
Bacteria [b]				
16S	F63	CAGGCCTAACACATGCAAGTC	55	Marchesi et al. 1998
	R1387	GGGCGGWGTGTACAAGGC		
	F341	CCTACGGGAGGCAGCAG	55	Muyzer et al. 1993
	R534	ATTACCGCGGCTGCTGG		
	F338	ACTCCTACGGGAGGCAGCAG	53	Lane 1991
	R533	TTACCGCGGCTGCTGGCAC		Lee et al. 1996
Fungi [c]				
28S	F45	ATCAATAAGCGGAGGAAAAG	60	Sandhu et al. 1995
	R843	CTCTGGCTTCACCCTATTC		
18S	F1773 (ITS1)	TCCGTAGGTGAACCTGCGG	55	White et al. 1990
28S	R57 (ITS4)	TCCTCCGCTTATTGATATGC		

[a] Annealing temperature for the listed primer set.
[b] Nucleotide positions of bacterial primers correspond to coordinates of a reference *E. coli* 16S gene.
[c] Nucleotide positions of fungal primers correspond to coordinates of a reference *S. cerevisiae* 28S gene.

Fungal Amplification. Target sequences of fungi were derived from two different, and yet highly-conserved regions of nuclear rRNA genes (Sandhu et al. 1995; White et al. 1990). Like bacteria, the rRNA genes have stretches of stable sequence interspersed with variable regions (Table 2-1). The first region targeted corresponded to base pair coordinates 45 to 64 and 825 to 843 of the reference *Saccharomyces cerevisiae* 28S gene, for the forward and reverse primers, respectively (Sandhu et al. 1995). Sandhu and colleagues (1995) reported that their fungal primers amplify a highly variable 799 bp product that is useful for sorting fungal species. The primers were identified by sequencing and aligning variable regions of 28S rRNA genes for all fungi amplified by their laboratory (Shandu et al. 1995). Primers of the second region evaluated are derived from the nuclear internal transcribed spacer (ITS) regions. The forward primer is positioned near the tail end of the small subunit (18S) and the reverse primer is positioned near the beginning of the large subunit (28S). These primers amplify a region that evolves quickly and varies among species within a genus or even among isolated populations of the same species (White et al. 1990). The repeat units have coding regions for forming a single ribosome; the number of repetitive regions may vary among species.

PCR reactions were carried out in 50 µL reaction volume. Each reaction tube contained 2.0 µL of each 10 uM ITS1 and 10 uM ITS4 primer, 5.0 µL of 10X PCR buffer, 5.0 µL of 25mM $MgCl_2$, 4 µL of 10 mM dNTPs, 5.0 µL of 2.5 mg mL^{-1} non-actylated BSA, 1.5 µL of Taq Gold polymerase, 2.0 µL of DNA template. The final volume was adjusted to 50 µL by adding UV-

treated water. Every fungal amplification reaction using ITS1 and ITS4 began with initial denaturing at 94°C for 10 minutes followed by 30 cycles of 94°C for 45 seconds, 55°C for 45 seconds, and 72°C for 60 seconds (White et al.1990). The last cycle was held at 72°C for seven minutes, before the samples were stored at 4°C.

Denaturing Gradient Gel Electrophoresis (DGGE). Extracted DNA from ARF soil was amplified using previously established primers with an additional 40-nucleotide GC-rich sequence affixed to the 5-prime end of the forward primer (Muyzer et al. 1993). This GC-clamp increases the stability of the transitional molecules as it denatures (Muyzer et al. 1993).

Thermocycling conditions consisted of an initial 10 minutes of for denaturing at 94°C, then 34 cycles of 94°C for 30 seconds, 60°C for 45 seconds, and 72°C for 45 seconds, followed by a final five minute extension phase at 72°C. Each PCR reaction contained 1.25 units of Clontech Advantage 2 polymerase (BD Biosciences: San Jose, CA) and 10 pmol of each primer. Final volume was adjusted to 25 µL by addition of nanopure water. Amplification was performed on a Robocycler™ PCR block (Stratgene: La Jolla, CA).

Denaturation was performed using a D-code 16/16 cm gel system, maintaining a constant temperature of 60°C in 0.5x TAE buffer (20 mM Tris-acetate. 0.5 mM EDTA, pH 8.0). Denaturing gradients were formed using 8-10% acrylamide and 30-60% denaturant where 100% denaturant is defines as 7M urea, formamide. Gels were run at 55 volts for 16 hours. Bands within the gel were stained in 0.5x TAE buffer with ethidium bromide (0.5 mg L^{-1}). Dominate bands were excised, eluted in 50 µL of nanopure water and placed at -20°C for one hour to overnight and re-amplified using the same primers and thermocycling conditions listed above. DNA purification of the PCR product was completed following the manufacture's specifications for the Ultra Clean PCR Clean-up DNA Purification Kit (MoBio Laboratories: Carlsbad, CA). The purified product was sequenced using the 341-forward primer by capillary electrophoresis.

Next-Generation Sequencing. Extracted and purified DNA was amplified using universal bacterial primers F63 and R1387 of the 16S rRNA gene to produce a 1.3kb PCR product. The amplicon product was submitted for high-throughput sequencing using Roche® 454 Life Sciences (Branford, CT) instrument, which combined emulsion PCR (emPCR) and pyrosequencing (Ronaghi et al. 1998) in high-density picoliter reactors (Margulies et al. 2005).

The 1.3kb PCR product was reamplified using 454-specific primer adapters A and B and a nested primer pair of F338 and R533. The fusion primers A and B were affixed to the 5-prime

end of each strand. The fusion primers consisted of a 20-mer sequence that included a 4-bp bead-binding tag that facilitated the binding of amplicons to the capture oligonucleotide already annealed to the streptavidin-biotin bead for downstream emPCR and pyrosequencing. The fusion primers also contained an 8-bp bar-code. Barcodes were specific to individual samples and where combined and analyzed together. The barcoded samples allowed specific samples to be segregated from the mixture during data analysis. A 2-bp internal binding set was attached to the 3-prime end of the barcode that was attached to either the 5-prime end of either F338 or R553 universal bacterial primer (Lane 1991). The double-stranded nested PCR products that contained the A and B adapters were subject to traditional PCR amplification to generate millions of DNA target amplicons that included the fusion sequences, bookended on the target amplicon sequence.

The amplified product containing fusion primers A and B were purified and concentrated following standard molecular laboratory techniques. One to five nanograms of purified double-stranded DNA of the amplicon library was immobilized on a streptavidin-biotin bead that contained a capture oligonucleotide. Following the emPCR amplification the isolation and capture of the DNA-positive beads were placed in a PitoTiterPlate™ for sequencing-by synthesis.

Analyses of Molecular Data. Data from Next Generation Sequencing were trimmed and aligned using the pyrosequencing pipeline of the Ribosomal Database Project (RDP) (Cole et al. 2009). Trimmed sequences removed the key tags and fusion primers, while the alignment algorithm positioned the sequence files against *E. coli*. The trimmed and aligned sequences were assigned to the most parsimonious bacterial taxonomy following *Bergey's Taxonomic Outline of the Prokaryotes* (Garrity et al. 2005) using RDP-Classifier (Wang et al. 2007). Sequences were assigned using a Naïve Bayesian classification algorithm and the RDP-recommended 50% bootstrap cut-off for 200 bp length amplicons. At the 50% bootstrap confidence threshold each 200 bp queried sequence produced an overall correct classification of 99.5% at the phylum level (Wang et al 2007). The algorithm assumed independence of all data features (i.e., sequences) and permitted only parent-child relationships (Cheng and Greiner 2001).

RDP was also used to calculate Shannon biodiversity (H'), species evenness, and rarefaction statistics. Evenness is an ecological measure that describes the equality of proportions of taxa distributed in a sample. A value close to 1 indicates an equal distribution of organisms among the represented taxa. The Shannon diversity index is the sum of proportions of individuals

belonging to the *i*-th taxon in a population. High positive H' values are suggestive of high diversity. Rarefaction was used to assess taxon richness. Richness is the total number of unique taxon in a sample. This measure is sensitive to sample size and is also susceptible to populations with high evenness. If taxa are evenly distributed, then the probability of sampling one of any taxon is as likely as sampling any other taxon. Rarefaction curve analysis controls the effects of sample size and evenness by plotting sample abundance by taxon richness, which permits an evaluation of genuine differences in taxon richness. All rarefaction curves were generated at the 0.03% genetic distance cutoff threshold, unless specified otherwise. Rarefaction curves were generated using Microsoft Excel (Redman, WA).

The RDP-classified sequences were imported into Microsoft Excel (Redman, WA) and abundance tables were generated for all tested samples. Sample abundance was plotted using matched rank order abundance curves and relative abundance charts. Unless specified elsewhere, identified phylotypes that contributed > 0.2% of the overall abundance were listed, while those that contributed less were consolidated into a single "other" group.

All bacterial abundance data were imported to PRIMER v6 (Clarke and Gorley 2006), which was used to investigate the statistical effects of decomposition and PMI on soil and bone. This multivariate statistical package applies methods that make few assumptions on data structure and uses nonparametic alternatives for assessing change in bacterial community structure (Clarke 1993). Following the recommended guidelines for statistical analyses on abundance data, the dataset were standardized and log-transformed in order to reduce the influence of highly abundant taxa, and in turn give weight to less abundant or rare taxa. After data transformation, a Bray-Curtis (BC) similarity matrix was created. The BC similarity coefficients were generated on the data using 50 restarts, producing a sample-by-sample matrix, where similarity was determined by a value between 0 and 100. High values indicated more similarity and lower values indicated less similarity.

Analysis of Similarity (ANOISM) on the BC similarity matrix was used only to test the effect of decomposition on *a priori* structured ARF sample groups (Chapter 4). ANOSIM is a nonparametric multivariate corollary to ANOVA (Clarke 1993). All other analyses were performed on unstructured datasets, which permitted genuine groups to form based on patterns in the data. To do so, hierarchical cluster analysis using nearest neighbor linkage on the BC matrix was performed. Significant clusters were identified by similarity profile permutation tests

(SIMPROF), a routine of PRIMER v6. Multi-Dimensional Scaling (MDS) of the BC matrix was used to create nonparametric ordination plots; a method similar to principal components analysis (PCA). The MDS plots maximized the sum of pairwise differences between all possible combinations of samples and placed the samples in two dimensional space. Results of the cluster analysis and SIMPROF were layered on the MDS plot in order to highlight the significant clusters of samples.

Investigations of higher order taxa permitted consistency in phylotype representation across subjects. Observations of complex ecosystems at lower microbial taxa have shown significant intersubject variability of human gastrointestinal track(Eckburg et al 2005) and mouth (Keijser et al. 2008), as well as soils (Roesch et al 2007; Nacke et al. 2011) and deep seas (Venter et al. 2004). Therefore, the investigation into the effects of PMI on bacterial community analyses remained at the highest taxonomic order, as this project represented one of the first applications of next generation sequencing of bacterial communities in gravesoils and human bone.

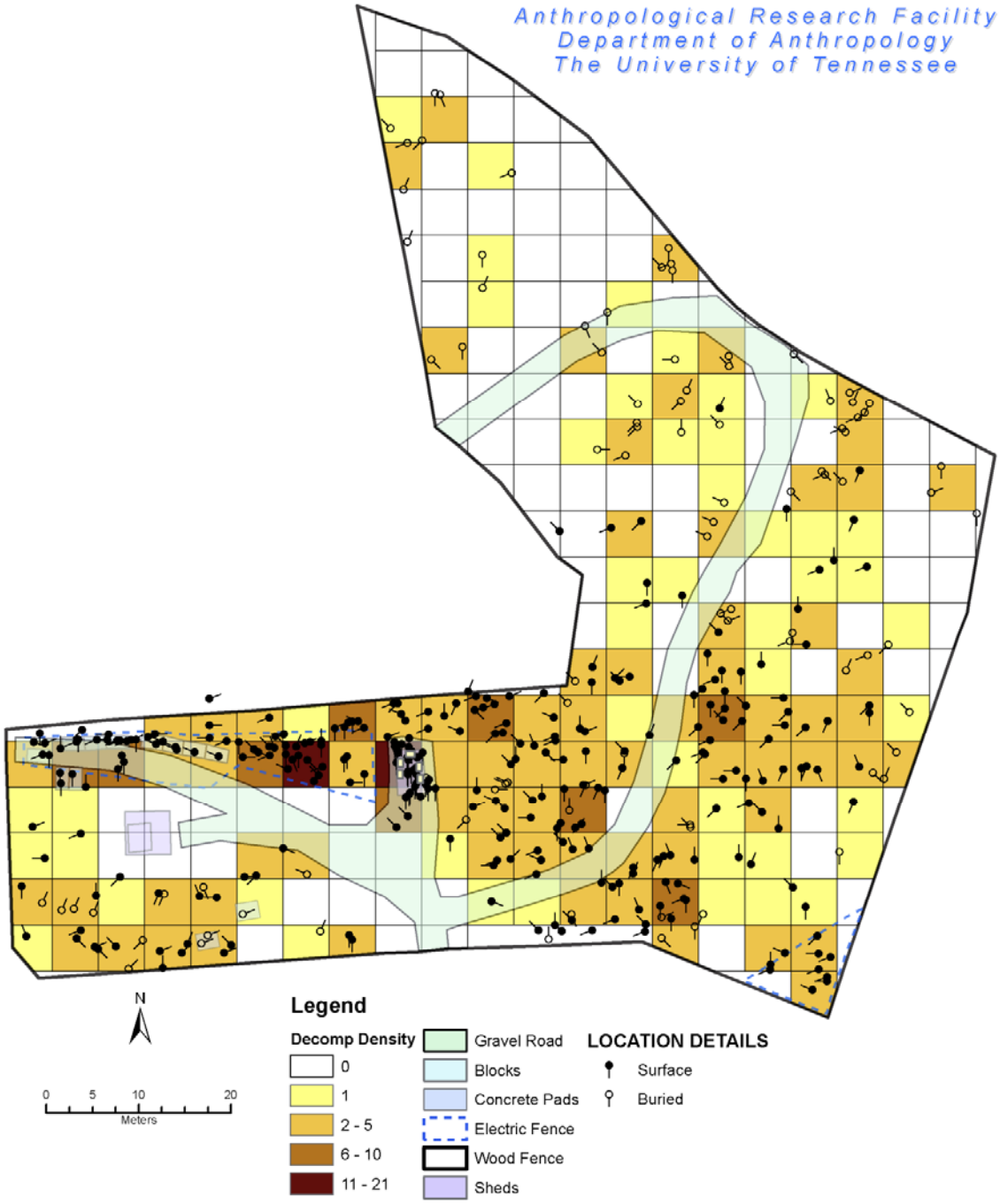

Figure 2-1. Density distribution of decomposing corpses per 5-x-5-meter grid units. Distribution indicates non-random placement of corpses at the ARF (figure from Damann 2010).

Chapter 3 Physicochemical Environment of the ARF Soil Landscape

3.1 Introduction

At the initiation of this project 1,089 bodies decomposed at the University of Tennessee Anthropology Research Facility (ARF). That figure produced a density of 850 corpses per acre. The amount and consistency of human decomposition over a relatively small space presented an opportunity to evaluate the effect of decomposition on basal physicochemical soil properties. If sites with constant decomposition are different from those with no decomposition, then the same would be expected to occur with longer postmortem intervals (PMI). To that end, the ARF was partitioned based on decomposition intensity, and soil samples were collected and evaluated for eight different soil parameters:

- Soil moisture content (SMC)
- Soil organic content (SOM)
- Soil pH (pH)
- Total percent carbon(C)
- Total percent nitrogen (N)
- Carbon to nitrogen ratio (CN)
- Lipid-bound phosphorus (Lipid-P)
- Total extracted DNA (DNA)

3.2 Sample Selection

Soil samples were collected from units within the ARF following a stratified semi-random sampling strategy. The semi-random strategy was chosen since there were few units of high decomposition intensity. Therefore, all units that contained six or more bodies were included in the High study set. Units containing less than five bodies were randomized using the Microsoft Excel ™ (Redman, WA) random number generator. The first ten units from each remaining strata were selected for inclusion. Forty (40) units were selected inside the ARF (Figure 3-1). Soil samples were collected within a two-meter radius of the marked unit centroids. Ten additional samples were used from the non-ARF sample series that were collected outside the facility.

3.3 Analytical Methods

The distribution of raw data values (SMC, pH, SOM, C, N, CN, Lipid-P, and DNA) by sample group (None, Low, Middle, High, and non-ARF) were visualized with box and whisker plots, outliers were identified and removed, and the data were reassessed for normality. The data were standardized by log transformation. Significant deviations from the null hypothesis of no difference were determined by one-way Analysis of Variance (ANOVA) and Tukey's post-hoc test for pairwise differences was performed. Principal Components Analysis (PCA) on ANOVA determined significant variables was performed. The first and second principal component scores (PC1 and PC2) were factored by decomposition group and evaluated by ANOVA. The PC1 and PC2 scores were plotted against each other.

3.4 Results and Discussion

The distribution of log-transformed data for the eight soil parameters factored by decomposition sample group was visualized with box and whisker plots (Figure 3-2). The ANOVA model was significant ($p \leq 0.05$), and identified the variables SMC, SOM, pH, N, CN, and Lipid-P as significant (Table 3-1). Post-hoc Tukey's test indicated significant differences ($p \leq 0.05$) between the sample group taken outside the facility and all sample groups inside in pH, SMC, and SOM.

A PCA on Euclidean distances for the six significant variables extracted two component scores. The PC1 and PC2 values accounted for 79% of the total variation in the sample distribution. PC1 contributed 54% and PC2 contributed 25% (Figure 3-3). One-way ANOVA of the PC1 and PC2 scores were statistically significant ($p < 0.001$). The samples from outside the facility clustered, while all other samples were much more dispersed. Additionally, samples from the High group were loosely clustered relative to the location of samples composing the None, Low, and Middle groups.

Within the ARF, the elevated levels of nitrogen, Lipid-P, and water were consistent with an influx of high-quality nutrients into the ARF soil, which was further supported by a lower CN ratio in the High sample group when compared to the non-ARF samples. These findings were consistent with other work (Carter et al. 2007; McGuire and Treseder 2010; Swift 1979) that discussed increased biological activity surrounding the decay of nutrient-rich resources.

3.5 Conclusions

Recorded soil properties identified significant differences among sample groups inside the facility to the samples collected outside the facility, while few differences among the sampled areas within the ARF were supported by the data. A PCA of the soil data supported this finding by separating only the non-ARF samples from the wider distribution of ARF samples. These findings suggested homogeneity of physicochemical parameters across the ARF soil landscape, while also maintaining separation from the non-decomposition soil outside the facility. Higher nitrogen, moisture, and Lipid-bound phosphorus and lowered CN values in an area specifically designed for human decomposition, may have defined a signature of human decomposition in the terrestrial landscape. This interpretation based solely on the recorded physicochemical parameters was taken with caution however, since there were no observed differences among the stratified sample groups inside the ARF. Despite similarity in parent material, the basal soil properties outside the facility may in fact have been different, regardless of decomposition. At the same time, the sampling strategy of general landscape soils may have missed the specific effects of decomposition on the landscape (Benninger et al. 2008; Carter et al 2007).

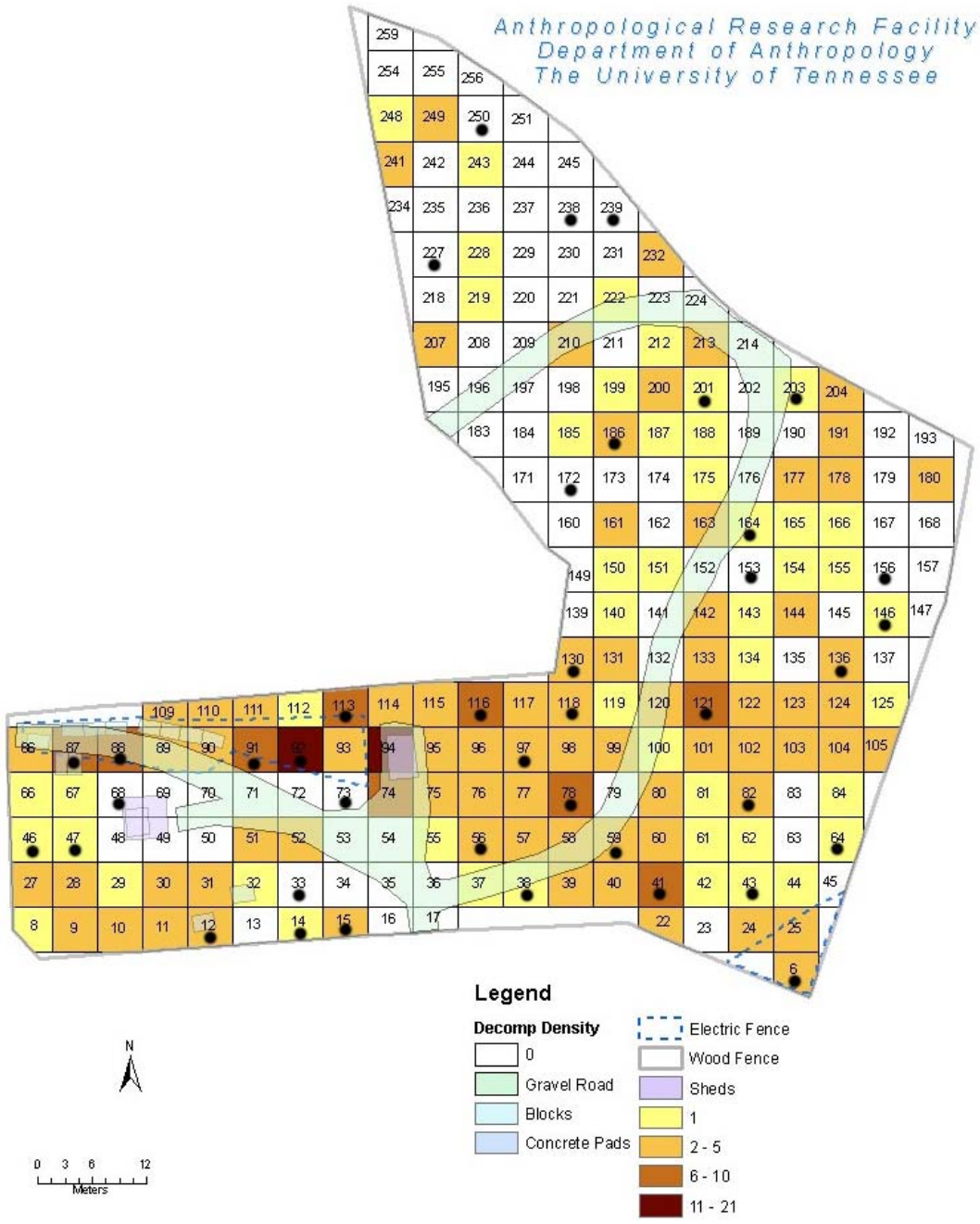

Figure 3-1. Sampled units are marked with a black dot (figure from Damann 2010).

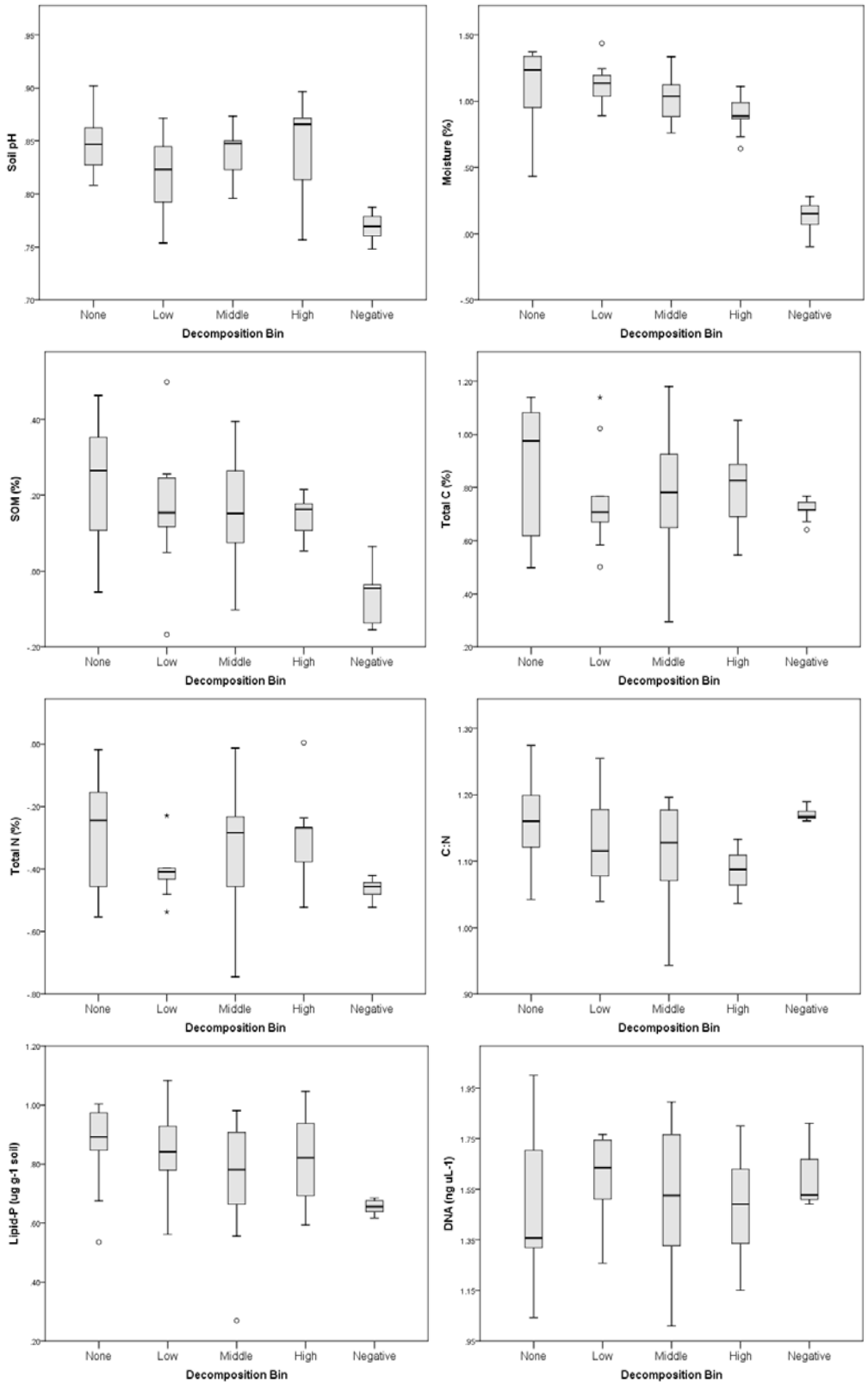

Figure 3-2. Box and whisker plots of the eight soil parameters recorded at the ARF. From top to bottom and left to right the plots are soil pH, moisture, and organic content, total carbon, total nitrogen, carbon-nitrogen ratio, lipid-P, and DNA (figure from Damann et al. 2012).

Table 3-1. One-way ANOVA on ARF sample groups. Asterisk denotes a significant model ($p \leq 0.05$) (table from Damann et al. 2012).

Variables		Sum of Squares	df	Mean Square	F	Sig.
SOM	Between Groups	.477	4	.119	6.161	.001*
	Within Groups	.832	43	.019		
	Total	1.308	47			
Moisture	Between Groups	6.839	4	1.710	45.439	.000*
	Within Groups	1.693	45	.038		
	Total	8.532	49			
pH	Between Groups	.040	4	.010	10.079	.000*
	Within Groups	.043	44	.001		
	Total	.083	48			
N	Between Groups	.235	4	.059	2.771	.039*
	Within Groups	.934	44	.021		
	Total	1.169	48			
CN	Between Groups	.039	4	.010	2.807	.037*
	Within Groups	.151	43	.004		
	Total	.191	47			
Lipid-P	Between Groups	.278	4	.069	3.029	.027*
	Within Groups	1.032	45	.023		
	Total	1.309	49			
C	Between Groups	.149	4	.037	1.003	.416
	Within Groups	1.672	45	.037		
	Total	1.821	49			
DNA	Between Groups	.130	4	.032	.531	.714
	Within Groups	2.261	37	.061		
	Total	2.391	41			

SOM, soil organic matter
moisture, soil moisture content
pH, soil pH
C, total carbon content
N, total nitrogen content
CN, carbon / nitrogen ratio
Lipid-P, lipid-bound phosphorus
DNA, total extracted DNA.

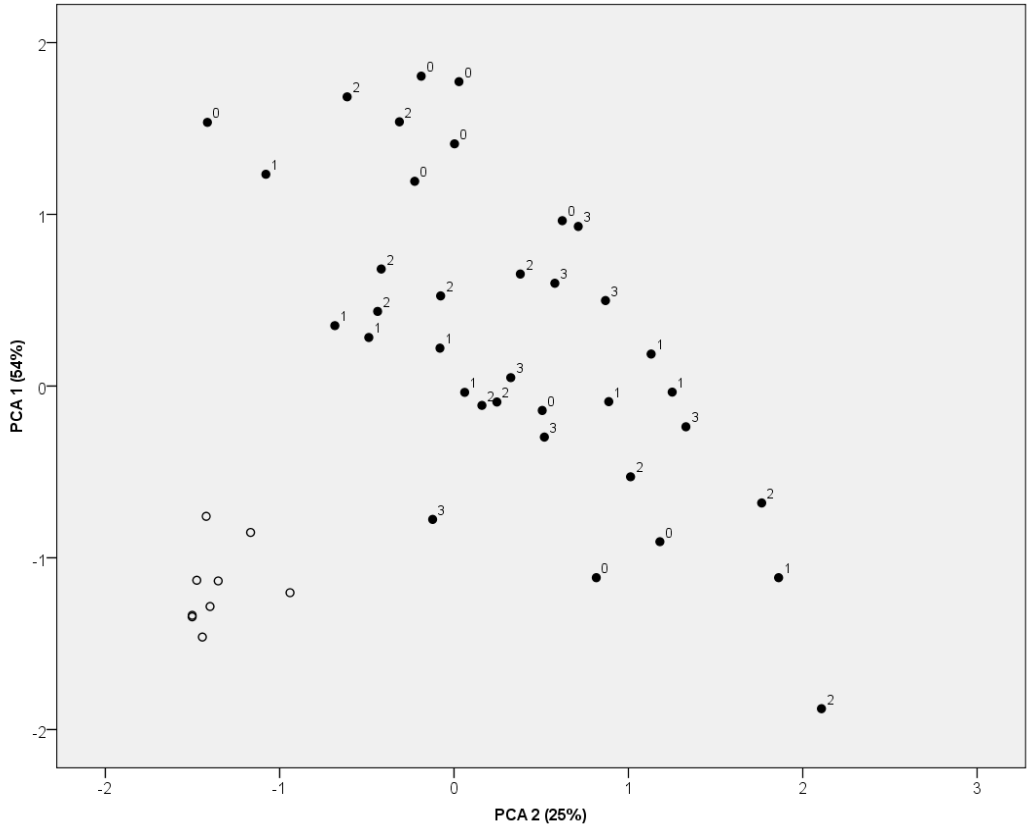

Figure 3-3. PCA plot of ARF landscape samples. Samples are labeled by decomposition group (None = 0, Low =1, Middle=2, and High=3). PC1 and PC2 accounted for 79% of the observed variation among the variables tested, which include soil moisture content, soil organic matter, soil pH, total N, CN ratio, and Lipid-P. Facility soils (filled circles) are clearly separated from the negative control group collected outside the facility (empty circles) (figure from Damann et al. 2012).

Chapter 4 Bacterial Communities of the ARF Soil Landscape

4.1 Introduction

Microbes and bacteria in particular are highly sensitive to changes in the environment (Borneman and Triplett 1997). Slight variations observed in soil physicochemical parameters among the sample groups inside the facility may precipitate significant differences in bacterial communities that were not observed in the analyses of physicochemical parameters among the University of Tennessee Anthropology Research Facility (ARF) sample groups presented in Chapter 3. Therefore, the ARF landscape soil samples partitioned by decomposition intensity were evaluated for differences in bacterial community structure.

4.2 Sample Selection

Bacterial community structure of the ARF landscape was evaluated from forty soil samples taken inside the ARF. The 40 samples corresponded to the same ARF landscape samples that were evaluated for physicochemical differences among the four decomposition groups. Since no differences were observed between any of the sample groups inside the facility, the None group samples were set as the comparative sample. The soil samples outside the facility were not evaluated in this series of laboratory tests presented here.

4.3 Analytical Methods

An initial set of 15 soil samples were analyzed via Denaturing Gradient Gel Electrophoresis (DGGE). Unfortunately, results of the DGGE analysis were of limited value since excised and sequenced bands produced mixtures of organisms. Therefore, subsequent analyses occurred using next-generation sequencing (NGS) with the Roche 454 FLX sequencer. Quality-checked sequences from NGS were trimmed, aligned, and classified as described previously (see Chapter 2, Molecular Methods).

Univariate biodiversity statistics of the trimmed and aligned sequences using the Ribosomal Database Project (RDP) pyrosequencing pipeline generated rarefaction curves, Shannon diversity (H'), and species evenness statistics. These diversity measures reduced a complicated biological sample matrix into single mathematical values; thereby enabling comparison with standard parametric means testing, such as one-way Analysis of Variance (ANOVA). Rarefaction was assessed graphically at the 3% genetic distance cutoff by plotting the upper and lower 95% confidence intervals.

A similarity matrix on bacterial taxonomy by sample was created with the classified sequences. The samples (soil units) in this matrix were factored by decomposition group and analyzed using Microsoft Excel (Redland, WA) and PRIMER v6 (Clarke and Gorley 2006). Frequency distributions of RDP classified bacterial phylotypes were used to generate matched rank-ordered abundance curves, which were used as a quick visual assessment for the level of congruence among the sample groups. The None sample group was set as the reference plot for comparison to the other three groups (Low, Middle, and High).

Due to the high frequency of zeros in a biological matrix nonparametric analyses were applied using PRIMER v6. Group differences in classified sequences were assessed by Analysis of Similarity (ANOISM) on the Bray-Curtis (BC) generated distance matrix of sampled units. The BC matrix was computed on standardized and log-transformed sample abundance data. Multi-Dimensional Scaling (MDS) of the BC distance matrix was used to create ordination plots. The MDS plots maximized the sum of pairwise differences between all possible combinations of samples and placed them in two-dimensional space. Hierarchical cluster analysis (CLUSTER) was performed in on the BC matrix. Significant clusters were identified by Similarity Profile Permutation tests (SIMPROF). Cluster and SIMPROF results were layered on the MDS plots in order to visualize the significantly different clusters at varying levels of similarity.

4.4 Results and Discussion

Denaturing Gradient Gel Electrophoresis (DGGE). Initial screening of 15 soil samples produced results for 47% of the 67 identified bands. A small set of bacterial and fungal sequences of low diversity and abundance for the number of samples evaluated were provided (Table 4-1). The presence of many sulfur reducing chemoorganotrophic bacteria such as *Thiocapsa sp.* and *Desulfobacterium sp*. was observed. They are characterized as free-living phototrophic purple sulfur bacteria and anaerobic fermenters of pyruvate, respectively. The purple sulfur bacteria use H_2S as their reducing agent and produce elemental sulfur through oxidation of H_2S, a product of human decomposition (Vass et al. 1992). All subsequent DGGE profiles produced gels with many indistinct bands, which demonstrated a lack of separation. Due to the lack of resolution obtained from DGGE, NGS was used to provide a more detailed picture of overall bacterial diversity than that provided by DGGE.

Next Generation Sequencing (NGS). High-throughput sequencing produced 3.65 MB of raw sequence data for the amplified V3 region of the 16S rRNA gene. After trimming and aligning the raw sequences, a total of 6,410 bacterial sequences at 200 bp in length were identified.

The matched rank order abundance curves demonstrated overall similarity among the the 14 identified bacterial phyla across the four decomposition groups (i.e., None, Low, Middle, High) (Figure 4-1). The five most abundant phyla each contributed greater than 0.8% of the total classified sequences and accounted for 90% of all classified bacterial phyla (Figure 4-2). The "other" phyla (2%) and the unclassified group (8%) constituted the residual. Similar plots were generated for the 43 unique bacterial orders identified (Figure 4-3). There were 16 bacterial orders that contributed greater than 0.8% of the total observations. These 16 bacterial orders accounted for 82% of all classified sequences at this taxonomic level (Figure 4-4). The unclassified sequences (11%) and those listed as "other" (7%) constituted the residual. All samples regardless of decomposition group appeared to be dominated by Proteobacteria, Actinobacteria, Acidobacteria, Bacteroidetes, and Gemmatimonadetes. From these major phyla, common bacterial orders were also observed, which included common soil dwelling organisms of Actinomycetales and Rhizobiales. Based on visual inspection of the bacterial rank order curves some taxa (i.e., Burkholderiales and Desulfarculales) increased in rank with increasing human decomposition activity.

Rarefaction curve analysis was employed at the 97% similarity level (i.e., 3% genetic distance cutoff threshold) in order to measure how phylotype richness in the four sample groups varied with sample size. For each sample group the upper and lower 95% confidence levels were plotted (Figure 4-5). Richness values where similar to each other and each 95% confidence ellipse was congruent with all others, indicating no difference between any two groups or among the total. Shannon diversity and species evenness were negatively associated, indicating that as diversity increased, species evenness decreased. For example at the 3% distance cutoff the None group had the lowest diversity value (5.25) and the highest evenness score (0.95) among the four groups (Figures 4-6 and 4-7). An ANOVA of each univariate measures demonstrated overall agreement in community profile when the dataset was factored by decomposition group. The only significant difference observed between any two sample groups based on Tukey's post-hoc test occurred with the evenness scores for the groups of None and Middle ($p = 0.044$). Each additional measure failed to exclude the null hypothesis ($p > 0.05$).

Visual inspection of the MDS plot suggested partial separation among samples (Figure 4-8). A nonparametric multivariate analysis of the BC similarity matrix using ANOSIM on the four sample groups identified significant differences in bacterial community composition between the High sample group and the groups of None and Low. All other pairwise comparisons failed to exclude the null hypothesis (Table 4-2; Figure 4-9).

Given the significant difference identified between the High and None samples, a full library comparison of the DNA sequences using the RDP Library Comparison routine identified additional significant differences for specific taxa. The RDP Library Comparison algorithm estimated the likelihood that the frequency of membership in a given taxon was the same for the two libraries. The test is based on the assumption that the number of sequences assigned to any one taxon is less than 5% of the number of sequences (Audic and Claverie 1997). For larger frequencies, the standard two population proportions test assumes an approximate standard normal distribution, and the p-value is estimated from the z distribution (Cole et al. 2009).

The High sample group was characterized by elevated levels of (1) Actinomycetales ($p = 0.0002$), (2) Burkholderiales ($p = 0.0017$), and (3) Bacteroidetes ($p < 0.0000$) and the bacterial order Sphingobacteriales ($p = 0.0017$), while having (4) a reduced concentration of Acidobacteria ($p = 0.0128$) when compared to the None sample group. When layered on the MDS plot, the bacterial order Acidomicrbiales dominated the areas with no decomposition, whereas Burkholderials and Sphingobacteriales were more prevalent in areas with increased concentration of human decomposition (Figure 4-10).

4.5 Conclusions

Differences in the microbial community structure between sample groups inside the ARF were significant. Rarefaction analysis indicated that the differences among groups were not due to differences in sample abundance since all groups followed the same trajectory. Similarly, univariate measures demonstrated consistent trends among the four groups across all distance thresholds. However, bacterial community composition in areas with increased decomposition was statistically different from the areas with little to no decomposition. The separation of samples in two-dimensional space resulted from the presence of significantly different bacterial communities. Taken in sum, the slight variations observed in soil physicochemical parameters among the sample groups inside the facility precipitated significant differences between sample

groups based on bacterial community profiles. Given these findings, it may be possible to identify similar characteristics in gravesoils and bone with advancing PMI.

Table 4-1. Identified organisms from amplificaion of the 16S and 28S rDNA gene by DGGE (table from Damann 2010).

Band	Similar Genus	Similarity Index	Donors	Acceptors	Description
1.1	*Desulfitobacterium spp.*	0.76	H+	Sulfate, sulfite	Anaerobic
1.2	*Thiocapsa spp.*	0.85	H_2, H_2S	Sulfur compounds	Free-living anaerobic phototrophic purple sulfur bacteria, chemoorganotroph, on acetate, phototrophic
2.1	*Desulfitobacterium spp.*	0.74			Anaerobic
2.3	*Thiocapsa spp.*	0.90	H_2, H_2S	Sulfur compounds	Free-living anaerobic phototrophic purple sulfur bacteria, chemoorganotroph, on acetate, phototrophic
2.4	*Thiocapsa spp.*	0.88	H_2, H_2S	Sulfur compounds	Free-living anaerobic phototrophic purple sulfur bacteria, chemoorganotroph, on acetate, phototrophic
2.5	*Desulfobacterium spp.*	0.92	Short chain acids	SO_4-, S_2O_3-	Desulfobacterium autotrophicum ferments pyruvate
3.3	*Thiocapsa spp.*	0.88	H_2, H_2S	Sulfur compounds	Free-living anaerobic phototrophic purple sulfur bacteria, chemoorganotroph, on acetate, phototrophic
3.4	*Desulfobulbus spp.*	0.93	H2, sulfide, acetate	SO_4-	Desulfobulbus: sulfate-reducing
4.2	*Thiocapsa spp.*	0.86	H_2, H_2S	Sulfur compounds	Free-living anaerobic phototrophic purple sulfur bacteria, chemoorganotroph, on acetate, phototrophic
4.3	uncultured bacterium	1.00			
4.4	*Thiocapsa spp.*	0.84	H_2, H_2S	Sulfur compounds	Free-living anaerobic phototrophic purple sulfur bacteria, chemoorganotroph, on acetate, phototroph
5.1F	*Nectria spp*	0.95			
5.2F	*Penicillium spp.*	0.77			
5.5	*Desulfobacterium spp.*	0.93	Short chain acids	SO_4-, S_2O_3-	Desulfobacterium autotrophicum ferments pyruvate
6.3F	*Penicillium spp.*	0.94			
7.1F	*Helvella spp.*	0.83			

Table 4-1. Continued.

Band	Similar Genus	Similarity Index	Donors	Acceptors	Description
7.4	*Thiocapsa spp.*	0.89	H_2, H_2S	Sulfur compounds	Free-living anaerobic phototrophic purple sulfur bacteria, chemoorganotroph, on acetate, phototrophic
8.1F	uncultured soil fungi	0.79			
8.4	*Thiocapsa spp.*	0.89	H_2, H_2S	Sulfur compounds	Free-living anaerobic phototrophic purple sulfur bacteria, chemoorganotroph, on acetate, phototrophic
9.4	*Thiocapsa spp.*	0.89	H_2, H_2S	Sulfur compounds	Free-living anaerobic phototrophic purple sulfur bacteria, chemoorganotroph, on acetate, phototrophic
10.3F	uncultured soil fungi	0.86			
10.4F	*uncultured Zygomycete*	0.63			
11.1F	*Aspergillus*	0.97			
11.3	*Desulfitobacterium spp.*	0.93			
13.1F	*uncultured soil fungi*	0.88			
14.2F	*Helvella spp.*	0.98			
15.1F	*Thiocapsa spp.*	0.85	H_2, H_2S	Sulfur compounds	Free-living anaerobic phototrophic purple sulfur bacteria, chemoorganotroph, on acetate, phototrophic
16.1F	*Helvella spp.*	0.96			
16.4	*Desulfobacterium spp.*	0.75	Short chain acids	SO_4-, S_2O_3-	Desulfobacterium autotrophicum ferments pyruvate.
16.5	*Thiocapsa spp.*	0.85	H_2, H_2S	Sulfur compounds	Free-living anaerobic phototrophic purple sulfur bacteria, chemoorganotroph, on acetate, phototrophic
17.2	*Desulfobacterium spp.*	0.75	Short chain acids	SO_4-, S_2O_3-	Desulfobacterium autotrophicum ferments pyruvate
17.3	*Thiocapsa spp.*	0.85	H_2, H_2S	Sulfur compounds	Free-living anaerobic phototrophic purple sulfur bacteria, chemoorganotroph, on acetate, phototrophic

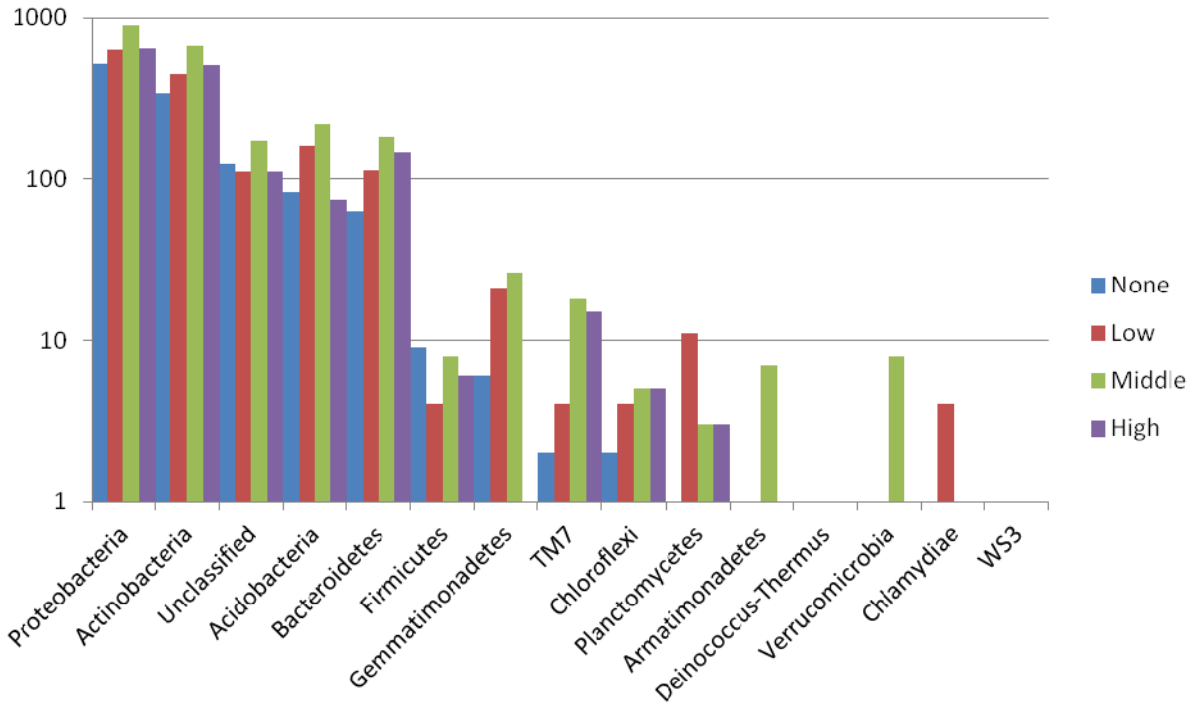

Figure 4-1. Matched rank order abundance plot of the 14 unique bacterial phyla. Samples are ranked based on the distribution of the None samples.

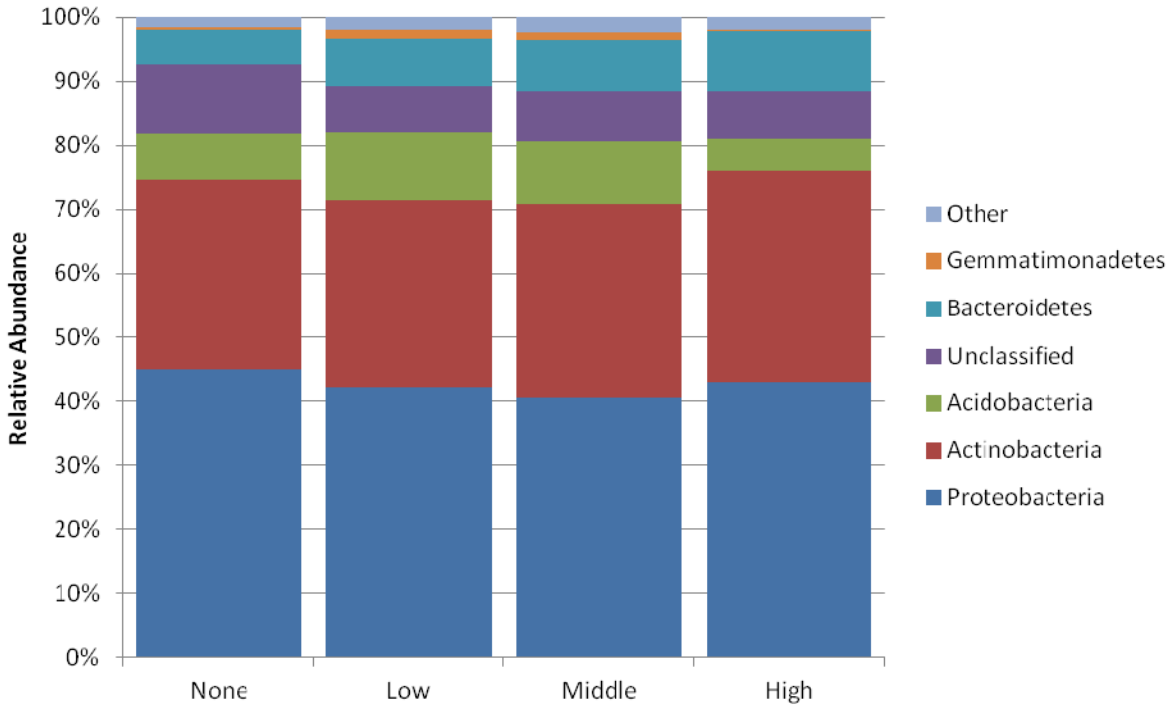

Figure 4-2. Distribution of the most abundant bacterial phyla across the four sample groups. Unclassified sequences are listed as such, and phyla accounting for < 0.8% of all classified sequences are included in the artificial group "others".

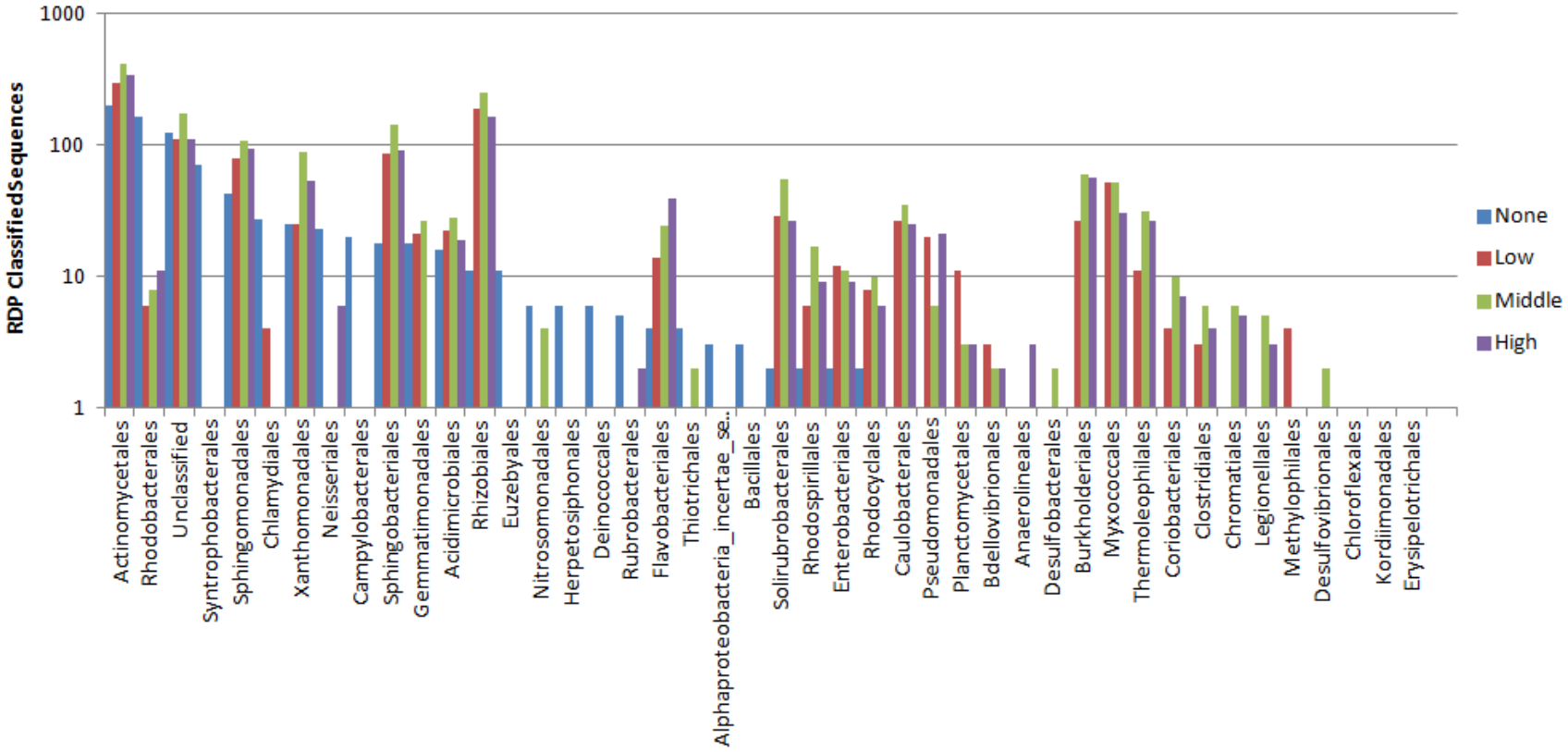

Figure 4-3. Matched rank order abundance plot of the 43 unique bacterial orders. Samples are ranked based on the frequency distribution of the None samples.

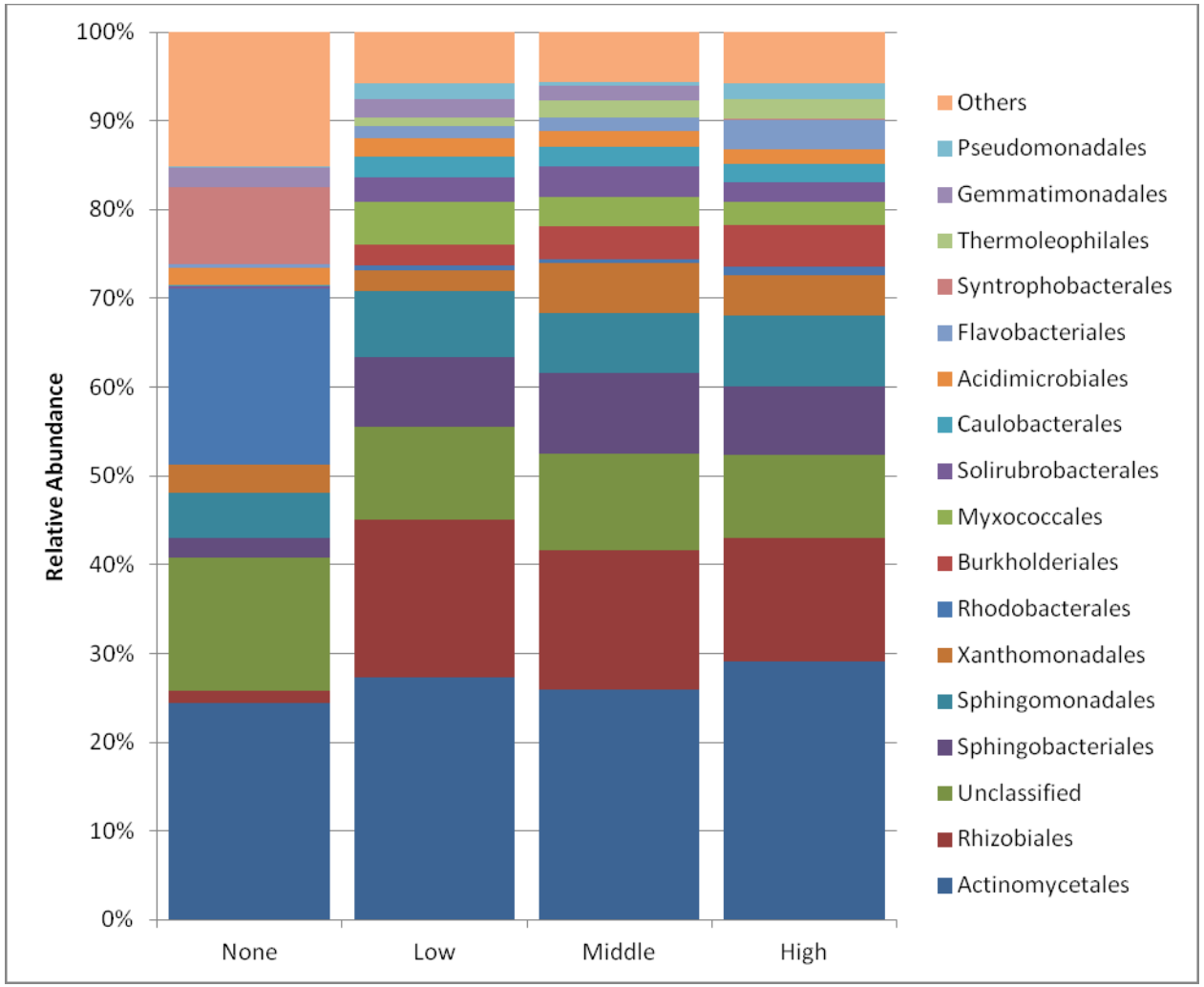

Figure 4-4. Distribution of the 17 most abundant bacterial orders across the four sample groups. Unclassified sequences are listed as such, and phyla accounting for < 0.8% of all classified sequences are included in the artificial group "others".

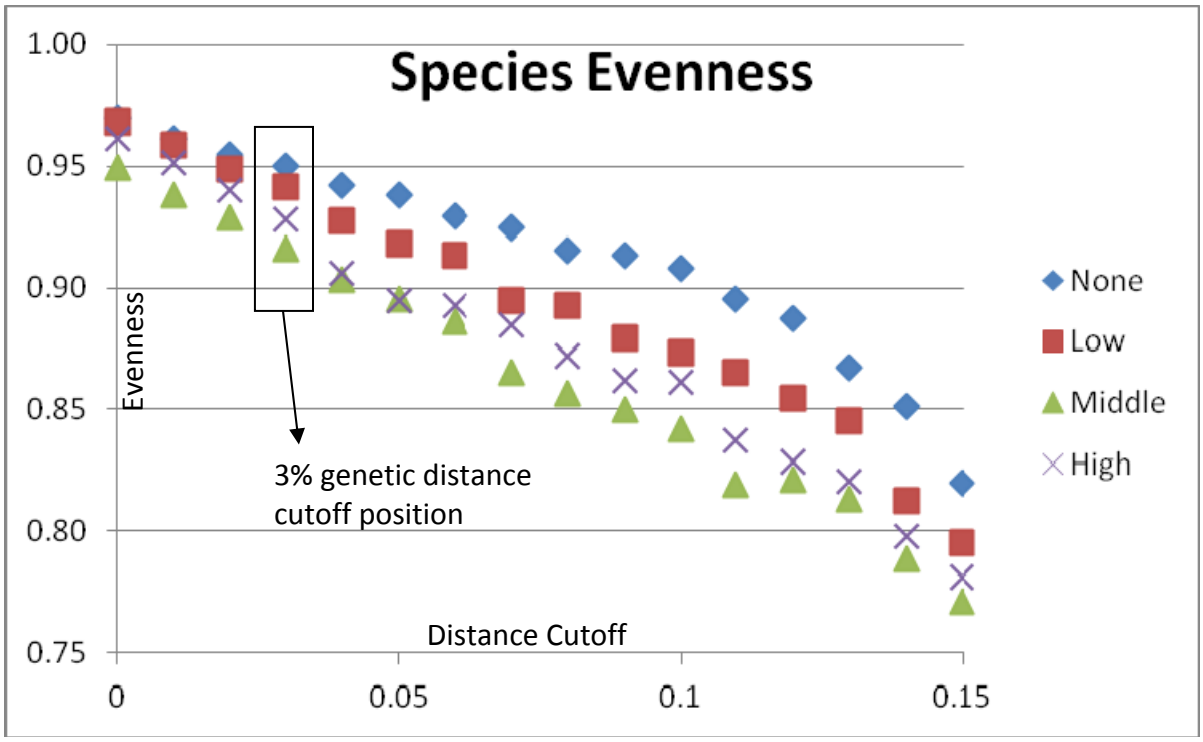

Figure 4-5. Evenness scores across various distance cutoff thresholds.

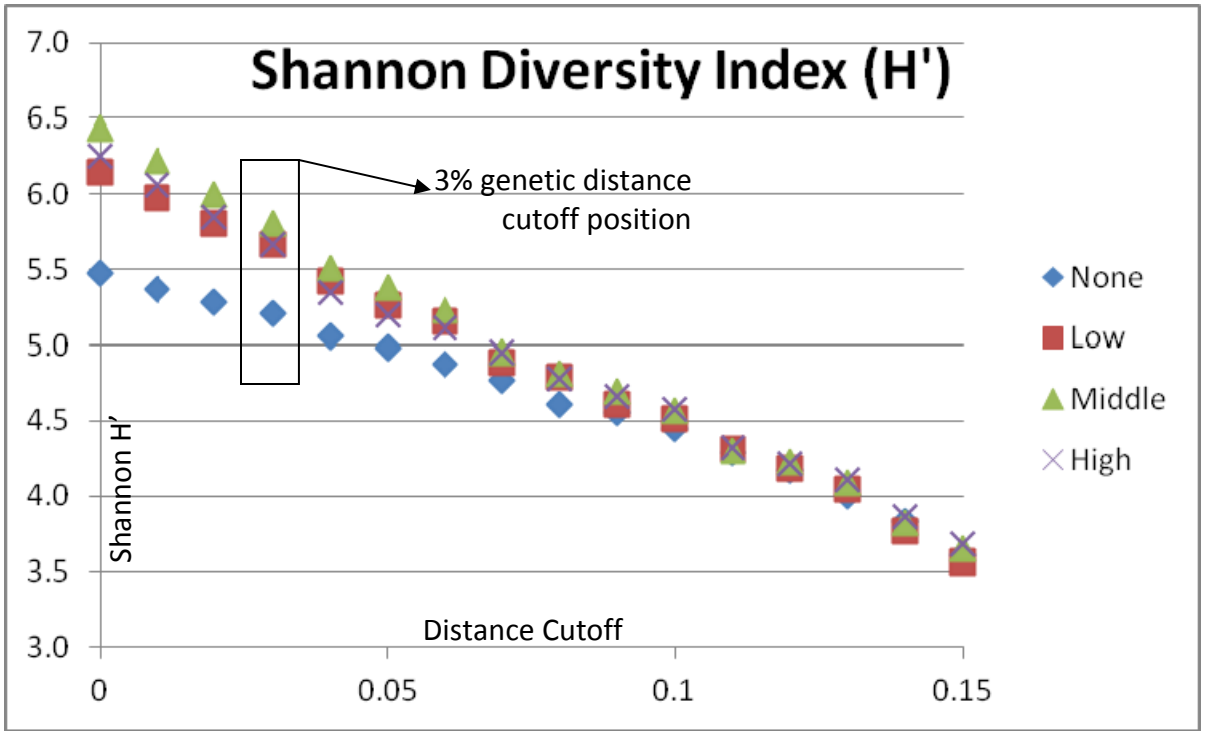

Figure 4-6. Shannon diversity estimators across various distance cutoff thresholds.

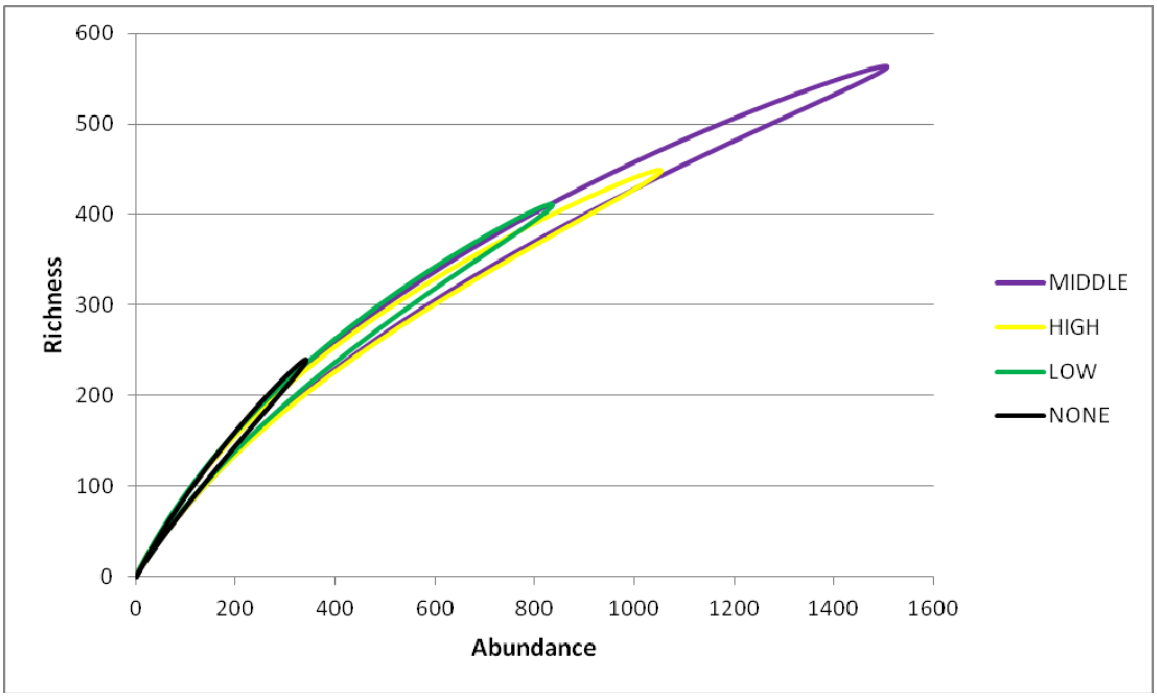

Figure 4-7. Rarefaction curves displaying taxon richness by sample abundance. Samples plotted at a genetic distance of 3%. Elipses are the upper and lower 95% confidence interval. This graph indicates no differences in taxon richness despite differences in abundance.

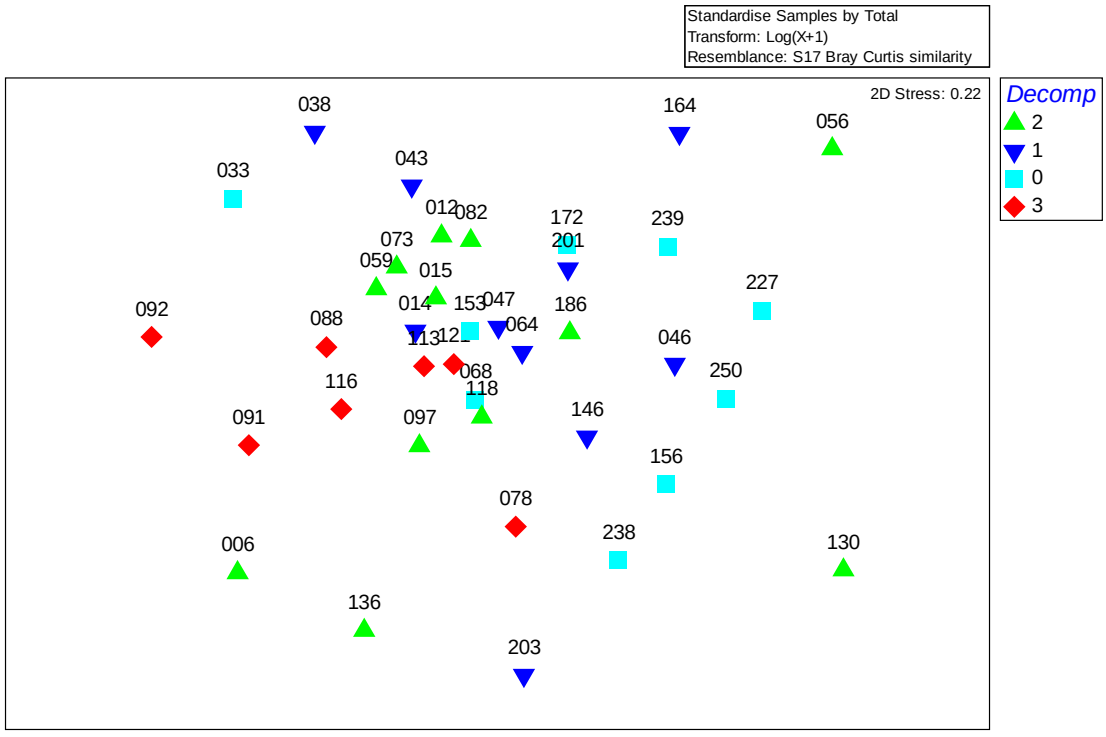

Figure 4-8. MDS plot of BC similarity matrix for the four sample groups inside the ARF. The four groups are differentiated by number and color (0=None, 1=Low, 2=Middle, 3= High) (figure from Damann 2010).

Table 4-2. ANOSIM for four sample groups (table from Damann 2010).

Global Test

Sample statistic (Global R): 0.04

Significance level of sample statistic: 0.186

Number of permutations: 999 (Random sample from a large number)

Number of permuted statistics greater than or equal to Global R: 185

Pairwise Tests

Group	R-statistic	Sig. Level (α=.05)	Possible Permutations	Actual Permutations	No. ≥ Obs.
0, 1	0.047	0.210	92378	999	209
0, 2	0.039	0.231	293930	999	230
0, 3	**0.36**	**0.001**	**11440**	**999**	**0**
1, 2	-0.09	0.983	646646	999	982
1, 3	**0.159**	**0.048**	**19448**	**999**	**47**
2, 3	-0.061	0.722	50388	999	721

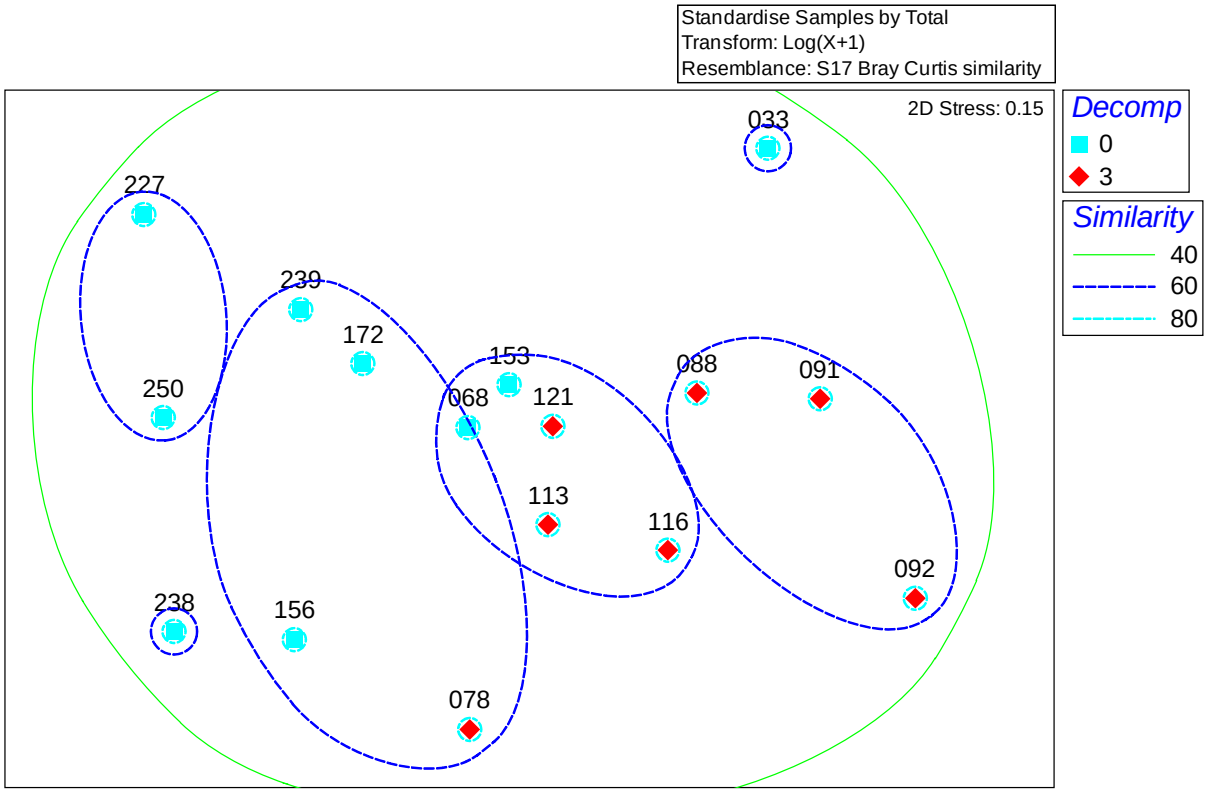

Figure 4-9. MDS of the BC similarity matrix for sample groups None and High (figure from Damann 2010).

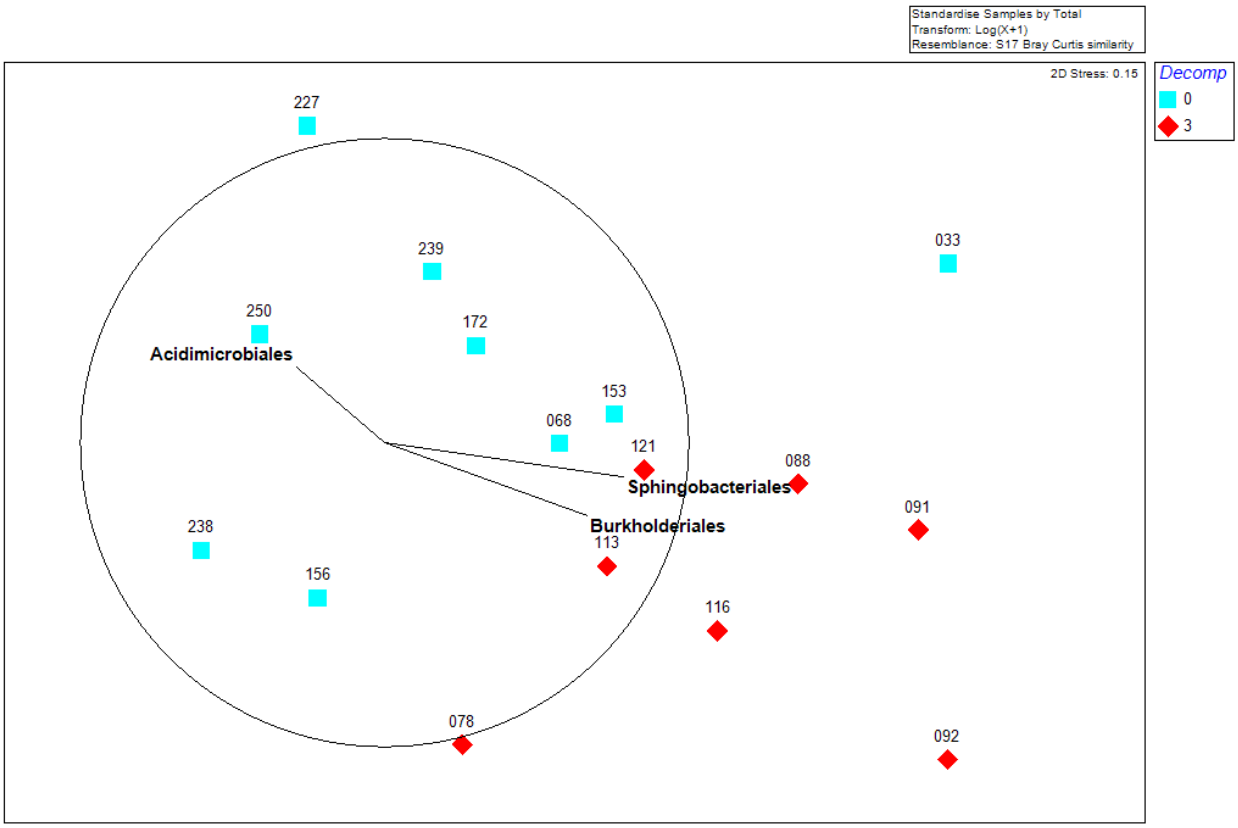

Figure 4-10. MDS of the BC similarity matrix for sample groups None and High. Significantly different bacterial orders that forced the separation between the two decomposition sample groups are layered. Red diamonds identify the High group.

Chapter 5 An Investigation into the Relationship of Postmortem Interval and the Physicochemical Parameters of Gravesoils

5.1 Introduction

The previous tests identified significant difference in certain physicochemical soil parameters between the samples taken outside the facility and the sample groups inside the facility, while virtually no significant differences existed among the sample groups within the University of Tennessee Anthropology Research Facility (ARF) (Chapter 3). This observation suggested a possible effect of human decomposition on the ARF landscape since all groups inside are different from those taken outside. This interpretation based solely on the recorded physicochemical parameters was taken with caution, since there were no observed differences among the stratified sample groups inside the ARF and the basal soil properties outside the facility may in fact have been different, regardless of decomposition. At the same time, the sampling strategy of general landscape soils may have missed the specific areas of the ephemeral and isolated islands of decomposition (Carter et al 2007). The lack of difference of physicochemical parameters for the general landscape soil samples inside the ARF precipitated further investigation into gravesoil collected from directly below decomposing corpses. In order to further explore the relationship of physicochemical soil parameters and postmortem interval (PMI), the same soil parameters were investigated from delineated decomposition sites with known PMI.

5.2 Sample Selection

Gravesoil samples were collected below 14 cadavers that varied from 1-48 months postmortem (Table 5-1). These samples were different from the landscape soil samples previously evaluated (Chapter 3 and 4), since these gravesoil samples were directly below actively decomposing corpse.

5.3 Analytical Methods

The analytical methods used in this assay to determine the physicochemical parameters of soil were identical to those reported in Chapter 2 General Field and Laboratory Methods of this report. The physicochemical data for the 14 soil samples collected below actively decomposing bodies were log-transformed and compared to those outside the facility (n = 10). An analysis of variance (ANOVA) on the eight test variables, factored by sample group was performed. The two groups included actively decomposing corpse soils and the non-ARF soils. The significant

variables were analyzed further by principal components analysis (PCA) on Euclidian distances, and the first two extracted principal component (PC) scores were plotted. A second ANOVA was applied to the two extracted components to test for significance. In order to assess the effect of PMI on the unstructured sample distribution, the principal component scores were tested using the PRIMER v6 cluster analysis and the similarity profile permutation test (SIMPROF). Cluster analysis of raw values was computed on group means. This analysis would identify any significant clusters within the *a priori* unstructured data set. The samples were plotted in two-dimensional space and overlaid with the results of cluster analysis in order to visualize relationships among samples based on similarity. Significance was assessed at $p \leq 0.05$.

5.4 Results and Discussion

Comparison of gravesoil from actively decomposing bodies to non-ARF soil via one-way ANOVA indicated seven significant variables ($p < 0.05$). Soil pH was the only variable that failed to exclude the null hypothesis of no difference ($p = 0.257$). The first two components of the PCA on the remaining seven variables accounted for 83% of the observed variation. Nitrogen (0.92), SOM (0.91), Lipid-P (0.88), and Carbon (0.85) were highly correlated with the first component axis (59.6%), whereas CN (0.96) had the greatest correlation with the second component axis (23.4%). The four variables that correlated with the first PC score were plotted and the values suggested an inverse relationship with time since death (Figure 5-1).

The two extracted component scores were plotted and labeled by months since death (Figure 5-2). The ANOVA model indicated significance ($p < 0.05$) for the first ($F = 29.2$, $df = 4$) and second ($F = 9.9$, $df = 4$) extracted component scores. Inspection of the scatter plot suggested a pattern where the soil samples with longer PMIs were more similar to those soil samples of shorter PMIs. Samples of early (one month postmortem) and late-stage decomposition (47 and 48 months postmortem), and the non-ARF samples had similar PC2 values, and differed from the mid-range decomposition sites. The majority of sample separation for the early, late, and non-ARF samples occurred along the first PC axis.

The effect of PMI was demonstrated through hierarchical cluster analysis of unstructured PC scores, which indicated three significant clusters of samples ($p < 0.05$). These data were plotted using the graphing function in PRIMER v6 and the significant clusters were layered, demonstrating the relationships among samples that coincided with PMI (Figure 5-3). Significant clustering of samples based on distance from group means were identified as samples

with a PMI of (a) one month, (b) 1-12 months, (c) 12-47 months, and (d) 48 months and normal, non-ARF soils.

5.4 Conclusions

Physicochemical parameters of gravesoils below actively decomposing corpses demonstrated a pattern related to the postmortem interval that may prove beneficial for estimating postmortem interval. Total nitrogen, soil organic matter, lipid-bound phosphorus, and total carbon content of the gravesoils created the greatest separation among the data points (i.e., the highest correlation) along the first PC score. As the PMI increased the values of the recorded physicochemical soil parameters decreased. The clustering of samples used in this assay, either pre-structured (ANOVA) or unstructured (SIMPROF) demonstrated significant time dependent effects ($p<0.05$). Significant clustering of the PC scores on group means were identified as (a) one month, (b) 2-12 months, (c) 12-47 months, and (d) 48 months and normal, non-ARF soils. This time-dependent pattern may prove applicable for estimating times since death. That stated, additional cross-sectional and longitudinal sampling and testing the physicochemical parameters of human gravesoils is necessary before becoming a viable and routine forensic method for refining PMI estimations.

Table 5-1. PMI and cadaver data for investigating the relationship between PMI and the physicochemical parameters of gravesoil.

PMI[1]	Age	Sex	Race	Weight	Body Description
1.1	43	M	W	225	skeletonized, maggots present, advanced
1.2	68	M	W	180	partially skeletonized, gooey, liquefied, maggots and beetles, covered with tarp, active
2	88	M	W	175	partially skeletonized, gooey, maggots still active, covered with tarp, active
7	53	M	W	n.d.	partially skeletonized, gooey, no maggots, active
9	50	F	W	185	partially skeletonized, gooey, pupal casings, covered with tarp, advanced
11	26	M	W	115	skeletonized
12.1	55	M	W	340	partially skeletonized, gooey, no maggots (pupal casings), covered with tarp, advanced
12.2	71	M	W	190	skeletonized, almost no soft tissue, semi covered with tarp
12.3	47	M	B	250	skeletonized, adipocere, semi-covered with tarp
18	70	M	B	200	half skeletonized, half mummified, uncovered
20	59	M	W	n.d.[2]	partly skeletonized, partly mummified, sun bleached on exposed bone, amputee
24	47	M	W	146	partly skeletonized, partly mummified
47	70	M	W	259	skeletonized, dry
48	67	M	W	114	skeletonized, dry

[1] Postmortem Interval (PMI) recorded in months. The additional 1 and 12 month samples were seriated since the date of placement was less than one month. In other words, body 12.3 was placed before 12.2; indicating that 12.3 had a longer PMI than 12.2.
[2] No Data (n.d.)

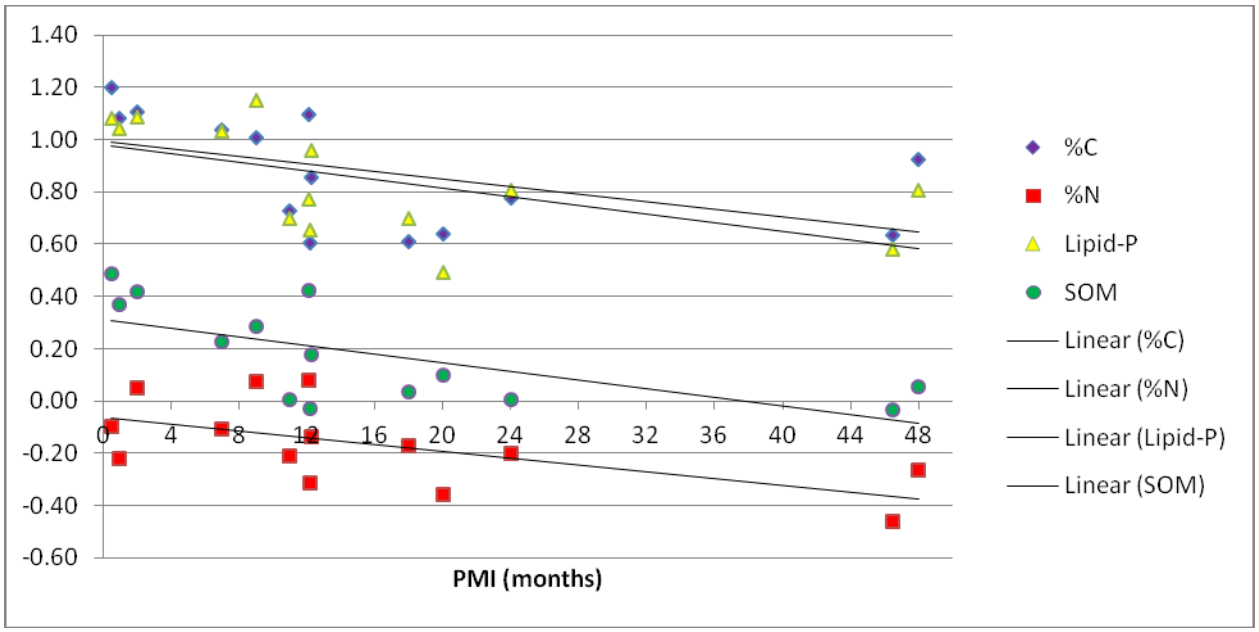

Figure 5-1. Graph of univariate soil parameters plotted against PMI. While slight, the log-transformed data indicated an inverse relationship with time since death. All parameters where highly correlated the first PC axis. Variables include total carbon (%C), lipid-bound phosphorus (Lipid-P), soil organic matter (SOM), and total nitrogen (%N) to months postmortem.

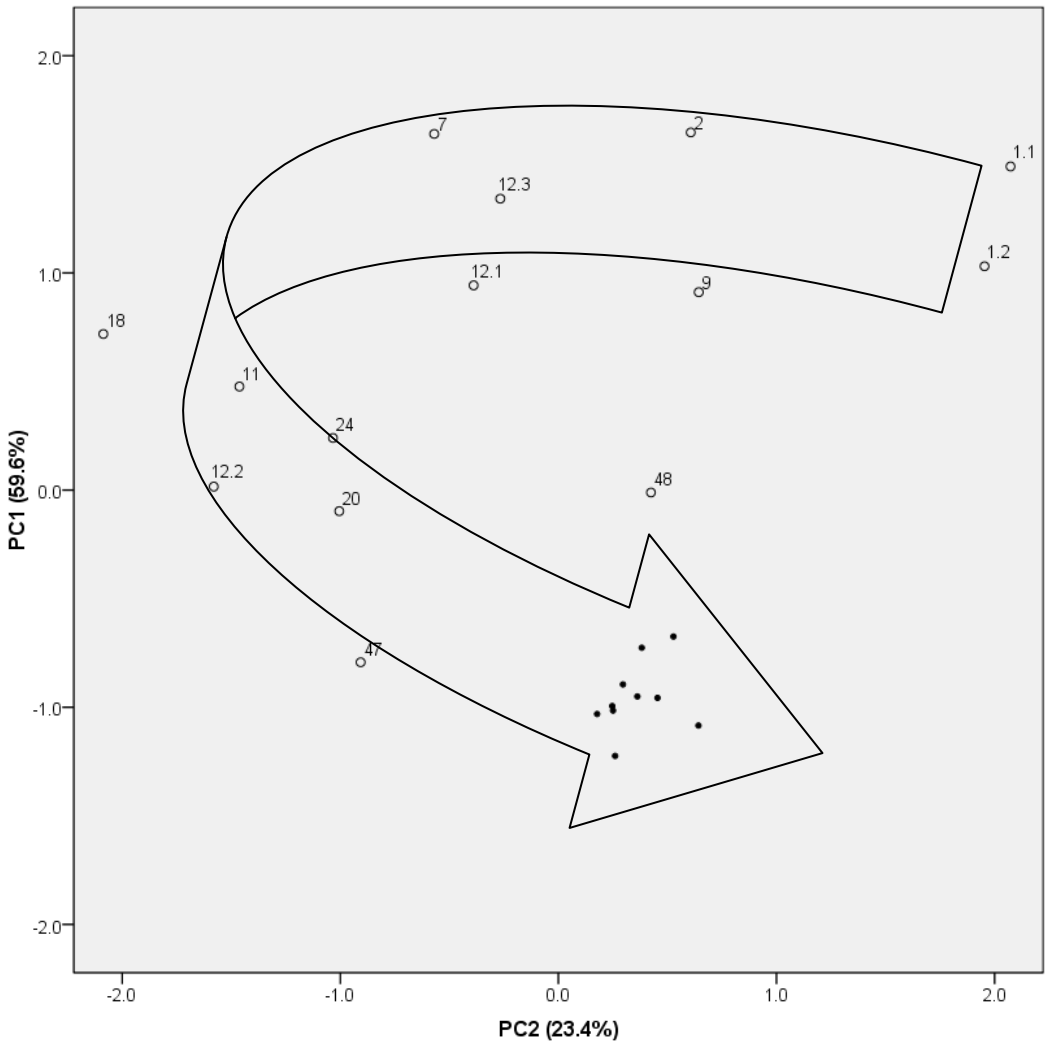

Figure 5-2. PCA of Active and non-ARF control samples. PC1 and PC2 accounted for 83% of the observed variation among the seven variables analyzed. The samples were labeled by months postmortem and varied from 1-48 months. A possible pattern emerged by which late-stage decomposition sites (47 and 48 months PM) approached the non-ARF soil samples (black filled circles) for the physicochemical soil characteristics evaluated. The arrow highlights the sample distribution pattern with time since death.

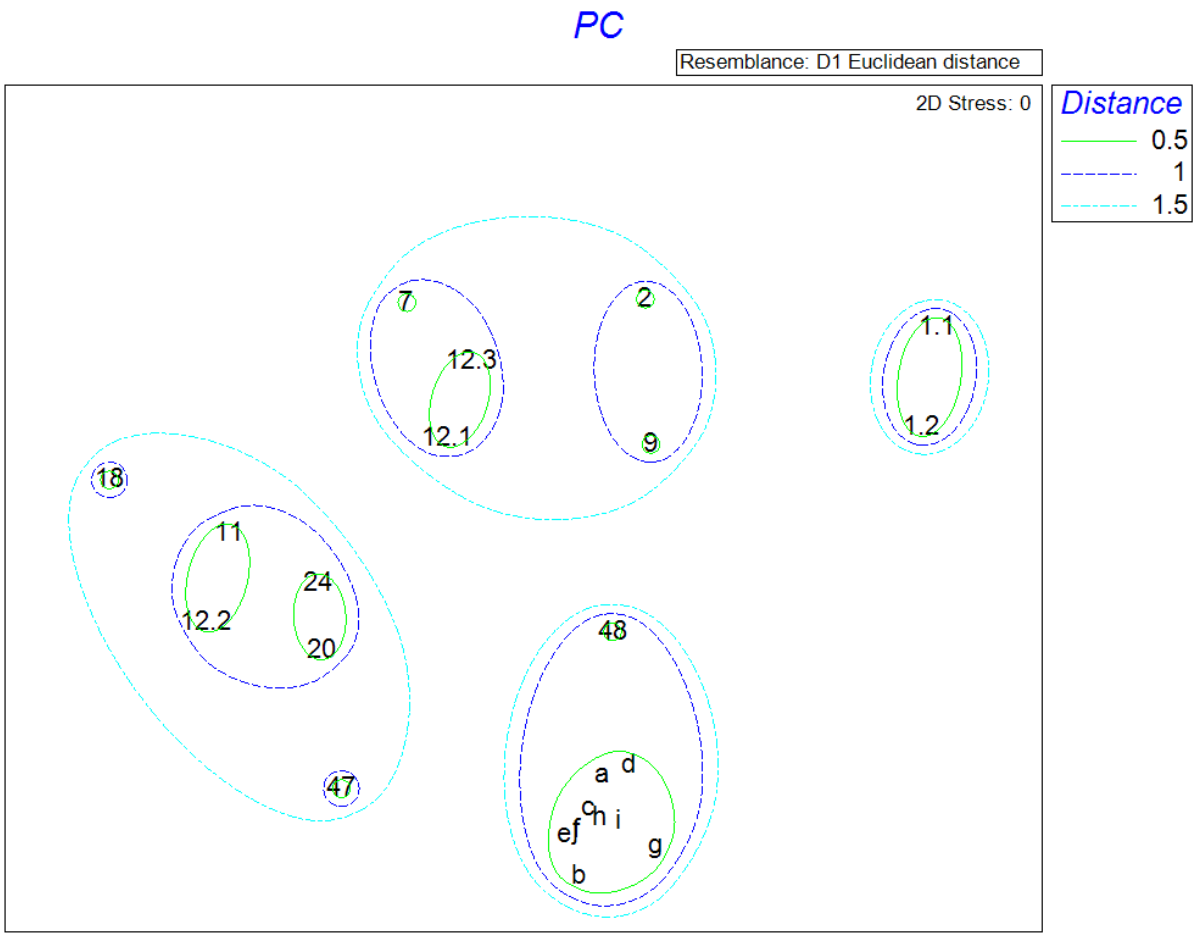

Figure 5-3. MDS of SIMPROF test on gravesoil PCA scores. Cluster analysis of the physicochemical data identified four significant clusters ($p < 0.05$) that coincided with PMI. The *a priori* unstructured data clustered by (a) one month, (b) two to 12 months, (c) 12 to 47 months, and (d) 48 months, plus the non-ARF soils. Note: Variables were re-labeled to account for data entry requirements of PRIMER; samples a-i are the non-ARF samples.

Chapter 6 An Investigation into the Relationship of Postmortem Interval and the Bacterial Communities of Gravesoils

6.1 Introduction

The effect of time since death on the recorded physicochemical parameters of gravesoil samples was observed (Chapter 5). If the physicochemical constitutes of gravesoils are different with advancing postmortem interval (PMI), then the bacterial community composition should have responded to those changes. Therefore, gravesoils below decomposing corpses were used to assess the effect of time since death on the bacterial community. Positive and/or negative relationships may provide additional information for aiding in the estimation of postmortem interval.

6.2 Sample Selection

Eleven gravesoil samples collected below actively decomposing bodies and three soil sample collected outside the University of Tennessee Anthropology Research Facility (ARF) were used in this assay. The soil from the 11 decomposing corpses spanned a postmortem interval from 1-47 months. The bodies varied from active decomposition with partial skeletal exposure to complete dry remains stage (Table 6-1). DNA extracted from the collected soil below the abdomen of each corpse enabled an investigation of bacterial communities based on amplification of the 16S rRNA gene using next generation sequencing (See Chapter 2).

6.3 Analytical Methods

The samples were sequenced using 454 GS FLX Titanium, which used a different chemistry than the previous bacterial community analysis that used non-Titanium reagents. Quality checked sequences from next generation sequencing (NGS) were trimmed, aligned, and classified as described previously.

Frequency distributions of classified bacterial phyla were used to generate relative abundance plots of dominate taxa. Rarefaction curves were created using the Ribosomal Database Project (RDP) pyrosequencing pipeline and assessed graphically at the 3% genetic distance cutoff by plotting the mean number of identified taxa by abundance. Investigation into the relationship of classified sequences with postmortem interval was assessed in PRIMER v6. The Bray-Curtis (BC) similarity coefficient was applied to log-transformed standardized phylotype abundance data for all 14 samples. The similarity profile permutation test (SIMPROF) was run in

conjunction with cluster analyses. The SIMPROF routine identified statistically significant evidence of clusters within unstructured data. Multi-Dimensional Scaling (MDS) of the BC distance matrix was used to create ordination plots and each plot was layered with the results of hierarchical cluster analysis.

6.4 Results and Discussion

Sequencing produced 128,148 sequences from the 14 samples analyzed. Four percent (4.24%; n=5,432) remained unclassified at the bacterial phylum level. The six most abundant phyla across all samples contributed greater than 0.2% of the total sequences and they accounted for 95.70% of all classified bacterial phyla (Figure 6-1). The classified sequences were dominated by Proteobacteria, Actinobacteria, Acidobacteria, Bacteroidetes, Firmicutes, and Gemmatimonadetes. The "other" phyla group (0.06%) and the unclassified group (4.24%) constituted the residual. This other group consisted of Chloroflexi, Cyanobacteria, TM7, Planctomycetes, Nitrospira, Deinococcus-Thermus, and Verrucomicrobia.

Rarefaction curve analysis (Figure 6-2) at the 97% similarity level (i.e., 3% genetic distance cutoff threshold), suggested that the non-ARF soils maintained an overall higher phylotype richness value than all other samples, except for the 47 months PMI sample. All samples were loosely ordered by PMI, suggesting an inverse relationship between richness and time since death.

Log-transformed and standardized abundance data for the 14 samples were converted to a BC similarity matrix and plotted by group means using MDS (Figure 6-3). Ellipses of various similarity distances were layered on the MDS plot demonstrating relationships among samples. The SIMPROF routine applied to the phylotype abundance data identified three genuine clusters ($p<0.05$) (Figure 6-4). One cluster was characterized by non-ARF samples. The second group consisted of samples from one month (1.1 and 1.2) and 20 months postmortem. The remaining samples with PMI of 2 to 12 months composed the third cluster.

The distribution of recovered genomic profiles from each soil sample (Figure 6-5) indicated a consistent relative abundance of Proteobacteria in all samples. Proteobacteria were most dominate among the 2, 7, 9, 11, 47 month, and non-ARF samples. Actinobacteria were present in all samples in varying proportions and the PMI appeared to have little effect on abundance, but they did appear in greater relative abundance for nearly all decomposition samples in comparison to the non-ARF samples. Acidobacteria were nearly nonexistent in the samples,

except for the earliest sample (1.1) and the non-ARF soils. This observation was consistent with the bacterial community profile for the High and None sample groups evaluated in Chapter 4, supporting the periodicity of Acidobacteria response to leached nitrogen-containing compounds.

Dominate phylotypes often mask underlying patterns in the data; therefore the Proteobacteria and Actinobacteria were removed from the relative distribution as well as the other phyla of low representation. The remaining phyla included Acidobacteria, Bacteroidetes, and Firmicutes (Figure 6-5). Inspection of these data suggested a possible trend that may prove important in the assessment of postmortem interval. From the samples used in this study there was an early dominance in the relative abundance of Firmicutes in the first three samples, followed by Bacteroidetes from 7 to 20 months postmortem. Acidobacteria dominated the 47 month PMI sample and most closely resembled the three non-ARF samples.

6.5 Conclusions

Bacterial community profiling of gravesoils presented potential for estimating postmortem interval. Specifically, the effect of time since death appeared to have an effect of the presence and relative abundance of Firmicutes, Bacteroidetes, and Acidobacteria, especially when viewed in relation to one another. The ordination and SIMPROF routines identified genuine clusters within the bacterial abundance data that loosely related with postmortem interval. One group consisted of 1.1, 1.2 and 20 month postmortem samples; another included the 2 month PMI sample. Samples with a PMI of 7-12 months formed a third cluster, while the remaining cluster was characterized by PMI sample 47 and the non-ARF samples. These findings were consistent with the clustering of physicochemical gravesoil samples; in so much as the non-ARF samples had greater similarity to the early postmortem samples than they did to the middle decomposition samples (7-12 months). Additional cross-sectional and longitudinal sampling accompanied by deep sequencing of human gravesoils is necessary before bacterial metagenomics of gravesoils becomes a viable and routine forensic method.

Table 6-1. PMI and cadaver data for investigating the relationship between PMI and the bacterial communities of gravesoils.

PMI[1]	**Age**	**Sex**	**Race**	**Weight**	**Body Description**
1.1	43	M	W	225	skeletonized, maggots present, advanced
1.2	68	M	W	180	partially skeletonized, gooey, liquefied, maggots and beetles, covered with tarp, active
2	88	M	W	175	partially skeletonized, gooey, maggots still active, covered with tarp, active
7	53	M	W	n.d. [2]	partially skeletonized, gooey, no maggots, active
9	50	F	W	185	partially skeletonized, gooey, pupal casings, covered with tarp, advanced
11	26	M	W	115	Skeletonized
12.1	55	M	W	340	partially skeletonized, gooey, no maggots (pupal casings), covered with tarp, advanced
12.2	71	M	W	190	skeletonized, almost no soft tissue, semi covered with tarp
12.3	47	M	B	250	skeletonized, adipocere, semi-covered with tarp
20	59	M	W	n.d.	partly skeletonized, partly mummified, sun bleached on exposed bone, amputee
47	70	M	W	259	skeletonized, dry

[1] Postmortem Interval (PMI) recorded in months. The additional 1 and 12 month samples were seriated since the date of placement was less than one month. In other words, body 12.3 was placed before 12.2; indicating that 12.3 had a longer PMI than 12.2.
[2] No Data (n.d.)

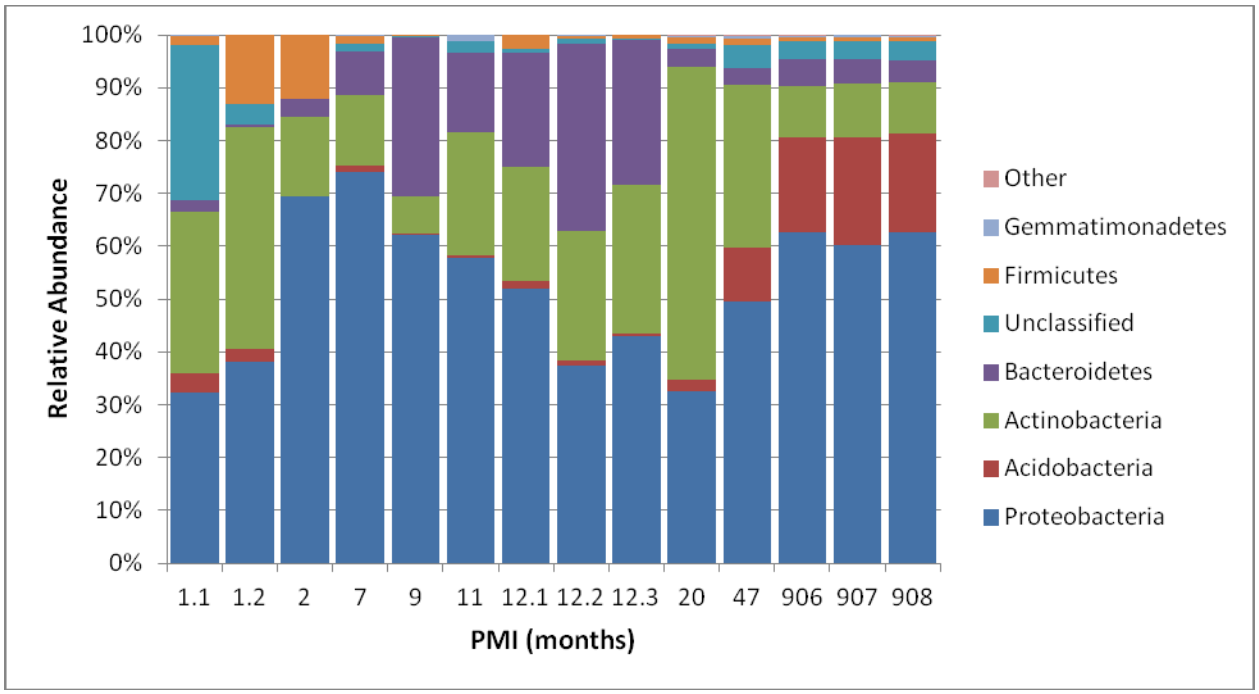

Figure 6-1. Distribution of bacterial phyla in gravesoils. Samples include 11 different decomposing corpses and three samples from outside the ARF with no indication of previous carcass decomposition (906, 907, and 908). Each sample is listed by months postmortem. Unclassified sequences were listed as such, and phyla accounting for < 0.2% of all classified sequences were included in the artificial group "other".

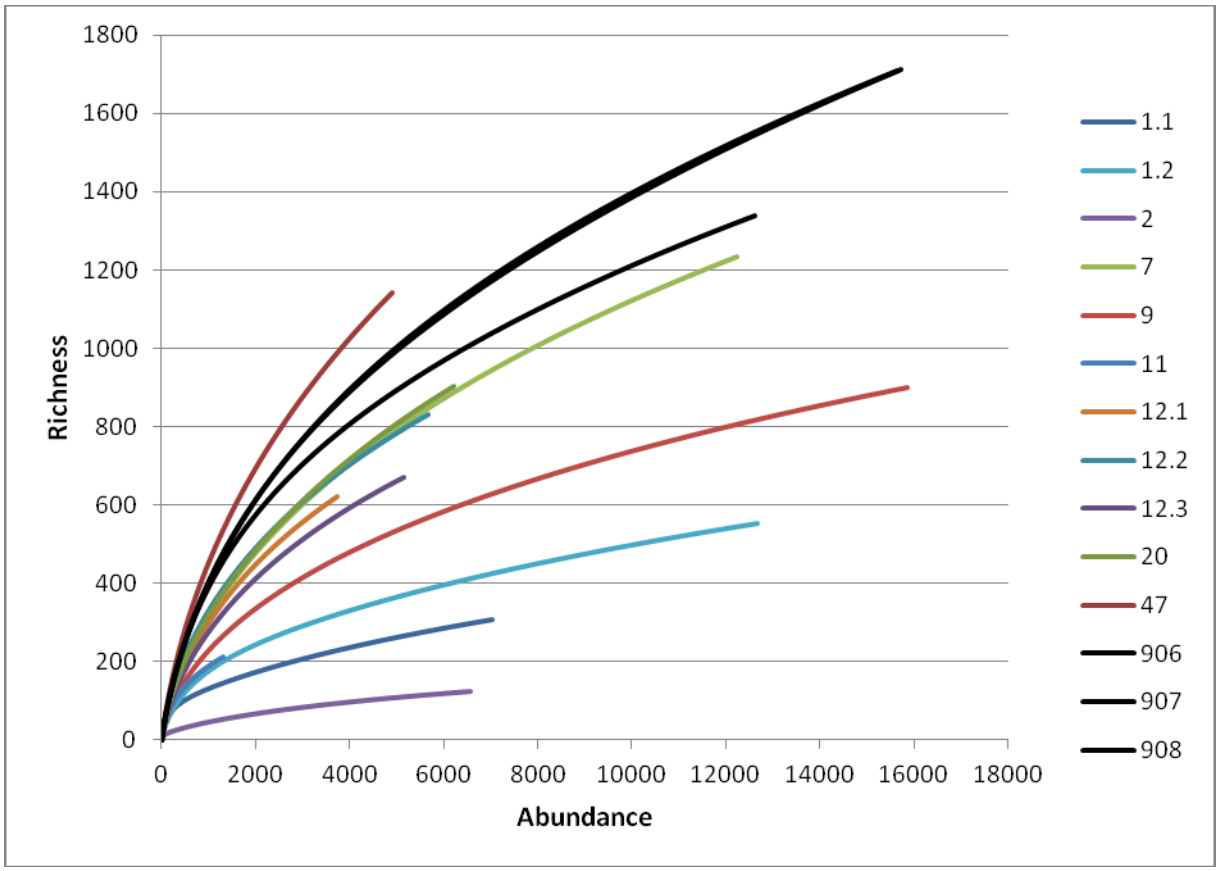

Figure 6-2. Rarefaction curves of bacterial phyla from gravesoils. All samples were graphed at a genetic distance of 3%. The non-ARF samples (black) had the greatest number of sequences and taxonomic units, with the exception of sample 47. This sample is the only one that exceeded the non-ARF samples in richness.

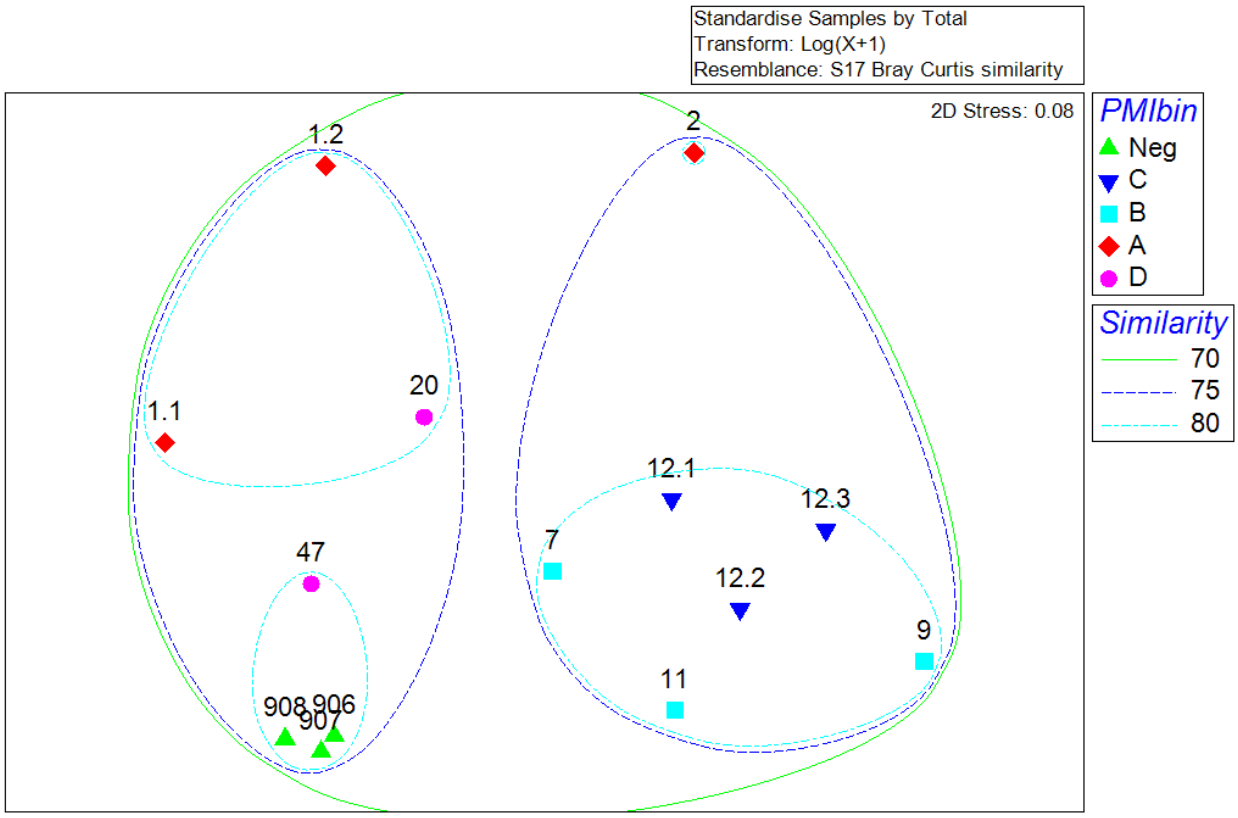

Figure 6-3. MDS on BC similarity matrix for bacterial communities in gravesoil. Each sample is labeled with month since death. Samples are grouped (labeled A, B, C, and D) by year of death 2007 (light blue), 2006 (dark blue), 2005 and earlier (purple), while the green triangles were the three non-ARF samples.

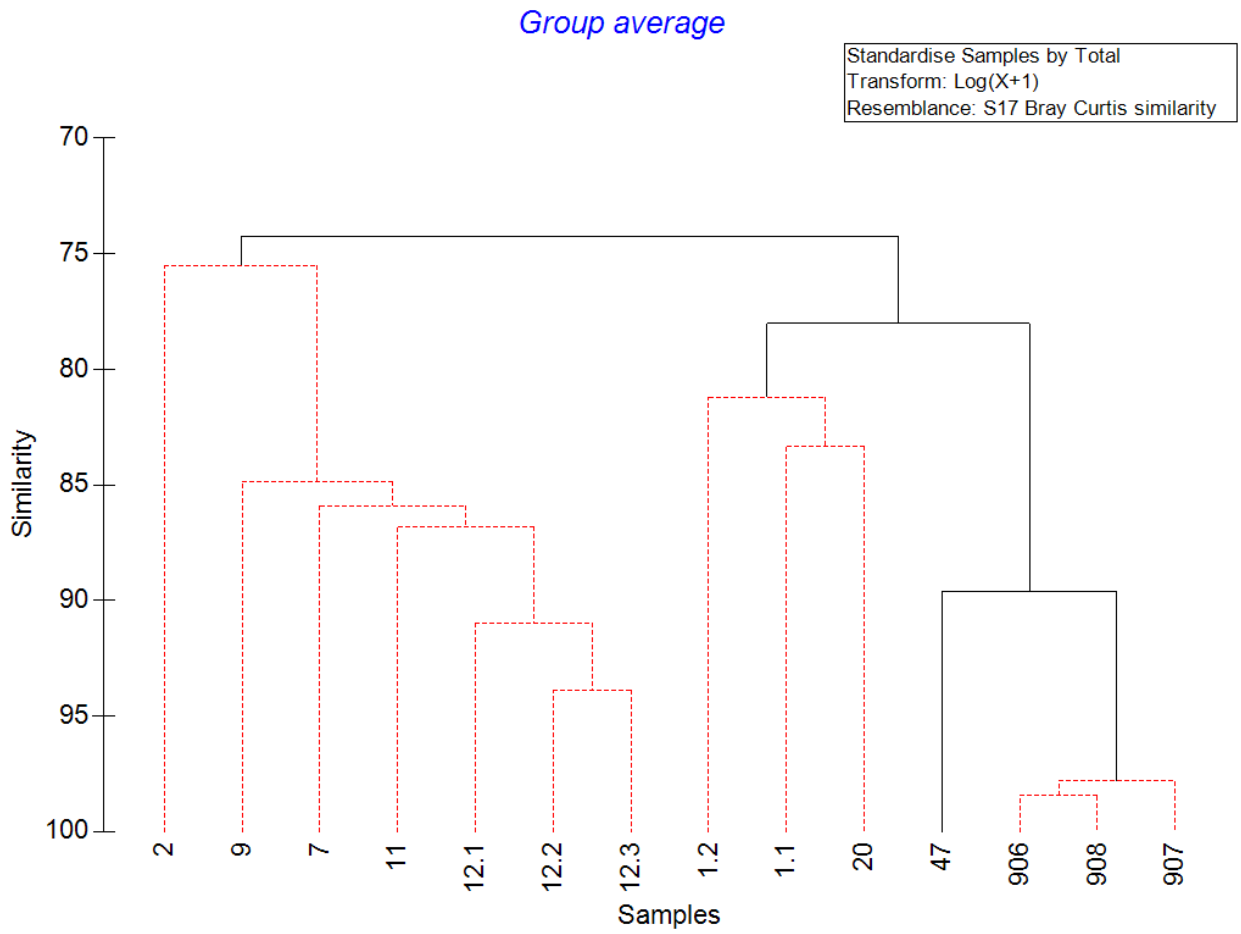

Figure 6-4. SIMPROF cluster analysis on group averages. Three significant clusters among the unstructured bacterial abundance data in gravesoils were identified. One cluster was characterized by non-ARF samples (i.e., 906, 907, 908). The second group consisted of PMI samples of 1.1, 1.2 and 20 months. The remaining samples with PMIs of 2 to 12 months composed the third cluster.

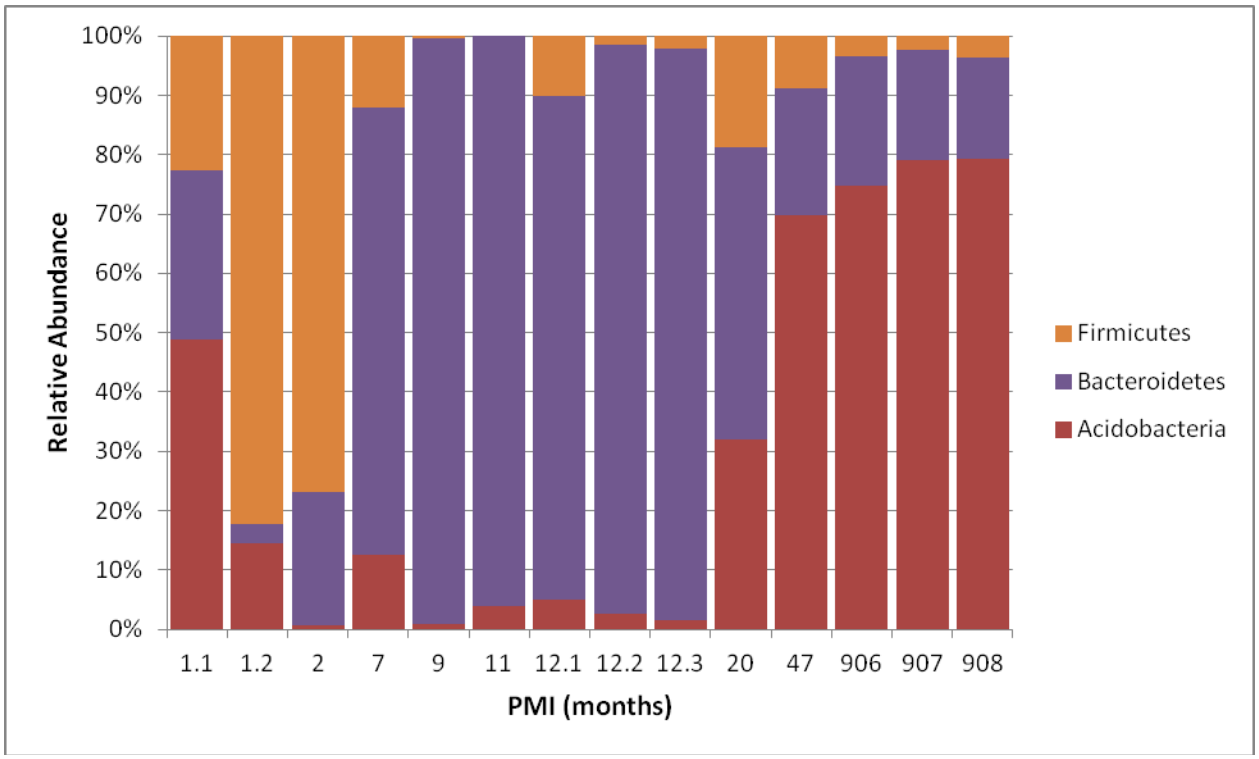

Figure 6-5. Relative abundance of select bacterial phyla in gravesoils by advancing PMI. The early PMI samples were dominated by Firmicutes (≤ 2). Samples with a PMI of 7 to 20 months dominated the second phase, and the oldest sample (47) was dominated by Acidobacteria, which was consistent with non-ARF samples.

Chapter 7 An Investigation into the Relationship of Postmortem Interval and Microbial Biomass of Bone

7.1 Introduction

Microbial populations, including those that facilitate organic decomposition, follow a positive sigmoidal population growth curve as they respond to fluctuations in nutrient availability, the physicochemical environment, and the organism itself. Bacteria are asexual and reproduce by binary fission every 15 to 20 minutes on average (Rousk and Bååth 2011). Non-yeast fungi on the other hand are multicellular and reproduce either sexually or asexually, and have a slower rate of reproduction than bacteria. Given the differences in reproductive strategies and energy acquisition, this test investigated the relationship between postmortem interval (PMI) and DNA concentration of bacteria and fungi recovered from human bone. The quantitative values of recovered DNA were used as a proxy measure of bacterial and fungal biomass. It was hypothesized that the concentration of bacteria will be more prevalent than fungi early in the decomposition process and - with increased decomposition and skeletonization - the lower-quality resource will be more susceptible to decay by fungi.

7.2 Sample Selection

Twelve lower rib samples (11 or 12) collected from decomposing bodies and three soil sample collected outside the ARF were used in this investigation. The bodies spanned a PMI from 1-48 months, and varied from active decomposition with partial skeletal exposure to complete dry remains stage (Table 7-1). Extracted DNA from the bone and soil enabled an investigation of microbial concentration based on quantitative amplification of highly conserved regions of bacteria and fungi (see Chapter 2).

7.3 Analytical Methods

Quantification of bacterial and fungal DNA in a sample was determined by SYBR Green JumpStart (Sigma, St. Louis, MO) assay. First, ten-fold serial dilutions of known bacterial and fungal DNA concentration were used to create a standard curve. Reaction inhibition and primer efficiencies were optimized using PCR products of the bacterial 16S rRNA gene from *E. coli* and an Internal Transcribed Spacer region (ITS) from *Fusarium solani*. Amplification of the standard curve PCR product and the unknown experimental test specimens were completed using

previously reported universal bacterial primers targeting a 200-bp fragment of the bacterial 16S rRNA gene and a 300-bp fragment of the ITS region of fungi (Table 7-2).

The recovered bone samples from the ARF were run simultaneously with the previously validated standard curve samples. To determine sample concentration, qPCR threshold CT values of the unknown bone and soil samples were compared to standard curves of amplified *E. coli* and *Fusarium solani*.

PCR reactions (20uL) contained 4uL of template DNA, 2X SYBR Green JumpStart reaction mix (Sigma, St. Louis, MO), 3 mM $MgCl_2$, 10n M fluorescein, 100 nM forward and reverse primers. The PCR condition consisted of an initial 5 minutes of denaturation at 95°C, 40 amplification cycles of 95°C for 30 seconds, annealing temperature of each primer set for 30 s, 72°C for 60 seconds, and a final extension step of 72°C for 10 minutes. All reactions were done in triplicate.

7.4 Results and Discussion

Bacterial universal primers were efficient for detecting bacteria in mixed samples based on a qPCR efficiency of 93%, while ITS primer sets gave a slightly lower efficiency (90%) than the bacterial primer set (Table 7-3). Amplification inhibition due to coelution of humic acids was resolved by using double purification with use of the MinElute PCR Purification Kit (Qiagen: Valencia, CA). The lower efficiency of the fungal standard was partially due to genetic variation at the primer annealing sites; thereby, indicating that the concentration values were a result of successful amplification, rather than an absolute total concentration of fungi. With that said, the reaction efficiencies between the bacterial and fungal primer sets were virtually the same.

Given the analytical conditions provided, the amount of bacterial and fungal DNA found in the samples varied from 0.2 to 17.0 pg uL^{-1} for bacterial DNA and 0.0 to 3.0 pg uL^{-1} for fungal DNA (Table 7-4). Bacterial concentrations were highest in the samples that had a postmortem interval less than 12 months, while the highest concentration of fungi were found in samples with a PMI greater than 12 months (Figures 7-1 and 7-2). The relative abundance of bacteria to fungi determined by the ratio of total bacteria to total fungi concentration indicated an overall decrease in the ratio across the four-year postmortem interval and appeared to stabilize from the 12 month period through the 48 month terminus of the study set (Figure 7-3).

These findings supported the hypothesis that a trend in the overall abundance of bacteria early in the decomposition process relative to fungi. Convergence between bacteria and fungi

was observed at the 12 month period in which bacteria and fungi began to be represented in equal proportions. Over the four-year period there was no point of secondary divergence in which fungi out competed bacteria in the bone samples analyzed.

7.5 Conclusions

The application of bacterial and fungal qPCR to human remains of different postmortem intervals demonstrated an overall decrease in the concentration of microbial DNA over time, and showed temporally related ecological patterns in the dominance of bacterial DNA over fungal DNA in samples from the first 12 months after death. After 12 months, bacterial concentration decreased and maintained levels similar to fungi. The overall decrease in bacterial DNA over time provided additional cause to investigate the composition of the bacterial communities for the exploration of bacterial community profiles from bone of different times since death.

Table 7-1. PMI and cadaver data for investigating the relationship between PMI and microbial biomass of human bone.

PMI[1]	Age	Sex	Race	Weight	Body Description
1.2	68	M	W	180	partially skeletonized, gooey, liquefied, maggots and beetles, covered with tarp, active
2	88	M	W	175	partially skeletonized, gooey, maggots still active, covered with tarp, active
7	53	M	W	n.d[2].	partially skeletonized, gooey, no maggots, active
9	50	F	W	185	partially skeletonized, gooey, pupal casings, covered with tarp, advanced
11	26	M	W	115	skeletonized
12.1	55	M	W	340	partially skeletonized, gooey, no maggots (pupal casings), covered with tarp, advanced
12.2	71	M	W	190	skeletonized, almost no soft tissue, semi covered with tarp
12.3	47	M	B	250	skeletonized, adipocere, semi-covered with tarp
18	70	M	B	200	half skeletonized, half mummified, uncovered
20	59	M	W	n.d.	partly skeletonized, partly mummified, sun bleached on exposed bone, amputee
24	47	M	W	146	partly skeletonized, partly mummified
48	67	M	W	114	skeletonized, dry

[1] Postmortem Interval (PMI) recorded in months. The additional 1 and 12 month samples were seriated since the date of placement was less than one month. In other words, body 12.3 was placed before 12.2; indicating that 12.3 had a longer PMI than 12.2.

[2] No Data (n.d.)

Table 7-2. Primer data for generating standard curves and quantifying bacterial and fungal DNA from human bone.

Target		**Forward**	**Reverse**	**bp**	**T_A (°C)**	**Reference**
Standards						
	Bacteria	63F	1387R	1500	55	Marchesi et al. 1998
	Fungi	ITS1	ITS4	600	55	White et al. 1990
Experimental						
	Bacteria	341F	534R	200	55	Muyzer et al. 1993
	Fungi	5.8S	ITS1	300	53	Fierer et al. 2005

Table 7-3. Standard curve analyses for quantifying bacterial and fungal DNA.

	Bacteria	*Fungi*
R	0.998	0.999
R^2	0.996	0.999
M	-3.493	-3.598
B	13.979	18.080
Efficiency	0.93	0.90

Table 7-4. Concentration of bacterial and fungal DNA.

PMI	Bacteria			Fungi		
	CT	CT (s.d.)	DNA Conc. (pg/uL)	CT	CT (s.d.)	DNA Conc. (pg/uL)
1.2	18.57	0.05	0.2647	31.74	0.57	0.0016
2	15.60	0.09	2.3017	32.74	0.47	0.0008
7	16.28	0.16	1.4092	33.03	0.76	0.0007
9	13.03	0.11	14.9836	24.74	0.26	0.1404
11	13.28	0.08	12.4727	20.87	0.14	1.6705
12.1	12.83	0.17	17.3329	23.14	0.47	0.3892
12.2	14.83	0.17	4.0362	20.03	0.12	2.8591
12.3	18.19	0.25	0.3490	24.28	0.07	0.1876
18	15.03	0.07	3.4788	19.99	0.12	2.9238
20	15.47	0.21	2.5332	19.96	0.07	2.9929
24	16.69	0.18	1.0451	22.20	0.29	0.7119
48	18.23	0.14	0.3394	22.09	0.07	0.7663

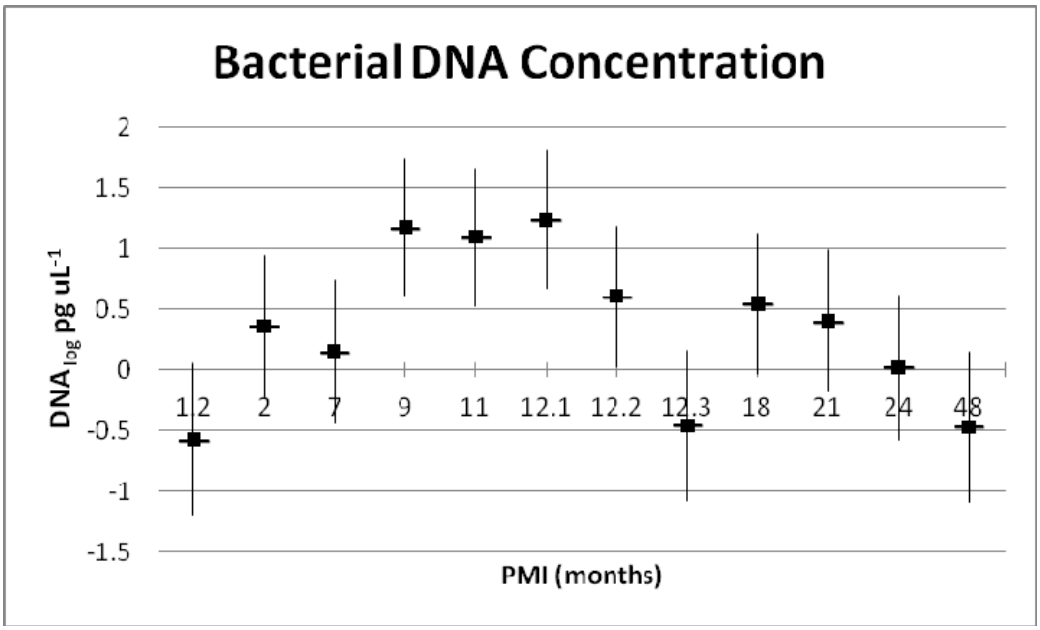

Figure 7-1. Concentration of bacterial DNA isolated from bone with advancing PMI. Box and whisker plots indicate mean and upper and lower 95% confidence intervals for each sample.

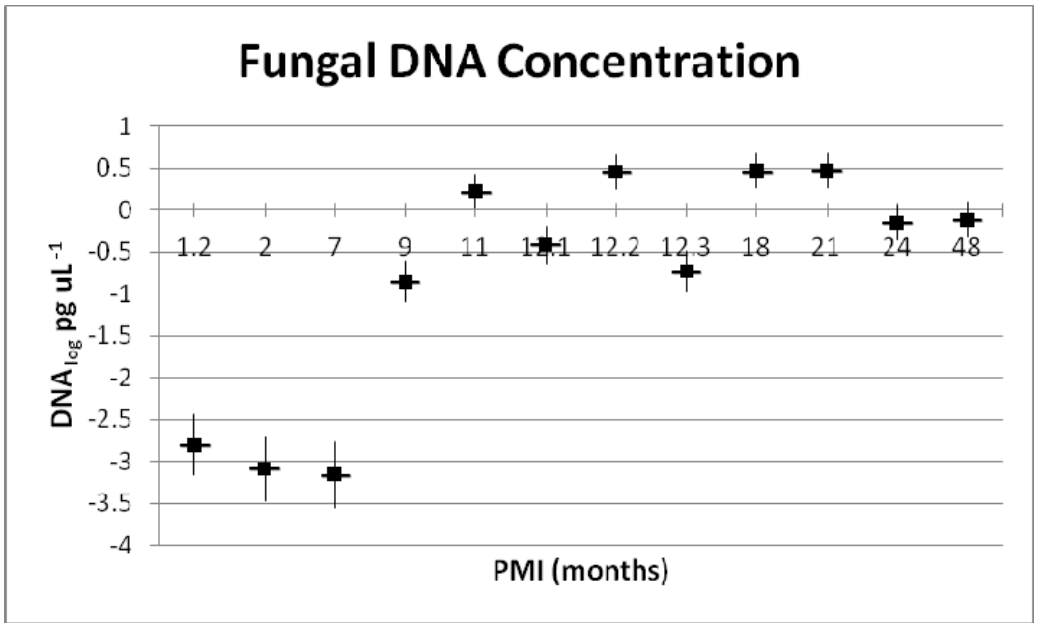

Figure 7-2. Concentration of fungal DNA isolated from bone with advancing PMI. Box and whisker plots indicate mean and upper and lower 95% confidence intervals for each sample.

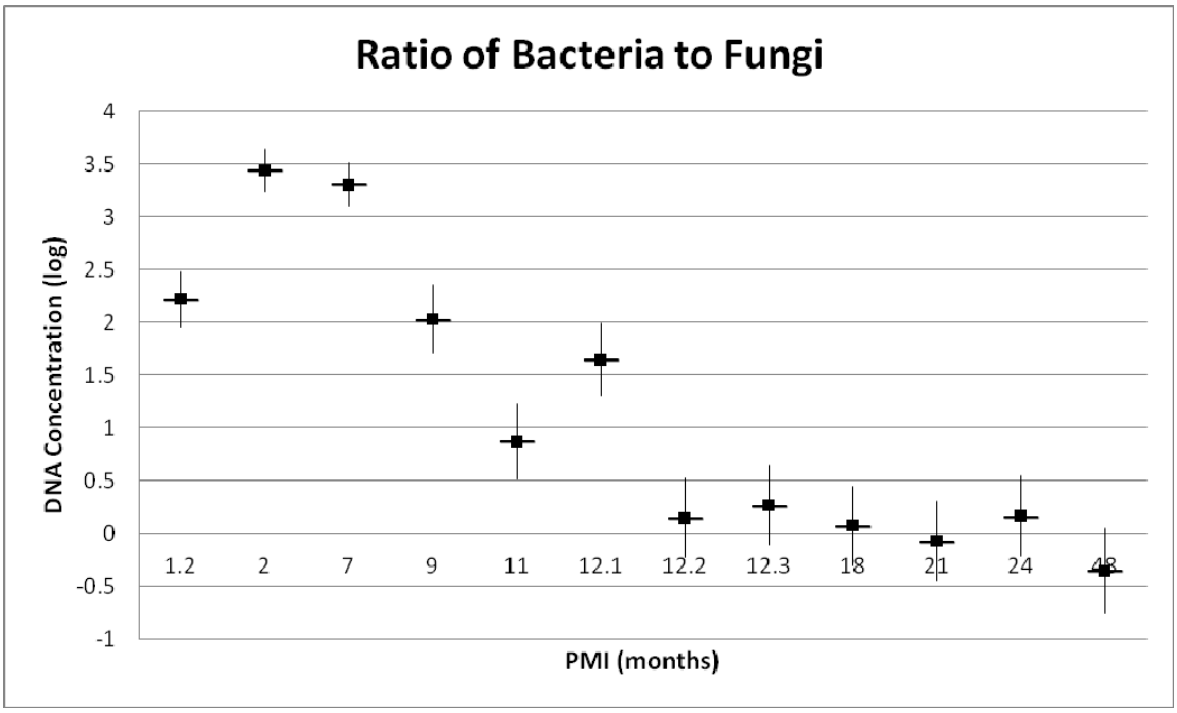

Figure 7-3. Ratio of bacteria to fungi with advancing PMI. Box and whisker plots indicate mean concentration and upper and lower 95% confidence intervals for each sample.

Chapter 8 An Investigation into the Relationship of Postmortem Interval and Bacterial Metagenomics of Bone

8.1 Introduction

The investigation into bacterial biomass in human bone revealed a pattern whereby DNA concentration increased until the first year after death. At which point, the concentration of all subsequent samples decreased. By applying next generation sequencing the bacterial composition and relative distribution of dominate phyla can be identified. This additional information may prove useful by identifying patterns of specific phyla over the postmortem interval assessed in these series of laboratory investigations.

8.2 Sample Selection

Twelve lower ribs collected from decomposing bodies and three soil sample collected outside the UT Anthropology Research Facility (ARF) were used. The 12 decomposing corpses spanned a postmortem interval (PMI) of 1-48 months. The bodies varied from active decomposition with partial skeletal exposure to complete dry remains (Table 8-1). DNA extracted from the ribs enabled an investigation of bacterial communities based on amplification of the 16S rRNA gene using next generation sequencing.

8.3 Analytical Methods

The samples were sequenced using 454 GS FLX Titanium chemistry. Quality checked sequences from NGS were trimmed, aligned, and classified as described previously. Frequency distributions of classified bacterial phyla were used to generate relative abundance plots of dominate phyla. Rarefaction curves were created using the Ribosomal Database Project (RDP) pyrosequencing pipeline to assess phylotype richness. The mean number of identified taxa was plotted by sequence abundance at the 3% genetic distance cutoff. Investigation into the relationship of classified sequences with postmortem interval was assessed in PRIMER v6. A Bray-Curtis (BC) similarity coefficient of log-transformed and standardized abundance data for all 15 samples was generated. The similarity profile permutation test (SIMPROF) was run in conjunction with cluster analyses. The SIMPROF routine identified statistically significant clusters within unstructured data. Multi-Dimensional Scaling (MDS) of the BC distance matrix was used to create ordination plots, and each plot was layered with the results of hierarchical cluster analysis on group means.

8.4 Results and Discussion

Sequences from all rib samples provided 124,164 classified sequences (Figure 8-1). The results of bacterial community analysis suggested a consistency in the presence of specific bacterial phyla. The six most abundant phyla across all bone samples each contributed greater than 0.2% of the total sequences and accounted for 94.37% of all classified bacterial phyla. The six most abundant phyla were Protebacteria (64%), Firmicutes (12%), Bacteroidetes (10%), Actinobacteria (7%), Acidobacteria (1%), and Gemmatimonadetes (0.26%). Nearly six percent (5.62%; n = 6,976) of the trimmed and aligned sequences remained unclassified at the bacterial phylum level. The "other" phyla group (0.008%) included Chloroflexi, TM7, and Deferribacteres.

Rarefaction curve analysis at the 97% similarity level (i.e., 3% genetic distance cutoff threshold), indicated a greater abundance per taxa for the three non-ARF soil samples than the bone PMI samples. Interestingly, the bone samples were loosely grouped by PMI, following a general pattern whereby the longer PMI samples were more consistent with the non-ARF samples (Figure 8-2).

Cluster analysis and the SIMPROF routine applied on phylum-level abundance data identified three significant clusters ($p<0.05$) (Figure 8-3). One cluster was characterized by non-ARF samples and the 24 and 48 month PMI bone samples. The second group consisted of samples 1.2, 2, and 12.3 months. The remaining samples with PMI between 7-20 months composed the third cluster. The MDS plots demonstrated a partial effect on time since death Ellipses at various similarity distances were layered on the MDS plot in order to highlight genuine groups determined by SIMPROF (Figure 8-4).

An investigation of the relative distribution of classified bacterial sequences for each of the bone samples suggested a possible trend toward greater similarity between non-ARF soils and bone as the time since death increased. The most abundant sequences in bone were derived from Proteobacteria, Firmicutes, Bacteroidetes, and Actinobacteria, while Acidobacteria appeared mostly in the non-ARF soil samples and the bone sample of 48 months postmortem (Figure 8-5). An additional time dependent effect was observed among the Firmicutes, Bacteroidetes, and Actinobacteria after removing the most abundant phylum from the relative distributions. Proteobacteria were removed because dominate phylotypes in relative distributions often mask underlying patterns in abundance data. The temporally-related transitions were most apparent

among Firmicutes, Bacteroidetes, and Actinobacteria (Figure 8-6). These three phyla undergo a temporal shift for the 12 bone samples evaluated. Firmicutes (Figure 8-7) dominated the early samples (< 7 months), followed by Bacteroidetes (Figure 8-8) that were most abundant between 9 and 20 months, followed by Actinobacteria (Figure 8-9) for the oldest two samples (24 and 48 months) in this investigation.

Across all methods applied in this investigation, sample 12.3 was an outlier with respect to the large abundance of Firmicutes and unclassified trimmed and aligned sequences. Individual variation of enteric bacterial composition may be one possible explanation for the non-conforming distribution (Costello et al. 2009). However, an observation of note that may warrant future investigation was the presence of adipocere. The saponification of fatty acids into adipocere precludes additional decay (Moses 2012) and may in fact have additional direct antimicrobial properties. Of the 4,948 Firmicutes identified in this sample, 4,517 were of the bacterial order Clostridiales, which have been identified as instrumental in microbially-mediated adipocere formation (Moses 2012, Takatori et al. 1986).

8.5 Conclusions

Bacterial metagenomic analyses of the 12 ribs identified consistent presence of specific bacterial phyla across all samples. Within this data, temporally-related transitions were observed following a pattern of dominance from Firmicutes, to Bacteroidetes, and ending with Actinobacteria. The distributions of these three bacterial phyla demonstrated the potential use of bacterial metagenomic analyses as postmortem temporal benchmarks. These findings seem plausible, given recent findings of human gut microbiome investigation where Firmicutes and Bacteroidetes constitute the most abundant phyla (Ley et al. 2006; Turnbaugh et al. 2007), implying the early postmortem samples were gut derived bacteria. Bacteroidetes is a diverse phylum whose members are widely distributed in soils, sea water, and the human gut. They generally metabolize sugars directly from the environment or release them from long-chain polysaccharides, such as cellulose and chitin. Chitin is a dominate polymer of fungi cell walls, insect exoskeletons and exuded puparia. The increase in Bacteroidetes by the nine month sample coincided with the increased concentration of fungi (Chapter 7). Actinobacteria are also gram-positive, mostly acid-fast bacteria with high GC content that are widely distributed in soil. They have been characterized as aerobic, with most species being facultative anaerobic chemoogranotrophs (Jones and Collins 1986), which are instrumental in organic decomposition

and humus formation of the soil. While these data on the relationship between postmortem interval and bacterial community composition are promising, caution should be applied as these findings are preliminary and offer insight from a limited sample size.

Table 8-1. PMI and cadaver data for investigating the relationship between PMI and bacterial communities of human bone.

PMI[1]	**Age**	**Sex**	**Race**	**Weight**	**Body Description**
1.2	68	M	W	180	partially skeletonized, gooey, liquefied, maggots and beetles, covered with tarp, active
2	88	M	W	175	partially skeletonized, gooey, maggots still active, covered with tarp, active
7	53	M	W	n.d. [2]	partially skeletonized, gooey, no maggots, active
9	50	F	W	185	partially skeletonized, gooey, pupal casings, covered with tarp, advanced
11	26	M	W	115	skeletonized
12.1	55	M	W	340	partially skeletonized, gooey, no maggots (pupal casings), covered with tarp, advanced
12.2	71	M	W	190	skeletonized, almost no soft tissue, semi covered with tarp
12.3	47	M	B	250	skeletonized, adipocere, semi-covered with tarp
18	70	M	B	200	half skeletonized, half mummified, uncovered
20	59	M	W	n.d.	partly skeletonized, partly mummified, sun bleached on exposed bone, amputee
24	47	M	W	146	partly skeletonized, partly mummified
48	67	M	W	114	skeletonized, dry

[1] Postmortem Interval (PMI) recorded in months. The additional 1 and 12 month samples were seriated since the date of placement was less than one month. In other words, body 12.3 was placed before 12.2; indicating that 12.3 had a longer PMI than 12.2.
[2] No Data (n.d.)

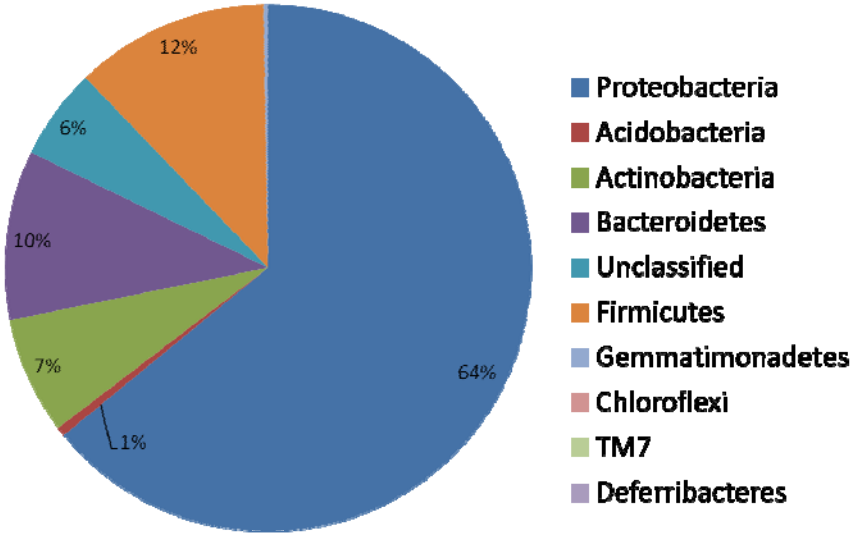

Figure 8-1. Distribution of 124,164 classified 16S sequences at the bacterial phyla level from human bones.

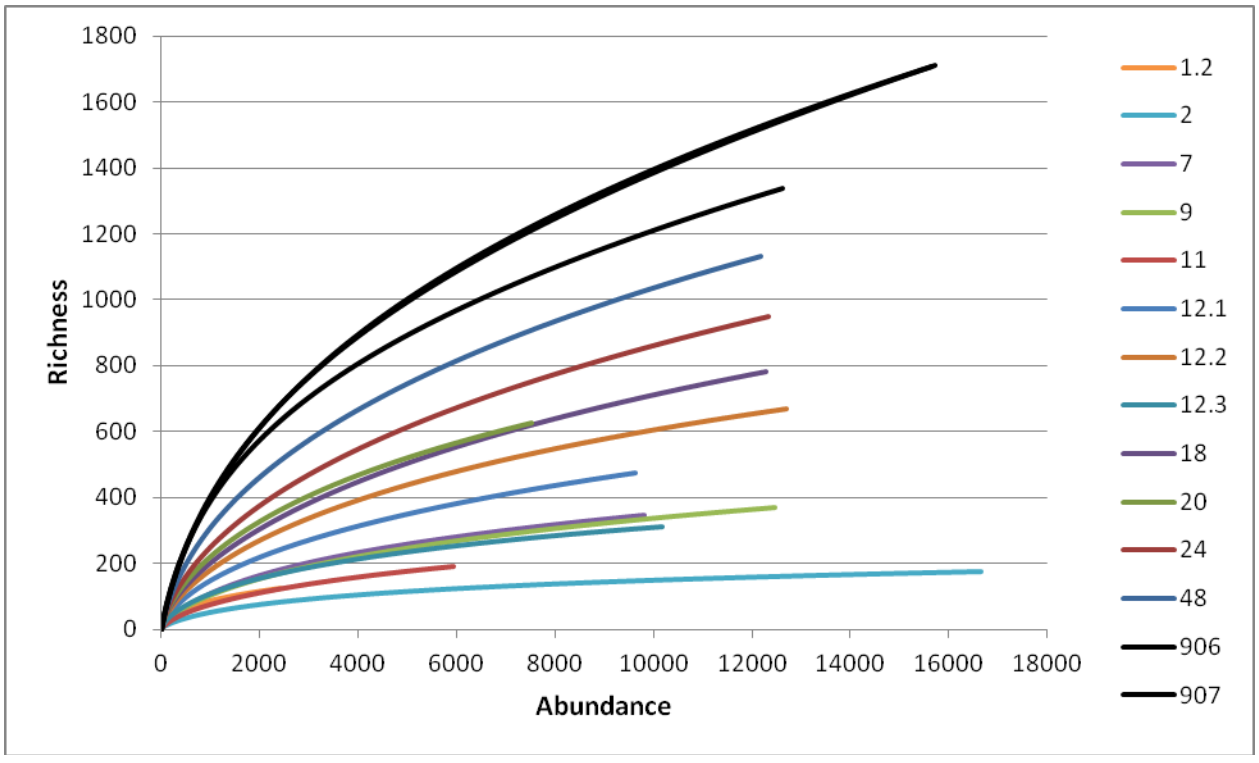

Figure 8-2. Rarefaction curves of bacterial phyla from bone. All samples were graphed at a genetic distance of 3% . The non-ARF samples (black) had the greatest number of taxonomic units by abundance that any one sample, suggesting agreater bacterial load in soil than all bone samples.

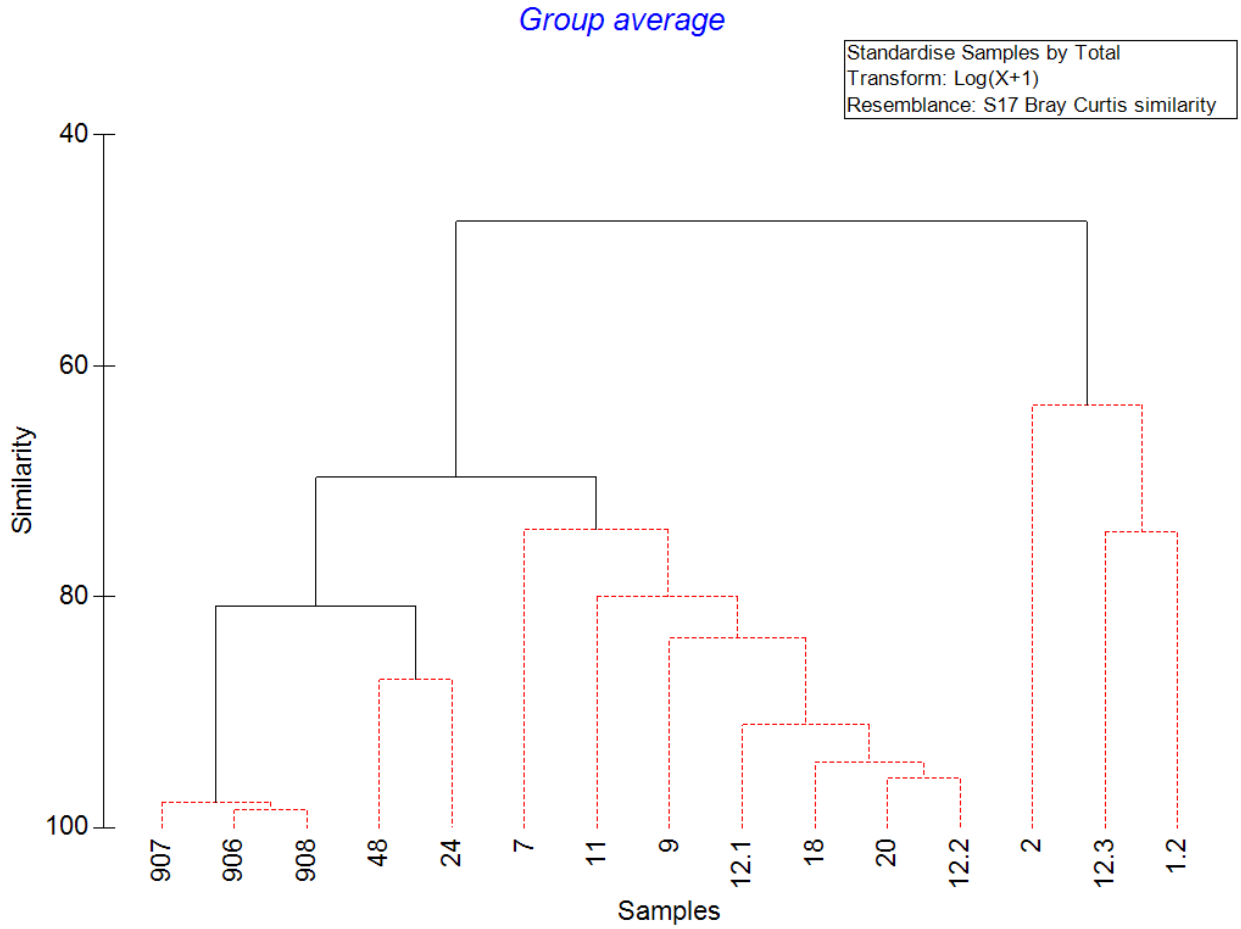

Figure 8-3. Cluster analysis of bone samples on group averages using the SIMPROF routine. Three significant clusters among the unstructured bacterial abundance data were identified ($p<0.05$). One cluster was characterized by non-ARF samples (i.e., 906, 907, 908) and the two oldest samples (24 and 48 months postmortem). The second group consisted of samples with a PMI of 1.2, 2, and 12.3, months. The remaining samples created the third significant cluster and covered an interval of 7 to 20 months postmortem.

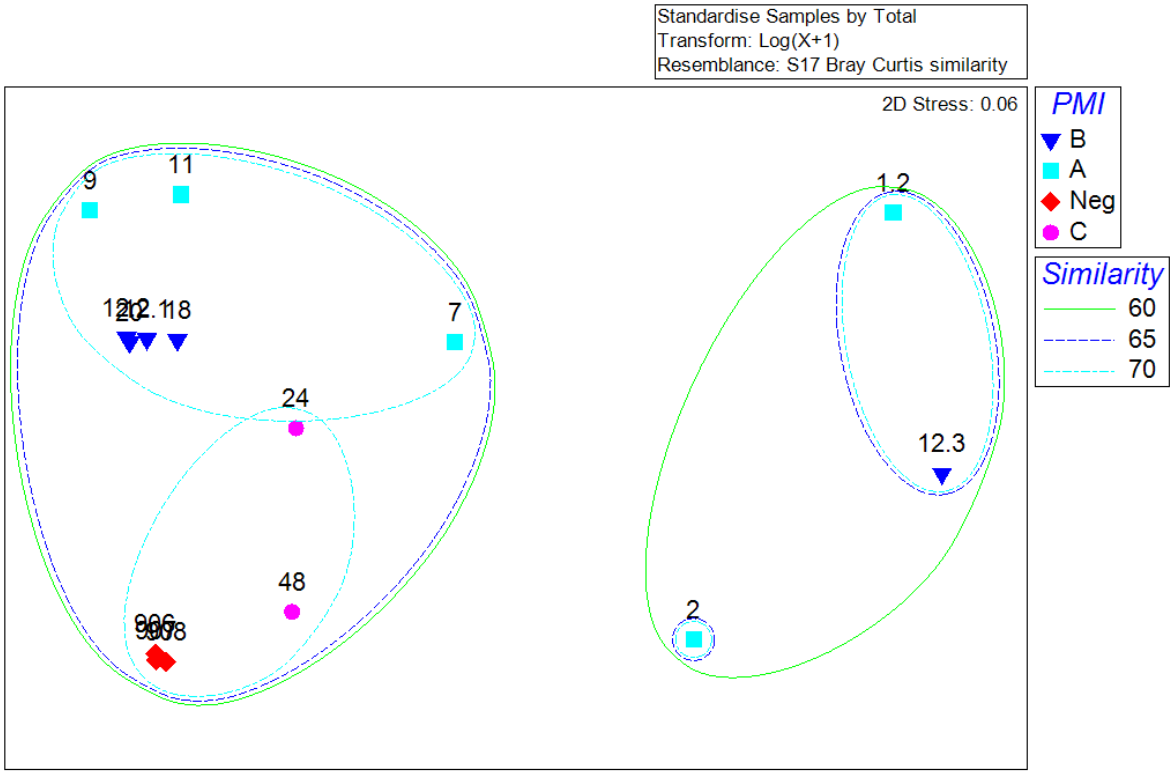

Figure 8-4. MDS of the BC similarity matrix of bone samples. Samples were labeled by months since death and were grouped by year of death 2007 (light blue), 2006 (dark blue), 2005 and earlier (purple).

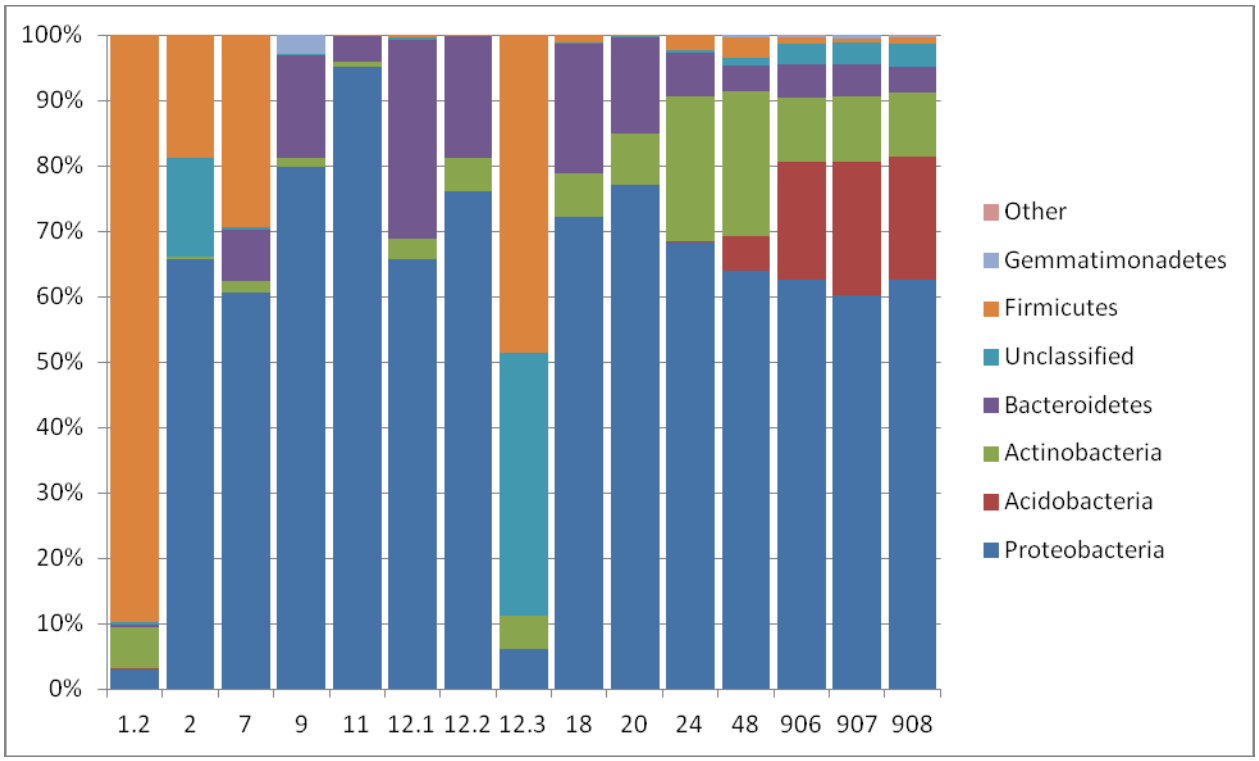

Figure 8-5. Relative abundance of bacterial phyla in bone. Samples were from 12 decomposing corpses and three normal soil samples outside the ARF (906, 907, 908). Unclassified sequences were listed as such, and phyla accounting for < 0.2% of all classified sequences were included in the artificial group "other".

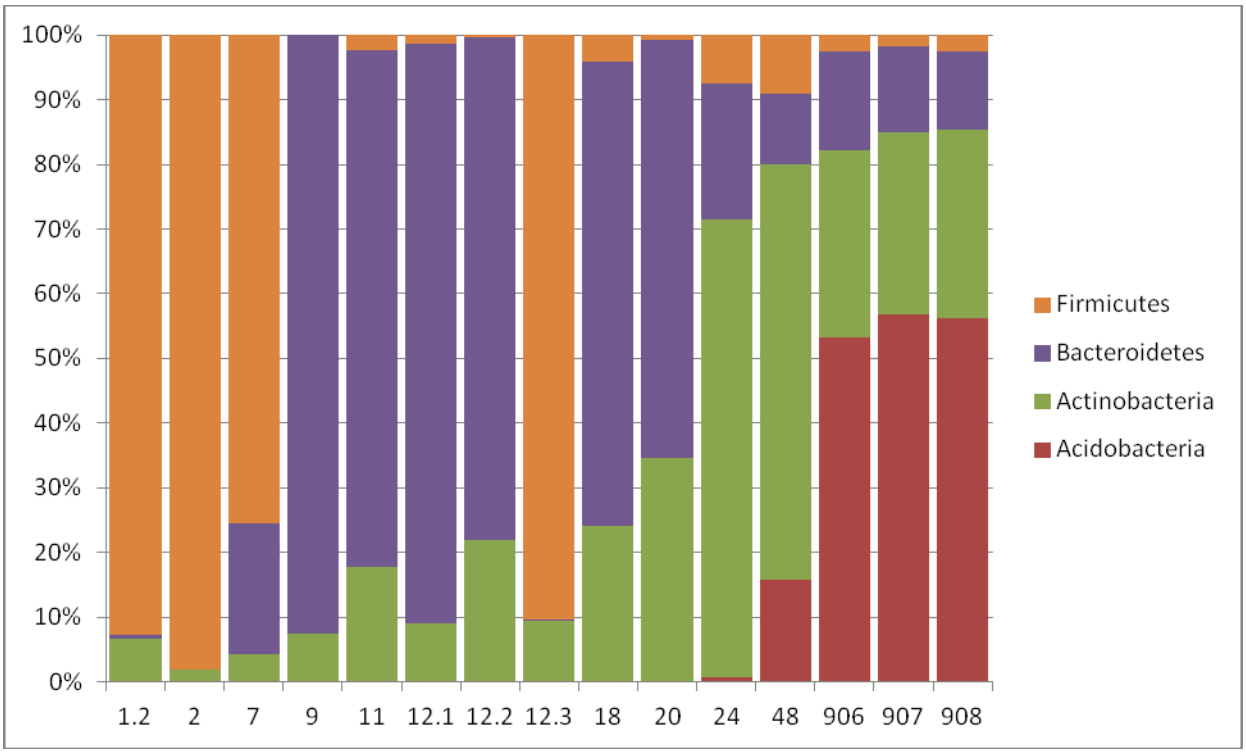

Figure 8-6. Relative abundance of four bacterial phyla from bone. Visual inspection of the data organized by increasing PMI demonstrated a possible trend important to understanding the relationship of PMI and bacterial metagenomics of decomposing human bone. The early PMI samples were dominated by Firmicutes. Bacteroidetes dominated the second phase of samples from 9 to 20 months, with the exception of the 12.3 month samples. The 24 and 48 month samples were dominated by Actinobacteria, and the level of Acidobacteria also increased between these two samples.

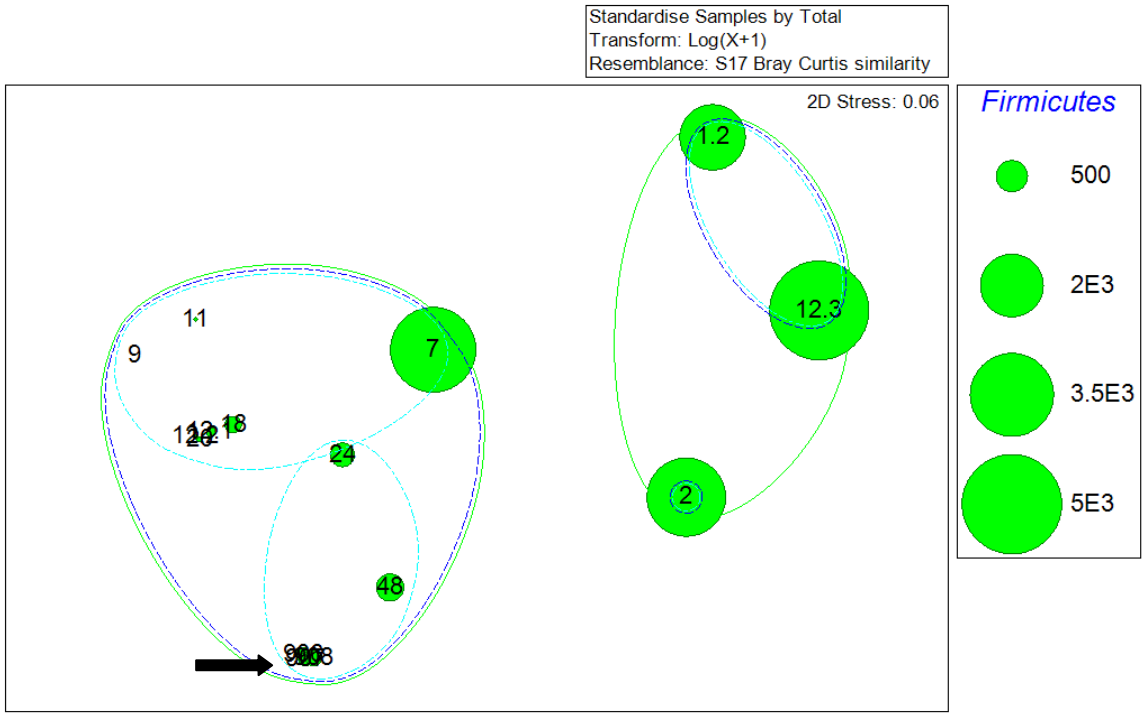

Figure 8-7. MDS of the BC similarity matrix of bone. Firmicutes were most abundant in samples with a PMI of 1.2, 2, 7, and 12.3 months. Non-ARF samples are marked with an arrow.

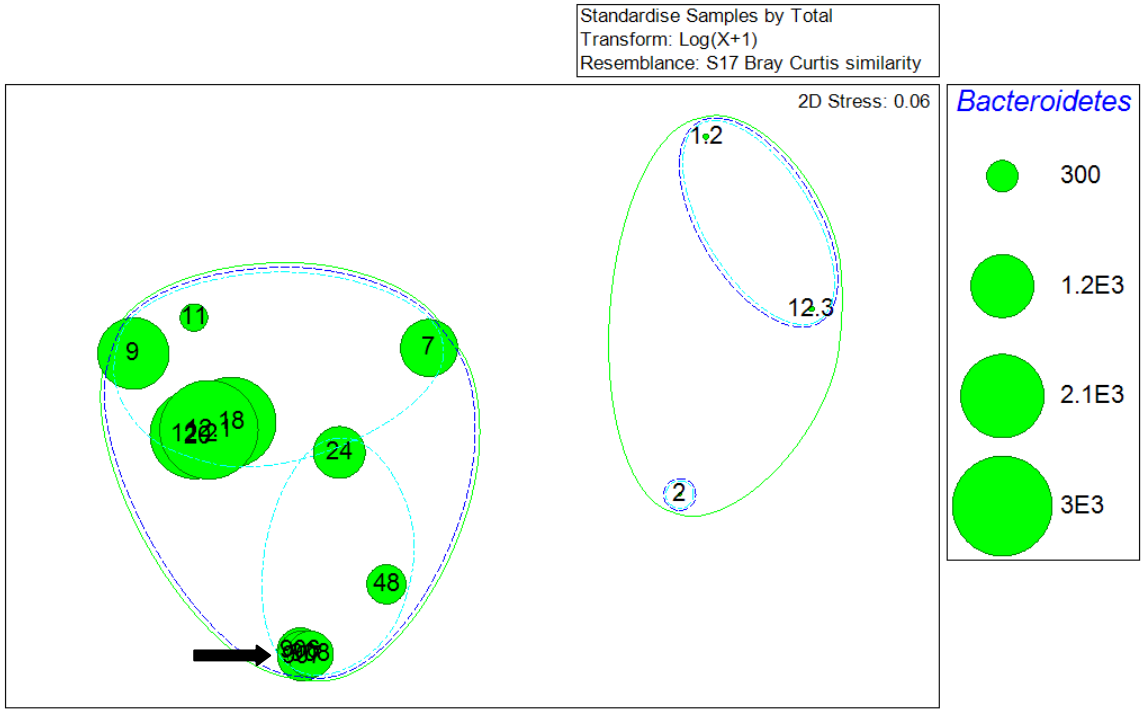

Figure 8-8. MDS of the BC similarity matrix of bone. Bacteroidetes were most abundant in samples with a PMI of 9 to 20 months. Non-ARF samples are marked with an arrow.

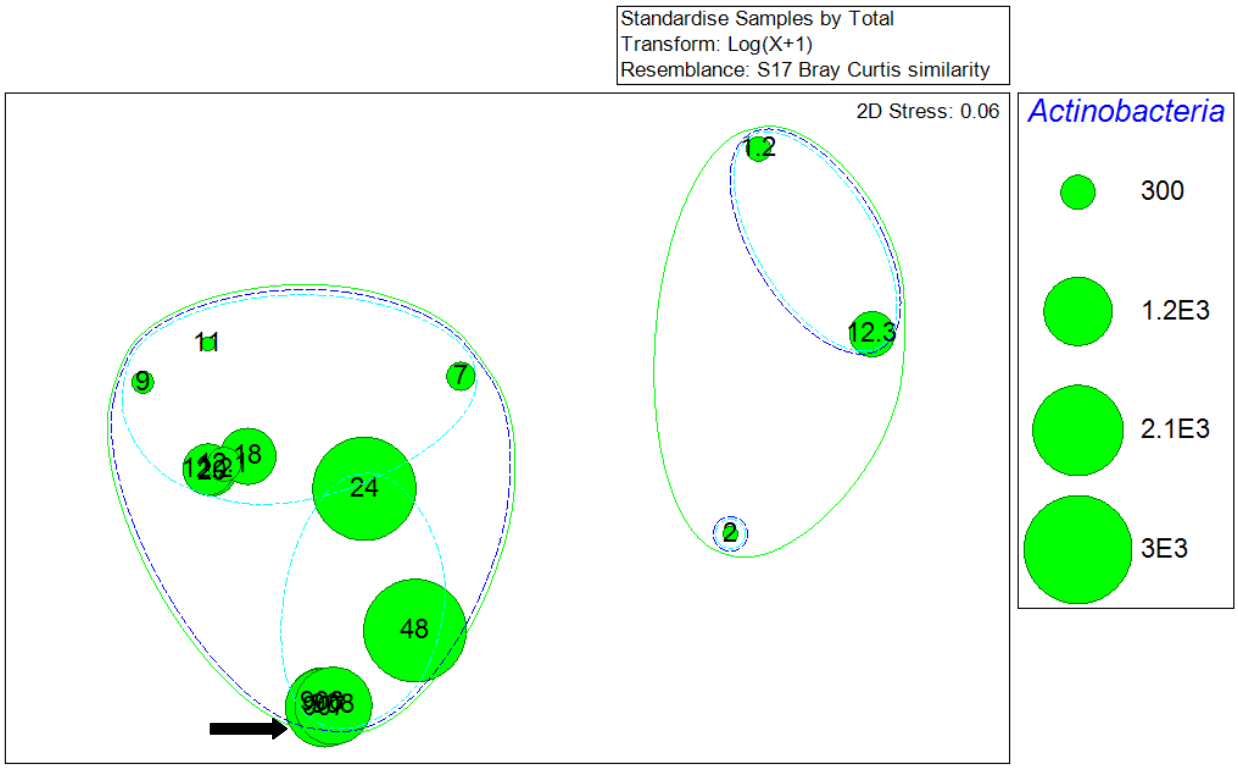

Figure 8-9. MDS of the BC similarity matrix of bone. Actinobacteria were most abundant in samples with a PMI of 24 and 48 months, and the non-ARF soil samples. Non-ARF samples are marked with an arrow.

Chapter 9 Conclusions

9.1 Discussion of Findings

An understanding of gravesoil characteristics and human microbial ecology in relation to human decomposition is essential for developing new models that estimate PMI with greater accuracy than those currently in practice. The development of next-generation sequencing has significantly changed our ability to understand the breadth and depth of microbial diversity; what was once preclude, due to expense and time required for culture, cloning, and Sanger sequencing, is now possible. By applying this novel approach in human decomposition sample analysis, a radically new understanding into the richness and diversity of microflora of the gravesoil-cadaver interface has been provided. The microbial diversity of gravesoils and bone were detected in a greater magnitude than previously described. This new insight presents a challenge not only to the forensic sciences community, but also to soil scientists, microbiologists, ecologists, and taxonomists as the microbial ecology of human decomposition becomes better explained in relation to advancing postmortem interval (PMI).

The ARF Soil Landscape. Systematic analyses of physicochemical parameters of ARF soils suggested a homogenous environment; however, significant shifts in the bacterial community structure were observed among ARF sample groups, partitioned by increasing decomposition. It has been reported that bacterial community structure is affected by land use through modification of soil characteristics (Jesus et al. 2009), and soil pH has been identified as a major factor influencing community composition (Lauber et al. 2009). Soil ecologists have stated that Acidobacteria constitute approximately 20% of bacterial soil communities (Dunbar et al. 2002). Correspondingly, the elevated pH at ARF sites of constant human decomposition maintained a lower relative abundance of Acidobacteria. Since decomposition had a significant effect on the underlying soil microbial structure, it was understood that the same characteristics would vary with advancing PMI, making PMI estimation based on soil characteristics and microbial structure possible.

PMI and Gravesoils. The physicochemical characteristics of the 14 gravesoil samples clustered into four significant groups that followed a trajectory of increasing PMI. The four groups had PMI of (i) one, (ii) 2-12, (iii) 12-47, and (iv) 48 months. The cluster with the longest PMI also included the normal, non-decomposition soils. The distribution of bacterial phyla in

gravesoil samples indicated a consistent relative abundance of Proteobacteria, Actinobacteria, Bacteroidetes, Firmicutes, and Acidobacteria, which is consistent with previous reports on soil bacterial communities (Roesch et al. 2007). There was an observable temporal succession in relative abundance for the 11 gravesoil samples subjected to NGS. The succession began with the Firmicutes, followed by the Bacteroidetes, and ended with Acidobacteria when the other dominate phyla were removed. The visual pattern was supported by identification of significant clustering of soil samples that loosely followed a trajectory of advancing PMI. The four groups had PMI of (i) 1.1, 1.2 and 20, (ii) 2, (iii) 7-12, and (iv) 47 months. Again, the cluster with the longest PMI also included the normal, non-decomposition soils.

PMI and Bone. Quantitative PCR not only demonstrated a decrease in the overall concentration of microbial DNA in bone over time, but showed temporally related ecological patterns in the dominance of bacterial DNA in the first 12 months following death. Overall bacterial concentration, as measured by the quantity of DNA recovered, reduced thereafter becoming equable with fungal DNA concentration for the same samples. The demonstrated relationship of microbial DNA with PMI provided the opportunity for additional exploration of the bacterial metagenomic profiles of the bone samples.

A consistent presence of specific bacterial phyla in human ribs was identified. Within these limited data points, temporally-related transitions were observed following a pattern of early dominance with the Firmicutes (≤ 7 months), followed by Bacteroidetes (9-20 months), and ended with Actinobacteria (24 and 48 months). The presence of these phyla corresponded to recent findings of deep sequencing of the human gut where Firmicutes and Bacteroidetes dominated the bacterial community (Ley et al. 2006; Turnbaugh et al. 2007); thus suggesting that the early postmortem samples were dominated by gut derived bacteria. Bacteroidetes, the second dominate group, are an ecologically and metabolically diverse phylum. Found in the human gut and soils, they generally metabolize sugars directly from their environment or release them from long-chain polysaccharides, such as cellulose and chitin. Chitin is a dominate polymer of fungi cell walls, insect exoskeletons, and exuded puparia. The increase in Bacteroidetes at the nine month PMI sample coincided with increased concentration of fungi that was determined by qPCR. The rise of Actinobacteria among these three phyla formed the last transition. They have been characterized as aerobic, with most species being facultative anaerobic chemoogranotrophs (Jones and Collins 1986), which are instrumental in organic

decomposition and humus formation of the soil (Moorhead and Sinsabaugh 2006). The dominance of Actinobacteria in the late-stage PMI samples may suggest active decay of skeletal tissue by bacterial constituents of the local soil environmental; however, much more work is required to support this hypothesis.

The relative abundance of bacterial phyla in gravesoils and bone determined by NGS demonstrated real potential for the application of bacterial metagenomic analyses to studies in human decomposition ecology and PMI estimation. While these data on the relationship between physicochemical and bacterial community structure of gravesoils and bone to PMI is promising, caution should be applied as these findings are preliminary and offer insight from a limited sample size. Additional cross-sectional and longitudinal sampling and testing of human gravesoils and bone is necessary before becoming a viable and routine forensic method for refining PMI estimations.

9.2 Implications for Policy and Practice

Given the results obtained from the analyses of the ARF soil landscape, outdoor research laboratories that evaluate cadaver decomposition should consider the long-term effects of consistent use. This work has demonstrated that over time a delineated research area devoted to constant human decomposition displayed a trend toward becoming saturated with higher soil pH values, nitrogen content and a lower carbon to nitrogen ratio; therefore, it is suggested that future research facilities incorporate an evaluation of a saturation hypothesis into their long-term strategic goals by performing ecological surveys, early and repeatedly, throughout the lifecycle of a decomposition facility. In doing so, a better understanding of the relationship between ecological change and the forensic goals of providing better models for estimating postmortem intervals may be forthcoming.

Postmortem microbiology is a new field of investigation, and as a result, requires much more study in order to fully implement microbial community structure as a means for better estimating postmortem interval. Next generation sequencing allows characterization of microbial communities that were previously not culturable. We now understand that while human bacterial community structure often shows minimal variability during an adult lifespan, it does vary significantly among individuals (Turnbaugh et al. 2007, Costello et al. 2009), indicating an individualized microbial community fingerprint. This, in turn, may result in a personalized postmortem microbiology, which could explain some of the significant variation associated with

cadaver decomposition (c.f. Shirley et al. 2011). Understanding the general modulators of decomposition such as these and their effect on the rate of human decomposition is important for furthering our understanding of the observable patterns of how humans decompose and how those patterns and changes in the landscape may be used to better estimate time since death.

9.3 Implications for Further Research

Decomposition is a complex series of biological and physicochemical processes that are directly linked to the surrounding ecological niche and functions to recycle nutrients and energy. As demonstrated, the decomposition of a human is no exception. At death and subsequent deposition, the body is a nutrient-rich resource that is reincorporated into the landscape as living biomass; in such a setting the microbial community performs an integral role.

In order to realize the full potential of decomposition ecology to the forensic sciences, additional taphonomic research is certainly required. Both experimental and evidenced-based data collection should continue to be employed to identify patterns of change in the physicochemical (e.g., soil pH, total carbon, nitrogen, and moisture content, ninhydrin reactive nitrogen, volatile fatty acids) and biological (e.g., bacteria, fungi, and nematodes) constituents of gravesoils and bones. These measures should be considered in addition to the descriptive gross observations and plotting of daily mean temperatures currently recorded.

The methods of collection, recording, and analysis of such information should be standardized to facilitate comparison between and among the various recovery sites and decomposition facilities across the United States. Standardized data collection may permit establishment of a nationwide registry of experimental and evidenced-based data that would create the opportunity for the necessary increase in sample size and the development of regional models of human decomposition that will assist in refining postmortem interval estimates.

References Cited

Benninger LA, Carter DO, and Forbes S (2008) The biochemical alteration of soil beneath a decomposing corpse. Forensic Sci Int 180:70-75.

Borneman J and Triplett EW (1997) Molecular microbial diversity in soils from eastern Amazonia: evidence for unusual microorganisms and microbial population shifts associated with deforestation. Appl Environ Microbiol. 63:2647-2653.

Carter DO and Tibbett M (2003) Taphonomic mycota: fungi with forensic potential. J Forensic Sci 48:168-171.

Carter DO, Yellowlees D, Tibbett M (2007) Cadaver decomposition in terrestrial ecosystems. Naturwissenschaften 94:12-24.

Carter DO, Yellowlees D, Tibbett M (2010) Moisture can be the dominant environmental parameter governing cadaver decomposition in soil. Forensic Sci Int 200:60-66.

Cheng J and Greiner R (2001) Learning Bayesian belief network classifiers: algorithms and system, p 141-151. In Stroulia E and Matwin S (eds) Advances in Artificial Intelligence, 14th Biennial Conference of the Canadian Society for Computational Studies of Intelligence, AI 2001 Ottawa, Canada, Proceedings. Springer-Verlag: Berlin.

Child AM (1995) Towards an understanding of the microbial decomposition of archaeological bone in the burial environment. J Archaeol Sci 22:165-174.

Clarke KR and Gorley RN (2006) PRIMER v6: Users Manual/Tutorial. PRIMER-E: Plymouth.

Clarke KR (1993) Non-parametric multivariate analyses of changes in community structure. Aust J Ecol 18: 117-143.

Cole JR, Wang Q, Cardenas E, Fish J, Chai B, Farris RJ, Kulam-Syed-Mohideen AS, McGarrell DM, Marsh T, Garrity GM, and Tiedje JM (2009) The Ribosomal Database Project: improved alignments and new tools for rRNA analysis. Nuc Acid Res 37 (Database issue).

Costello EK, Lauber CL, Hamaday M, Fierer N, Gordon JI, and Knight R (2009) Bacterial community variation in human body habitats across space and time. Sci 326:1694-1697.

Damann FE (2010). Human decomposition ecology at the University of Tennessee Anthropology Rsearch Facility. Dissertation, Knoxville, Tennessee.

Damann FE, Tanittaisong A, and Carter DO (2012) Potential carcass enrichment of the University of Tennessee Anthropology Research Facility: a baseline survey of edaphic features. Forensic Sci Int, 222:4-10.

Dunbar J, Barns SM, Ticknor LO, Kuske CR (2002) Empirical and theoretical bacterial diversity in four Arizona soils. Appl Environ Microbiol 68: 3035–3045.

Drijber RA, Doran JW, Parkhurst AM, and Lyon DJ (2000) Changes in soil microbial structure with tillage under long-term wheat-fallow management. Soil Biol Biochem 32:1419-1430.

Edson SM, Ross JP, Coble MD, Parson TJ, Barritt SM (2004) Naming the dead - confronting the realities of rapid identification of degraded skeletal remains. Forensic Sci Rev 16:63-88.

Evans WED (1963) The Chemistry of Death. Charles C. Thomas: Springfield.

Fierer N, Jackson JA, Vilgalys R, Jackson RB (2005) Assessment of soil microbial community structure by use of taxon-specific quantitative PCR assays. Appl EnvironMicrobiol 71: 4117-4120.

Garrity GM, Brenner D, Krieg NR, and Staley JT (2005) Bergey's Manual of Systematic Bacteriology, 2nd edition, Volume 2. Springer-Verlag: New York.

Hackett CJ (1981) Microscopical focal destruction (tunnels) in exhumed bones. Med Sci Law, 21: 243-65.

Hartgrove NT (2006) Soil Survey of Knox County, Tennessee. USDA: Natural Resources Conservation Services, National Cooperative Soil Survey.

Heiri O, Lotter AF, and Lemcke G (2001) Loss on ignition as a method for estimating organic and carbonate content in sediments: reproducibility and comparability of results. J Paleolimn 25:101-110.

Jesus ED, Marsh TL, Tiedje JM, Moreira FMD (2009) Changes in land use alter the structure of bacterial communities in Western Amazon soils. ISME J 3:1004–1011.

Jones D and Collins MD (1986) Irregular, nonsporing gram-positive rods. In Sneath PHA, Mair NS, Sharpe ME, and Holt JG (eds) Bergey's Manual of Systematic Bacteriology, Volume 2. William & Wilkins: Baltimore.

Kates M (1986) Techniques in lipidology: isolation, analysis, and identification of lipids. In: Burdon RH and Van Kippenberg PH (eds), Laboratory techniques in Biochemistry and Molecular Biology, Volume 3, Part 2:123-127. Elsevier: New York.

Keijser BJF, Zaura E, Huse SM, van der Vossen JMBM, Schuren FHJ, et al. (2008) Pyrosequencing analysis of the oral microflora of healthy adults. J Dent Res 87:1016-1020.

Lane D (1991) 16s/23s rRNA sequencing, pp 115-175. In Stackebrandt E and Goodfellow M (eds), Nucleic Acid Techniques in Bacterial Systematics. John Wiley & Sons: West Sussex.

Lauber CL, Hamady M, Knight R, Fierer N (2009) Pyrosequencing-based assessment of soil pH as a predictor of soil bacterial community structure at the continental scale. Appl Environ Microbiol 75: 5111–5120.

Layton A, Mckay L, Williams D, Garrett V, Gentry R, and Sayler G (2006) Development of Bacteroides 16S rRNA gene TaqMan-based real-time PCR assays for estimation of total, human, and bovine fecal pollution in water. Appl EnvironMicrobiol 72:4214-4224.

Lee DH, Zo YG, and Kim SJ (1996) Non-radioactive method to study genetic profiles of natural bacterial communities by PCR-single-strand-conformation polymorphism. Appl EnvironMicrobiol 62:3112-3120.

Ley RE, Turnbaugh PJ, Klein S, Gordon JI (2006) Microbial ecology: human gut microbes associated with obesity. Nature 444:1022-1023.

Loreille OM, Diegoli TM, Irwin JA, Coble MD, and Parsons TJ (2007) High efficiency DNA extraction from bone by total demineralization. Forensic Sci Int: Genetics 1:191-195.

Marchiafava V, Bonucci E, and Ascenzi A (1974) Fungal osteoclasia: a model of dead bone resorption. Calcified Tissue Research 14:195–210.

Marchesi JR, Sato T , Weightman AJ, Martin TA, Fry JC, Hiom SJ, and Wade W (1998) Design and evaluation of useful bacterium-specific PCR primers that amplify genes coding for bacterial 16S rRNA. Appl EnvironMicrobiol 64:795-799.

Margulies M, Egholm M, Altman WE, Attiya S, Bader JS, Bemben LA, Berka J, et al (2005) Genome sequencing in microfabricated high-density picolitre reactors. Nature 437:376-380.

McGuire KL and Treseder KK (2010) Microbial communities and their relevance for ecosystem models: Decomposition as a case study. Soil Biology and Biochemistry 42:529-535.

Melvin JR Jr, Cronholm LS, Simson LR, and lsaacs AM (1984) Bacterial transmigration as an indicator of time of death. J Forensic Sci 29:412-417.

Moorhead DL and Sinsabaugh RL (2006) A theoretical model of litter decay and microbial interaction. Ecolog Monograph 76: 151–174.

Moses RJ (2012) Experimental adipocere formation: implications for adipocere formation on buried bone. J Forensic Sci 57:589-595.

Muyzer G, De Waal EC, Uitierlinden AG (1993) Profiling of complex microbial populations by denaturing gradient gel electrophoresis analysis of polymerase chain reaction-amplified genes coding for 16S rRNA. Appl EnvironMicrobiol 59:695-700.

Nacke H, Thu¨rmer A, Wollherr A, Will C, Hodac L, et al. (2011) Pyrosequencing-based assessment of bacterial community structure along different management types in German forest and grassland soils. PLoS ONE 6(2): e17000.

Parkinson RA (2009) Bacterial Communities Associated with Human Decomposition. Dissertation, Victoria University of Wellington.

Parkinson RA, Dias KR, Horswell J, Greenwood P, Banning N, Tibbett M and Vass AA (2009) Microbial community analysis of human decomposition in soil. In Ritz K, Dawson LA, Miller D (eds), Criminal and Environmental Soil Forensics. Springer: New York.

Roesch LFW, Fulthorpe RR, Riva A, Casella G, Hadwin AKM, et al. (2007)Pyrosequencing enumerates and contrasts soil microbial diversity. ISME J 1:283–290.

Ronaghi M, Uhlen M and Nyren, P (1998) A sequencing method based on real-time pyrophosphate. Sci 281:363–365.

Rousk J and Bååth E (2011) Growth of saprotrophic fungi and bacteria in soil. FEMS Microbiol Ecol 78: 17-30.

Sandhu GS, Kline BC, Stockman L, and Roberts GD (1995) Molecular Probes for Diagnosis of Fungal Infections. J Clinical Microbiol 33:2913-2919.

Shirley NR, Wilson RJ, and Meadows-Jantz L (2011) Cadaver use at the University of Tennessee's Anthropological Research Facility. Clinical Anat 24:372-380.

Sidrim JJC, Moreira Filho RE, Cordeiro RA, Rocha MFG, Caetano EP, Monteiro AJ and Brilhante RSN (2010) Fungal microbiota dynamics as a postmortem investigation tool: focus on Aspergillus, Penicillium and Candida species. J Appl Microbiol 108:1751–1756.

Storer DA (1984) A simple high sample volume ashing procedure for determining soil organic matter. Comm Soil Sci Plant Anal 15:759-772.

Swift MJ, Heal OW, Anderson JM (1979) Decomposition in terrestrial ecosystems. Blackwell Scientific: Oxford.

Takatori T, Ishiguro N, Tarao H, Matsumiya H (1986). Microbial production of hydroxy and oxo fatty acids by several microorganisms as a model of adipocere formation. Forensic Sci Int. 32:5-11.

Turnbaugh PJ, Ley RE, Hamady M, Fraser-Liggett, Knight R, and Gordon JI (2007) The human microbiome project. Nature 449:804-810.

Vass AA, Bass WM, Wolt JD, Foss JE, Ammons JT (1992) Time since death determinations of human cadavers using soil solution. J Forensic Sci 37:1236–53.

Vass AA, Barshick S-A, Sega G, Caton J, Skeen JT, Love JC, Synstelien JA (2002) Decomposition chemistry of human remains: a new methodology for determining the postmortem interval. J Forensic Sci 47:542-553.

Vass AA, Smith RR, Thompson CV, Burnett MN, Dulgerian N, Eckenrode BA (2008) Odor Analysis of Decomposing Buried Human Remains. J Forensic Sci 53:384-391.

Venter JC, Remington K, Heidelberg JF, Halpern AL, Rusch D, et al. (2004) Environmental genome shotgun sequencing of the Sargasso Sea. Science 304(5667): 66-74.

Wang Q, Garrity GM, Tiedje JM, and Cole JR (2007) Naïve Bayesian Classifier for Rapid Assignment of rRNA Sequences into the New Bacterial Taxonomy. Appl EnvironMicrobiol 73:5261-7.

White TJ, Bruns T, Lee S, Taylor J (1990) Amplification and direct sequencing of fungal ribosomal RNA genes for phylogenetics. In Innis MA, Gelfand DH, Sninsky JJ, and White TJ (eds) PCR Protocols: A Guide to Methods and Applications. Academic Press: San Diego.

Dissemination of Research Findings

Presentations

Damann FE. Human Decomposition Ecology and Estimating Time Since Death University of Tennessee Department of Anthropology. Knoxville, Tennessee, August 27, 2009

Damann FE. Human Decomposition Ecology and Estimating Time Since Death. NIJ Grantees Update Meeting, NIJ OJP DOJ. Alexandria, Virginia, December 7, 2009

Damann FE. Human Decomposition Ecology and Estimating Time Since Death. Regularly Scheduled Conference, Armed Forces Institute of Pathology. Washington, District of Columbia, December 9, 2009.

Damann FE. Human Decomposition Ecology and Estimating Time Since Death New York University, Department of Anthropology. New York, New York, April 23, 2009.

Damann FE and Marks MK. Temporal Information: Microbe-mediated soft tissue decomposition, American Academy of Forensic Sciences, Workshop #10 Taphonomy of Bone Destruction: Information Lost, Information Gained. Seattle, Washington, February 22, 2010.

Damann FE. Human Decomposition Ecology at the University of Tennessee Anthropology Research Facility Symposium on Time Since Death, Decomposition, and Taphonomy. Published abstract for the 62nd annual meeting of the AAFS. Seattle, Washington, February 26, 2010.

Damann FE. Patterns in Human Decomposition Ecology and the Potential for Time Since Death estimation, Harvard Associates in Police Science. Easton, Maryland, June 22, 2010.

Damann FE. Human Decomposition Ecology and Estimating Time Science Death, USA Science and Engineering Festival, Nifty 50 Speakers. Columbia, Maryland, October 2010.

Tanittaisong A and Damann FE. An investigation on the relationship of postmortem interval to microbial biomass in bone. Published abstract for the 64th annual meeting of the AAFS. Atlanta, Georgia, February 23, 2012.

Damann FE, The Science of Forensics: Decomposition and Estimating Time Science Death, USA Science and Engineering Festival, Nifty 50x2 Quince Orchard, Maryland, March 21, 2012.

Publications

Damann FE (2010) Human Decomposition Ecology at the University of Tennessee. A Dissertation, University of Tennessee: Knoxville.

Damann FE, Tanittaisong A, and Carter DO (2012) Potential Carcass Enrichment of the University of Tennessee Anthropology Research Facility: A Baseline Survey of Edaphic Features Forensic Sci Int, 222:4-10.

Damann FE and Carter DO (In Press) Human decomposition ecology and postmortem microbiology. A Manual of Forensic Taphonomy, Pokines J and Symes S, editors. CRC Press.

Damann FE and Tanittaisong A (In Preparation). An investigation on the relationship of postmortem interval to microbial biomass in bone.

Damann FE and Layton AC (In Preparaion). Bacterial metagenomics of human decomposition.